Passivity-Based Wind Estimation for Aircraft Maneuvering in Steady and Uniform Wind Fields

Jeremy W. Hopwood* and Craig A. Woolsey†
Virginia Tech, Blacksburg, VA 24060

Wind measurements in the lower atmosphere are vital to the expansion of air mobility operations, providing boundary condition data for numerical weather models and supporting planning and control systems for improved weather tolerance and safety. Traditional approaches to wind estimation from flight data rely on linearization of the flight dynamic model and are therefore only valid near the nominal flight condition. To obtain accurate wind estimates in maneuvering flight, this "small perturbations" restriction must be relaxed. This paper presents the design and simulation of a nonlinear, passivity-based observer for aircraft in wind with global exponential convergence guarantees. The main results include explicit formulas for implementing the observer as well as a linear matrix inequality that can be used to optimize wind estimate convergence. The wind observer is implemented using flight test data, demonstrating good performance even in maneuvering flight through turbulent air.

I. Introduction

Weather patterns over complex terrain are complicated and ever-changing, yet are crucially important to understand for safe air mobility operations [1]. The importance of accurate, real-time weather prediction only increases as Advanced Air Mobility (AAM) and Urban Air Mobility (UAM) missions mature to provide safe, efficient, and ubiquitous automated air transportation services in urban and suburban areas [2]. As the air mobility concept matures, the need grows for higher weather tolerance and thus relaxed margins for flight safety [3–6]. The expansion of weather-tolerant operations will not just be made possible through more accurate model-based atmospheric predictions on the mesoscale and microscale, but also through improved atmospheric measurements at the vehicle level. In fact, the latter can contribute to the former by providing timely, *in situ* measurements of wind and related atmospheric parameters such as pressure, temperature, and humidity as illustrated in Figure 1.

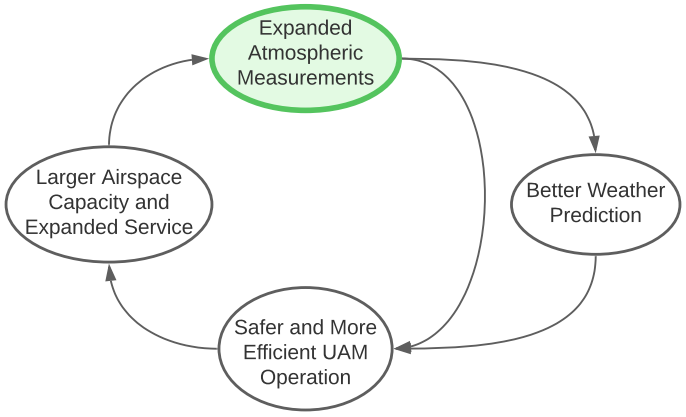

Fig. 1 Enabling air mobility.

Traditional *in situ* sampling methods such as weather balloons are impractical in an urban setting and only capture a few data points within the atmospheric boundary layer (ABL) at sparsely distributed locations. One of the

*Ph.D. Candidate, Crofton Department of Aerospace and Ocean Engineering, AIAA Student Member, jeremyhopwood@vt.edu
†Professor, Crofton Department of Aerospace and Ocean Engineering, AIAA Associate Fellow, cwoolsey@vt.edu

fastest-emerging solutions to bring higher temporal and spatial resolution to atmospheric measurements is the use of small unmanned aircraft systems (UAS) [7–12]. The use of UAS enables better ABL profiling and microscale numerical weather prediction (NWP) using high-rate *in situ* measurements. Of particular interest are approaches that do not require specialized sensors such as anemometers to measure wind velocity. The motion of the aircraft in response to external disturbances can be used to continuously estimate the wind at the aircraft's location. Minimal instrumentation requirements make aircraft-based wind estimation at low altitudes viable for a variety of small crewed and uncrewed aircraft. The opportunity for "crowdsourced" sensing could provide a rich data set that can be used across disciplines and applications to enable safer, more efficient, and weather-tolerant air mobility operations [13, 14].

While the incorporation of weather sensing on air mobility vehicles presents a great opportunity, there are concerns that current approaches would not enable access to some regions where data may be needed, such as areas subject to high winds. Most approaches to aircraft-based wind estimation rely on a linear flight dynamic modeling approach that assumes small perturbations from a nominal flight condition (e.g., forward flight at constant altitude). While these methods work well close to the designed operating condition, the underlying assumptions can be violated in the presence of strong wind. These concerns present a need to expand the range of flight conditions for which accurate wind estimates and atmospheric measurements can be made.

To improve capability to predict weather in an urban environment, this paper presents the design and simulation of a global nonlinear passivity-based wind observer for aircraft. This observer provides real-time estimates of the wind valid across the entire flight envelope. Such an observer creates a capability to expand the range of flight conditions for which accurate wind estimates can be made. One of the main benefits of this nonlinear observer is that it comes with rigorous guarantees on the wind estimate convergence over the entire flight envelope, thus increasing the level of trust in whatever autonomous mission for which the estimation scheme is employed. This is where traditional linear approaches and linearization-based approaches such as the extended Kalman filter can come up short. Kalman filtering approaches to wind estimation tend to be very sensitive to assumptions about the statistics of the wind disturbance, which is only exacerbated for flight across a wide variety of conditions.

This paper is organized as follows. Section II introduces the aircraft in question and derives the equations of motion in wind for which the observer is designed. Section III provides an overview of the theory of passivity-based observers as presented in [15, 16]. Next, the main result of this paper is detailed in Section IV where the passivity-based observer for aircraft in wind is designed. Finally, Section V presents both simulation and flight test results for the observer, enabling the evaluation of the observer's performance even when assumptions are violated.

II. Aircraft Dynamics in Wind

A. Rigid-Body Dynamics

Consider an aircraft, modeled as a rigid body of mass m. Let unit vectors $\{\boldsymbol{i}_1, \boldsymbol{i}_2, \boldsymbol{i}_3\}$ define an earth-fixed North-East-Down (NED) orthonormal reference frame, $\mathcal{F}_{\mathrm{I}}$. As the notation $\mathcal{F}_{\mathrm{I}}$ suggests, we take this frame to be an inertial reference frame over the time and space scales of vehicle motion. Let the unit vectors $\{\boldsymbol{b}_1, \boldsymbol{b}_2, \boldsymbol{b}_3\}$ define the orthonormal body-fixed frame, $\mathcal{F}_{\mathrm{B}}$, centered at the aircraft center of gravity (CG) with $\boldsymbol{b}_1$ out the front of the aircraft, $\boldsymbol{b}_2$ out of the right-hand side, and $\boldsymbol{b}_3$ out of the bottom completing the right-hand rule. The position of the body frame with respect to the inertial frame is given by the vector $\boldsymbol{q} = [x\ y\ z]^{\mathsf{T}}$. The attitude of the aircraft is given by the rotation matrix, $\boldsymbol{R}_{\mathrm{IB}}$, that maps free vectors from $\mathcal{F}_{\mathrm{B}}$ to $\mathcal{F}_{\mathrm{I}}$. Consider the Euler angle parameterization

$$\boldsymbol{R}_{\mathrm{IB}} = e^{\boldsymbol{S}(\boldsymbol{e}_3)\psi} e^{\boldsymbol{S}(\boldsymbol{e}_2)\theta} e^{\boldsymbol{S}(\boldsymbol{e}_1)\phi} \tag{1}$$

where ϕ, θ, and ψ are the roll, pitch, and yaw angles of the aircraft, respectively. Here, $\boldsymbol{e}_1 = [1\ 0\ 0]^{\mathsf{T}}$, etc., and $\boldsymbol{S}(\cdot)$ is the skew-symmetric cross product equivalent matrix satisfying $\boldsymbol{S}(\boldsymbol{a})\boldsymbol{b} = \boldsymbol{a} \times \boldsymbol{b}$. Let $\boldsymbol{v} = [u\ v\ w]^{\mathsf{T}}$ and $\boldsymbol{\omega} = [p\ q\ r]^{\mathsf{T}}$ be the translational and rotational velocity of the aircraft with respect to $\mathcal{F}_{\mathrm{I}}$ expressed in $\mathcal{F}_{\mathrm{B}}$, respectively. Thus, we have the kinematic equations of motion

$$\dot{\boldsymbol{q}} = \boldsymbol{R}_{\mathrm{IB}} \boldsymbol{v} \tag{2a}$$

$$\dot{\boldsymbol{R}}_{\mathrm{IB}} = \boldsymbol{R}_{\mathrm{IB}} \boldsymbol{S}(\boldsymbol{\omega}) \tag{2b}$$

With $\boldsymbol{\Theta} := [\phi \;\; \theta \;\; \psi]^\mathsf{T}$, Eq. (2b) becomes

$$\dot{\boldsymbol{\Theta}} = \underbrace{\begin{bmatrix} 1 & \sin\phi\tan\theta & \cos\phi\tan\theta \\ 0 & \cos\phi & -\sin\phi \\ 0 & \sin\phi\sec\theta & \cos\phi\sec\theta \end{bmatrix}}_{\boldsymbol{L}_{\mathrm{IB}}} \begin{bmatrix} p \\ q \\ r \end{bmatrix} \tag{3}$$

Alternatively, we may parameterize the attitude of the aircraft using the heading vector, $\boldsymbol{\lambda} = \boldsymbol{R}_{\mathrm{IB}}^\mathsf{T}\boldsymbol{e}_1$, and tilt vector, $\boldsymbol{\zeta} = \boldsymbol{R}_{\mathrm{IB}}^\mathsf{T}\boldsymbol{e}_3$, as done in [17–20]. Then, the attitude kinematics become

$$\dot{\boldsymbol{\lambda}} = \boldsymbol{\lambda} \times \boldsymbol{\omega} \tag{4a}$$

$$\dot{\boldsymbol{\zeta}} = \boldsymbol{\zeta} \times \boldsymbol{\omega} \tag{4b}$$

where the rotation matrix, $\boldsymbol{R}_{\mathrm{IB}}$, may be reconstructed as

$$\boldsymbol{R}_{\mathrm{IB}}(\boldsymbol{\lambda}, \boldsymbol{\zeta}) = \begin{bmatrix} \boldsymbol{\lambda} & \boldsymbol{S}(\boldsymbol{\zeta})\boldsymbol{\lambda} & \boldsymbol{\zeta} \end{bmatrix}^\mathsf{T} \tag{5}$$

Let us represent the aerodynamic force and moment acting on the aircraft expressed in $\mathcal{F}_{\mathrm{B}}$ as $\boldsymbol{F} = [X \; Y \; Z]^\mathsf{T}$ and $\boldsymbol{M} = [\mathcal{L} \; \mathcal{M} \; \mathcal{N}]^\mathsf{T}$. Define $\boldsymbol{p} = m\boldsymbol{v}$ to be the linear momentum of the aircraft and $\boldsymbol{h} = \boldsymbol{I}\boldsymbol{\omega}$ to be the angular momentum vector about the center of mass, both expressed in $\mathcal{F}_{\mathrm{B}}$. Here, $\boldsymbol{I}$ is the moment of inertia matrix about the center of mass in $\mathcal{F}_{\mathrm{B}}$. Altogether, the equations of motion in still air are

$$\dot{\boldsymbol{q}} = \boldsymbol{R}_{\mathrm{IB}}(\boldsymbol{\lambda}, \boldsymbol{\zeta})\boldsymbol{v} \tag{6a}$$

$$\dot{\boldsymbol{\lambda}} = \boldsymbol{\lambda} \times \boldsymbol{\omega} \tag{6b}$$

$$\dot{\boldsymbol{\zeta}} = \boldsymbol{\zeta} \times \boldsymbol{\omega} \tag{6c}$$

$$\dot{\boldsymbol{p}} = \boldsymbol{p} \times \boldsymbol{\omega} + mg\boldsymbol{\zeta} + \boldsymbol{F} \tag{6d}$$

$$\dot{\boldsymbol{h}} = \boldsymbol{h} \times \boldsymbol{\omega} + \boldsymbol{M} \tag{6e}$$

where we have mixed momentum and velocity notation.

B. Dynamics in a Wind Field

Before addressing the aerodynamic forces and moments, consider the aircraft's motion in wind. In general and independent of the aircraft's motion, the wind is a time-varying vector field, $\boldsymbol{W} : \mathbb{R}^3 \times \mathbb{R} \to \mathbb{R}^3$, defined in the inertial frame. Let the instantaneous wind vector as experienced by the aircraft be

$$\boldsymbol{w}(t) = \boldsymbol{W}(\boldsymbol{q}(t), t) \tag{7}$$

The *apparent wind*, $\boldsymbol{w}$, is the part of the aircraft state defined by evaluating the wind field, $\boldsymbol{W}$, at the aircraft's position, $\boldsymbol{q}$, at time t. Using the chain rule, the time derivative of $\boldsymbol{w}$ is

$$\frac{\mathrm{d}\boldsymbol{w}}{\mathrm{d}t} = \frac{\partial \boldsymbol{W}}{\partial t}(\boldsymbol{q}, t) + \nabla \boldsymbol{W}(\boldsymbol{q}, t)\frac{\mathrm{d}\boldsymbol{q}}{\mathrm{d}t} \tag{8}$$

in agreement with [12]. Note the we have arrived at Eq. (8) under the implicit assumption that the vehicle does not affect the flow field in which it is immersed. When the aircraft's velocity through a wind field is significantly faster than the time rate of change of the eddies (such as for fixed-wing aircraft), we can make a *frozen turbulence* assumption [21], meaning $\frac{\partial \boldsymbol{W}}{\partial t}(\boldsymbol{q}, t) = \boldsymbol{0}$. Therefore, Eq. (8) becomes

$$\dot{\boldsymbol{w}} = \nabla \boldsymbol{W}(\boldsymbol{q})\dot{\boldsymbol{q}} \tag{9}$$

Since we cannot deterministically model the gradient of the wind field evaluated along the aircraft's path, $\nabla \boldsymbol{W}(\boldsymbol{q})$, the apparent wind is typically modeled as Brownian motion: "$\dot{\boldsymbol{w}} =$ noise." Conversely, if the aircraft is not moving, the eddies are being convected over the aircraft by the bulk flow. Therefore, $\dot{\boldsymbol{w}}$ would instead become

$$\dot{\boldsymbol{w}} = \frac{\partial \boldsymbol{W}}{\partial t}(t) \tag{10}$$

where $\frac{\partial \boldsymbol{W}}{\partial t}$ is the time rate of change of wind velocity at the aircraft's position due to the convected eddies. This process is also considered random, leading to the same Brownian motion model.

In addition to the wind velocity, one may also want to estimate the gradient of the wind field. Independent of the air vehicle's geometry, we may define the gradient of the wind in the body frame as

$$\boldsymbol{\Phi}_W := \boldsymbol{R}_{\mathrm{IB}}^{\mathsf{T}} \nabla \boldsymbol{W} \boldsymbol{R}_{\mathrm{IB}} \tag{11}$$

Then, the body-frame gradient of the wind field can be decomposed into its symmetric and skew-symmetric parts [22],

$$\boldsymbol{\Phi}_W = \frac{1}{2}(\boldsymbol{\Phi}_W + \boldsymbol{\Phi}_W^{\mathsf{T}}) + \frac{1}{2}(\boldsymbol{\Phi}_W - \boldsymbol{\Phi}_W^{\mathsf{T}}) \tag{12}$$

The *angular velocity of the wind* in the body frame, $\boldsymbol{\omega}_W$, is defined by

$$\boldsymbol{\omega}_W := \frac{1}{2}(\boldsymbol{\Phi}_W - \boldsymbol{\Phi}_W^{\mathsf{T}})^{\vee} \tag{13}$$

where $(\boldsymbol{S}(\boldsymbol{a}))^{\vee} = \boldsymbol{a}$.

While $\boldsymbol{\omega}_W$ is in fact the vector field of body-frame wind angular velocity, each aircraft will experience a different gradient based on its geometry. In the case of fixed-wing aircraft, for example, Etkin [23] presents that the only non-negligible gradients due to the apparent wind in the body frame, $\boldsymbol{w}_b = [u_w \; v_w \; w_w]^{\mathsf{T}} = \boldsymbol{R}_{\mathrm{IB}}^{\mathsf{T}} \boldsymbol{w}$, are

$$p_w = \frac{\partial w_w}{\partial y} \qquad q_w = -\frac{\partial w_w}{\partial x} \qquad r_w = \frac{\partial v_w}{\partial x} \tag{14}$$

Here, x, y, and z are coordinates for $\mathcal{F}_{\mathrm{B}}$. Eq. (14) reflects an assumption that

a) the body-longitudinal component of wind is constant/uniform over the entire aircraft,
b) the body-lateral component of wind varies only along the aircraft's length, and
c) the body-vertical component of wind varies only along the aircraft's length and span.

The vector $\boldsymbol{\omega}_w = [p_w \; q_w \; r_w]^{\mathsf{T}}$ as defined by Eq. (14) is called the *apparent angular velocity of the wind*. Therefore, a fixed-wing aircraft experiences the body frame wind gradient

$$\boldsymbol{\Phi}_w := \begin{bmatrix} 0 & 0 & 0 \\ r_w & 0 & 0 \\ -q_w & p_w & 0 \end{bmatrix} \tag{15}$$

For other types of aircraft, $\boldsymbol{\Phi}_w$ may take on a different structure, and $\boldsymbol{\omega}_w$ will be defined accordingly.

If one wants to estimate gradients of the wind, a dynamic model for $\boldsymbol{\omega}_w$ must be obtained. In general, we can take the time derivative of Eq. (11) to obtain

$$\dot{\boldsymbol{\Phi}}_W = \dot{\boldsymbol{R}}_{\mathrm{IB}}^{\mathsf{T}} \nabla \boldsymbol{W}(\boldsymbol{q},t) \boldsymbol{R}_{\mathrm{IB}} + \boldsymbol{R}_{\mathrm{IB}}^{\mathsf{T}} \frac{\mathrm{d}}{\mathrm{d}t} \left(\nabla \boldsymbol{W}(\boldsymbol{q},t) \right) \boldsymbol{R}_{\mathrm{IB}} + \boldsymbol{R}_{\mathrm{IB}}^{\mathsf{T}} \nabla \boldsymbol{W}(\boldsymbol{q},t) \dot{\boldsymbol{R}}_{\mathrm{IB}} \tag{16}$$

which requires computing the time rate of change of the wind gradient along the path of the aircraft, $\frac{\mathrm{d}}{\mathrm{d}t} \left(\nabla \boldsymbol{W}(\boldsymbol{q},t) \right)$. This cannot be deterministically modeled due to the randomness of turbulence and is thus treated as noise. Since $\boldsymbol{\Phi}_w$ is the body frame gradient experienced by the aircraft, we define $\dot{\boldsymbol{\omega}}_w$ using the respective elements of the matrix equation in Eq. (16) according to the structure of $\boldsymbol{\Phi}_w$. Then using Eqs. (2b) and (3) in Eq. (16), we obtain

$$\dot{\boldsymbol{\omega}}_w = \left. \frac{\partial \boldsymbol{\omega}_W}{\partial \boldsymbol{\Theta}} \boldsymbol{L}_{\mathrm{IB}} \boldsymbol{\omega} \right|_{\nabla \boldsymbol{W} = \boldsymbol{R}_{\mathrm{IB}} \boldsymbol{\Phi}_w \boldsymbol{R}_{\mathrm{IB}}^{\mathsf{T}}} + \text{noise} \tag{17}$$

where $\frac{\partial \boldsymbol{\omega}_W}{\partial \boldsymbol{\Theta}}$ is computed using the right-hand side of Eq. (11). In general, this expression may be quite complicated since it depends on the structure of $\boldsymbol{\Phi}_w$. For a fixed-wing aircraft, however, it simplifies to

$$\dot{\boldsymbol{\omega}}_w = \begin{bmatrix} r q_w \\ p r_w - r p_w \\ -p q_w \end{bmatrix} + \text{noise} \tag{18}$$

We recognize the aerodynamic forces and moments only depend on the air-relative velocity. Therefore, $\boldsymbol{F} = \boldsymbol{F}(\boldsymbol{v}_\mathrm{r}, \boldsymbol{\omega}_\mathrm{r}, \boldsymbol{u})$ and $\boldsymbol{M} = \boldsymbol{M}(\boldsymbol{v}_\mathrm{r}, \boldsymbol{\omega}_\mathrm{r}, \boldsymbol{u})$, where $\boldsymbol{u}$ are the aircraft control inputs and

$$\boldsymbol{v}_\mathrm{r} = \boldsymbol{v} - \boldsymbol{R}_\mathrm{IB}^\mathsf{T}\boldsymbol{w} \tag{19a}$$

$$\boldsymbol{\omega}_\mathrm{r} = \boldsymbol{\omega} - \boldsymbol{\omega}_w \tag{19b}$$

Taking the time derivative of Eq. (19a) gives

$$\begin{aligned}\dot{\boldsymbol{v}}_\mathrm{r} &= \dot{\boldsymbol{v}} - \dot{\boldsymbol{R}}_\mathrm{IB}^\mathsf{T}\boldsymbol{w} - \boldsymbol{R}_\mathrm{IB}^\mathsf{T}\dot{\boldsymbol{w}} \\ &= \boldsymbol{v}\times\boldsymbol{\omega} + g\boldsymbol{R}_\mathrm{IB}^\mathsf{T}\boldsymbol{e}_3 + \frac{1}{m}\boldsymbol{F}(\boldsymbol{v}_\mathrm{r}, \boldsymbol{\omega}_\mathrm{r}, \boldsymbol{u}) + \boldsymbol{R}_\mathrm{IB}^\mathsf{T}\boldsymbol{S}(\boldsymbol{\omega})\boldsymbol{w} - \boldsymbol{R}_\mathrm{IB}^\mathsf{T}\dot{\boldsymbol{w}}\end{aligned} \tag{20}$$

Noting that $\boldsymbol{R}_\mathrm{IB}^\mathsf{T}\boldsymbol{S}(\boldsymbol{\omega})\boldsymbol{w} = -\boldsymbol{R}_\mathrm{IB}^\mathsf{T}\boldsymbol{w}\times\boldsymbol{\omega}$ and making use of Eq. (19a), we have

$$\begin{aligned}\dot{\boldsymbol{v}}_\mathrm{r} &= (\boldsymbol{v}_\mathrm{r} + \boldsymbol{R}_\mathrm{IB}^\mathsf{T}\boldsymbol{w})\times\boldsymbol{\omega} + g\boldsymbol{R}_\mathrm{IB}^\mathsf{T}\boldsymbol{e}_3 + \frac{1}{m}\boldsymbol{F}(\boldsymbol{v}_\mathrm{r}, \boldsymbol{\omega}_\mathrm{r}, \boldsymbol{\delta}) - \boldsymbol{R}_\mathrm{IB}^\mathsf{T}\boldsymbol{w}\times\boldsymbol{\omega} - \boldsymbol{R}_\mathrm{IB}^\mathsf{T}\dot{\boldsymbol{w}} \\ &= \boldsymbol{v}_\mathrm{r}\times\boldsymbol{\omega} + g\boldsymbol{R}_\mathrm{IB}^\mathsf{T}\boldsymbol{e}_3 + \frac{1}{m}\boldsymbol{F}(\boldsymbol{v}_\mathrm{r}, \boldsymbol{\omega}_\mathrm{r}, \boldsymbol{u}) - \boldsymbol{R}_\mathrm{IB}^\mathsf{T}\dot{\boldsymbol{w}}\end{aligned} \tag{21}$$

Here we have chosen to use variables $\boldsymbol{v}_\mathrm{r}$ and $\boldsymbol{w}$, but any pair of vectors from the wind triangle relation Eq. (19a) could be used. While we have used relative velocity $\boldsymbol{v}_\mathrm{r}$ for translation, we choose the angular velocity states $\boldsymbol{\omega}$ and $\boldsymbol{\omega}_w$ because typically $\boldsymbol{\omega}$ is directly measurable. Using $\dot{\boldsymbol{w}}$ as given by Eq. (8) along with $\dot{\boldsymbol{q}}$ from Eq. (2a), we obtain

$$\begin{aligned}\dot{\boldsymbol{v}}_\mathrm{r} &= \boldsymbol{v}_\mathrm{r}\times\boldsymbol{\omega} + g\boldsymbol{R}_\mathrm{IB}^\mathsf{T}\boldsymbol{e}_3 + \frac{1}{m}\boldsymbol{F}(\boldsymbol{v}_\mathrm{r}, \boldsymbol{\omega}_\mathrm{r}, \boldsymbol{u}) - \boldsymbol{R}_\mathrm{IB}^\mathsf{T}\nabla\boldsymbol{W}\left(\boldsymbol{R}_\mathrm{IB}\boldsymbol{v}_\mathrm{r} + \boldsymbol{w}\right) - \boldsymbol{R}_\mathrm{IB}^\mathsf{T}\frac{\partial\boldsymbol{W}}{\partial t} \\ &= \boldsymbol{v}_\mathrm{r}\times\boldsymbol{\omega} + g\boldsymbol{R}_\mathrm{IB}^\mathsf{T}\boldsymbol{e}_3 + \frac{1}{m}\boldsymbol{F}(\boldsymbol{v}_\mathrm{r}, \boldsymbol{\omega}_\mathrm{r}, \boldsymbol{u}) - \boldsymbol{\Phi}_W\left(\boldsymbol{v}_\mathrm{r} + \boldsymbol{R}_\mathrm{IB}^\mathsf{T}\boldsymbol{w}\right) - \boldsymbol{R}_\mathrm{IB}^\mathsf{T}\frac{\partial\boldsymbol{W}}{\partial t}\end{aligned} \tag{22}$$

Altogether, the equations of motion of an aircraft in a non-uniform, time-varying wind field are

$$\dot{\boldsymbol{q}} = \boldsymbol{R}_\mathrm{IB}\boldsymbol{v}_\mathrm{r} + \boldsymbol{w} \tag{23a}$$

$$\dot{\boldsymbol{\lambda}} = \boldsymbol{\lambda}\times\boldsymbol{\omega} \tag{23b}$$

$$\dot{\boldsymbol{\zeta}} = \boldsymbol{\zeta}\times\boldsymbol{\omega} \tag{23c}$$

$$\dot{\boldsymbol{v}}_\mathrm{r} = \boldsymbol{v}_\mathrm{r}\times\boldsymbol{\omega} + g\boldsymbol{\zeta} + \frac{1}{m}\boldsymbol{F}(\boldsymbol{v}_\mathrm{r}, \boldsymbol{\omega}_\mathrm{r}, \boldsymbol{u}) - \boldsymbol{\Phi}_W(\boldsymbol{v}_\mathrm{r} + \boldsymbol{R}_\mathrm{IB}^\mathsf{T}\boldsymbol{w}) - \boldsymbol{R}_\mathrm{IB}^\mathsf{T}\frac{\partial\boldsymbol{W}}{\partial t} \tag{23d}$$

$$\dot{\boldsymbol{w}} = \boldsymbol{R}_\mathrm{IB}\boldsymbol{\Phi}_W\left(\boldsymbol{v}_\mathrm{r} + \boldsymbol{R}_\mathrm{IB}^\mathsf{T}\boldsymbol{w}\right) + \frac{\partial\boldsymbol{W}}{\partial t} \tag{23e}$$

$$\dot{\boldsymbol{\omega}} = \boldsymbol{I}^{-1}\left(\boldsymbol{I}\boldsymbol{\omega}\times\boldsymbol{\omega} + \boldsymbol{M}(\boldsymbol{v}_\mathrm{r}, \boldsymbol{\omega}_\mathrm{r}, \boldsymbol{u})\right) \tag{23f}$$

$$\dot{\boldsymbol{\omega}}_w = \left.\frac{\partial\boldsymbol{\omega}_W}{\partial\boldsymbol{\Theta}}\boldsymbol{L}_\mathrm{IB}\boldsymbol{\omega}\right|_{\nabla\boldsymbol{W}=\boldsymbol{R}_\mathrm{IB}\boldsymbol{\Phi}_w\boldsymbol{R}_\mathrm{IB}^\mathsf{T}} + \text{noise} \tag{23g}$$

C. Simplified Dynamics for Passivity-Based Observer Design

In order to simplify the nonlinear observer design, consider the following two assumptions.

Assumption 1. *The wind field is uniform and steady. As a consequence,* $\boldsymbol{\Phi}_W = \boldsymbol{0} \implies \boldsymbol{\omega}_w \equiv \boldsymbol{0}$ *and* $\dot{\boldsymbol{w}} = \boldsymbol{0}$.

Assumption 2. *For the purpose of estimation, the aircraft's aerodynamics evolve on a time scale significantly slower than the observer dynamics such that at any point in time, the aerodynamics may be taken to be linear in* $\boldsymbol{v}_\mathrm{r}$ *and* $\boldsymbol{\omega}$ *with*

$$\boldsymbol{F} = \boldsymbol{F}_v\boldsymbol{v}_\mathrm{r} + \boldsymbol{F}_\omega\boldsymbol{\omega} + \boldsymbol{F}_0(\boldsymbol{u}) \tag{24}$$

$$\boldsymbol{M} = \boldsymbol{M}_v\boldsymbol{v}_\mathrm{r} + \boldsymbol{M}_\omega\boldsymbol{\omega} + \boldsymbol{M}_0(\boldsymbol{u}) \tag{25}$$

Note that in Eqs. (24) and (25), $\boldsymbol{F}_v$, $\boldsymbol{M}_v$, $\boldsymbol{F}_\omega$, and $\boldsymbol{M}_\omega$ are matrices, while $\boldsymbol{F}_0$ and $\boldsymbol{M}_0$ are vector-valued. The effect of Assumption 2 is that the quantities $\boldsymbol{F}_{(\cdot)}$ and $\boldsymbol{M}_{(\cdot)}$ are treated as slowly-varying parameters. For example, the values

of $\boldsymbol{F}_{(\cdot)}$ and $\boldsymbol{M}_{(\cdot)}$ for a fixed-wing aircraft generally depend on dynamic pressure, $\frac{1}{2}\rho \boldsymbol{v}_{\mathrm{r}}^{\mathsf{T}}\boldsymbol{v}_{\mathrm{r}}$, which we can assume to vary slowly compared to the observer dynamics. The plant dynamics for which we want to design a nonlinear observer are

$$\dot{\boldsymbol{q}} = \boldsymbol{R}_{\mathrm{IB}}\boldsymbol{v}_{\mathrm{r}} + \boldsymbol{w} \tag{26a}$$

$$\dot{\boldsymbol{\lambda}} = \boldsymbol{\lambda} \times \boldsymbol{\omega} \tag{26b}$$

$$\dot{\boldsymbol{\zeta}} = \boldsymbol{\zeta} \times \boldsymbol{\omega} \tag{26c}$$

$$\dot{\boldsymbol{\omega}} = \boldsymbol{I}^{-1}\big(\boldsymbol{I}\boldsymbol{\omega} \times \boldsymbol{\omega} + \boldsymbol{M}_v\boldsymbol{v}_{\mathrm{r}} + \boldsymbol{M}_\omega\boldsymbol{\omega} + \boldsymbol{M}_0(\boldsymbol{u})\big) \tag{26d}$$

$$\dot{\boldsymbol{v}}_{\mathrm{r}} = \boldsymbol{v}_{\mathrm{r}} \times \boldsymbol{\omega} + g\boldsymbol{\zeta} + \frac{1}{m}\big(\boldsymbol{F}_v\boldsymbol{v}_{\mathrm{r}} + \boldsymbol{F}_\omega\boldsymbol{\omega} + \boldsymbol{F}_0(\boldsymbol{u})\big) \tag{26e}$$

$$\dot{\boldsymbol{w}} = \boldsymbol{0} \tag{26f}$$

The state of this system is defined by the vector $\boldsymbol{x} = [\boldsymbol{q}^{\mathsf{T}}\ \boldsymbol{\lambda}^{\mathsf{T}}\ \boldsymbol{\zeta}^{\mathsf{T}}\ \boldsymbol{\omega}^{\mathsf{T}}\ \boldsymbol{v}_{\mathrm{r}}^{\mathsf{T}}\ \boldsymbol{w}^{\mathsf{T}}]^{\mathsf{T}} \in \mathbb{R}^n$ with dynamics $\dot{\boldsymbol{x}} = \boldsymbol{f}(\boldsymbol{x}, \boldsymbol{u})$, where the input vector, $\boldsymbol{u} \in \mathcal{U} \subset \mathbb{R}^m$, is known.

It is often the case that aircraft are instrumented with an accelerometer, gyroscope, magnetometer, and inertial positioning system (i.e. vision-based or GNSS) such that position, attitude, and angular velocity measurements can be readily obtained with negligible noise from a low-level estimation algorithm. Thus, we make the following assumption.

Assumption 3. *The aircraft position, attitude, and angular velocity are measured without noise.*

Therefore, let

$$\boldsymbol{y} = \boldsymbol{x}_1 := [\boldsymbol{q}^{\mathsf{T}}\ \boldsymbol{\lambda}^{\mathsf{T}}\ \boldsymbol{\zeta}^{\mathsf{T}}\ \boldsymbol{\omega}^{\mathsf{T}}]^{\mathsf{T}} \in \mathbb{R}^p \tag{27}$$

With $\boldsymbol{x} = [\boldsymbol{x}_1^{\mathsf{T}}\ \boldsymbol{x}_2^{\mathsf{T}}]^{\mathsf{T}}$ where $\boldsymbol{x}_2 = [\boldsymbol{v}_{\mathrm{r}}^{\mathsf{T}}\ \boldsymbol{w}^{\mathsf{T}}]^{\mathsf{T}} \in \mathbb{R}^{n-p}$, the dynamics are written as

$$\dot{\boldsymbol{x}}_1 = \boldsymbol{f}_1(\boldsymbol{x}_1, \boldsymbol{x}_2, \boldsymbol{u}) \tag{28a}$$

$$\dot{\boldsymbol{x}}_2 = \boldsymbol{f}_2(\boldsymbol{x}_1, \boldsymbol{x}_2, \boldsymbol{u}) \tag{28b}$$

where $\boldsymbol{f}_1$ contains the right-hand sides of Eqs. (26a)–(26d) and $\boldsymbol{f}_2$ contains the right-hand sides of Eqs. (26e)–(26f).

III. Observer Design via Passivation of Error Dynamics

We use the passivity-based observer described in [16]. The approach involves determining an output injection term $\boldsymbol{v}$ and a corresponding observer gain matrix $\boldsymbol{L}$ that render the state observation error dynamics strictly passive.

To begin, we recall that a dynamical system $\dot{\boldsymbol{x}} = \boldsymbol{f}(\boldsymbol{x}) + \boldsymbol{g}(\boldsymbol{x})\boldsymbol{u}$ with output $\boldsymbol{y} = \boldsymbol{h}(\boldsymbol{x})$ is *dissipative* with respect to the *supply rate* $w(\boldsymbol{u}, \boldsymbol{y})$ if there exists a non-negative smooth *storage function* $W(\boldsymbol{x})$ such that

$$W(\boldsymbol{x}(t)) - W(\boldsymbol{x}(0)) \leq \int_0^t w(\boldsymbol{u}(\tau), \boldsymbol{y}(\tau))\,\mathrm{d}\tau \tag{29}$$

The system is considered *passive* if it is dissipative with respect to the supply rate $w(\boldsymbol{u}, \boldsymbol{y}) = \boldsymbol{u}^{\mathsf{T}}\boldsymbol{y}$. It is *strictly passive* if there also exists a positive definite function ϕ such that the system is dissipative with respect to $w(\boldsymbol{u}, \boldsymbol{y}) = \boldsymbol{u}^{\mathsf{T}}\boldsymbol{y} - \phi$. Passive systems exhibit many desirable properties. For example, pure negative output feedback of a zero-state detectable, passive system asymptotically stabilizes the origin. This property among others is described in the seminal work of [24], where the authors also develop the conditions under which a system can be rendered passive by state feedback. In [25], these conditions were extended to output feedback passivation. Output feedback passivation was used in the passivity-based observer design approach described in [15, 16] for systems where only some of the states are available for feedback.

Here, we review the passivity-based observer design method detailed in [16]. Consider the Luenberger-like observer

$$\dot{\hat{\boldsymbol{x}}}_1 = \boldsymbol{f}_1(\hat{\boldsymbol{x}}_1, \hat{\boldsymbol{x}}_2, \boldsymbol{u}) + \boldsymbol{L}_1\boldsymbol{v}(\hat{\boldsymbol{x}}, \boldsymbol{y}, \boldsymbol{u}) \tag{30a}$$

$$\dot{\hat{\boldsymbol{x}}}_2 = \boldsymbol{f}_2(\hat{\boldsymbol{x}}_1, \hat{\boldsymbol{x}}_2, \boldsymbol{u}) + \boldsymbol{L}_2\boldsymbol{v}(\hat{\boldsymbol{x}}, \boldsymbol{y}, \boldsymbol{u}) \tag{30b}$$

with the nonlinear output injection term

$$\boldsymbol{v}(\hat{\boldsymbol{x}}, \boldsymbol{y}, \boldsymbol{u}) = -k(\hat{\boldsymbol{x}}, \boldsymbol{y}, \boldsymbol{u})\boldsymbol{y}_{\mathrm{p}} + \boldsymbol{v}_{\mathrm{p}} \tag{31}$$

where the output error $\boldsymbol{y}_\mathrm{p} = \hat{\boldsymbol{y}} - \boldsymbol{y}$ will become the passive output corresponding to the passive input $\boldsymbol{v}_\mathrm{p}$ – a dummy input – for the observer dynamics. Note that the observer formulation involves two gains – a *constant* gain $\boldsymbol{L} = [\boldsymbol{L}_1^T \ \boldsymbol{L}_2^T]^T$ and scalar gain *function* k. In Section IV, we will generalize the approach by allowing the scalar gain function, k, to be a matrix-valued function, $\boldsymbol{K}$, and allowing the matrix $\boldsymbol{L}_2$ to depend on measurements as in [26–28]. Define the estimate error as

$$\tilde{\boldsymbol{x}} := \hat{\boldsymbol{x}} - \boldsymbol{x} \tag{32}$$

and consider the notation

$$\tilde{\boldsymbol{f}}(\tilde{\boldsymbol{x}}; \boldsymbol{x}; \boldsymbol{u}) := \boldsymbol{f}(\tilde{\boldsymbol{x}} + \boldsymbol{x}, \boldsymbol{u}) - \boldsymbol{f}(\boldsymbol{x}, \boldsymbol{u}) \tag{33}$$

Then, the state estimate error dynamics are

$$\dot{\tilde{\boldsymbol{x}}}_1 = \tilde{\boldsymbol{f}}_1(\tilde{\boldsymbol{x}}_1, \tilde{\boldsymbol{x}}_2; \boldsymbol{x}_1, \boldsymbol{x}_2; \boldsymbol{u}) + \boldsymbol{L}_1 \boldsymbol{v}(\hat{\boldsymbol{x}}, \boldsymbol{y}, \boldsymbol{u}) \tag{34a}$$

$$\dot{\tilde{\boldsymbol{x}}}_2 = \tilde{\boldsymbol{f}}_2(\tilde{\boldsymbol{x}}_1, \tilde{\boldsymbol{x}}_2; \boldsymbol{x}_1, \boldsymbol{x}_2; \boldsymbol{u}) + \boldsymbol{L}_2 \boldsymbol{v}(\hat{\boldsymbol{x}}, \boldsymbol{y}, \boldsymbol{u}) \tag{34b}$$

The observer design involves two main steps. First, with $\boldsymbol{y}_\mathrm{p}$ viewed as the output, a proper Lyapunov function $V^*(\tilde{\boldsymbol{x}}_2, \boldsymbol{x})$ and a positive definite function φ^* are found that prove the error system in Eq. (34) augmented with the plant dynamics is globally minimum phase with respect to the manifold

$$\mathcal{M} = \{(\tilde{\boldsymbol{x}}, \boldsymbol{x}) \mid \tilde{\boldsymbol{x}} = \boldsymbol{0}\} \tag{35}$$

with

$$\dot{V}^* \leq -\varphi^*(\|\tilde{\boldsymbol{x}}_2\|) \tag{36}$$

This step can be thought of like the first step in integrator backstepping, where one stabilizes a subsystem using a state variable as an artificial input [29], ensuring the unmeasured state estimates asymptotically approach their true values when the measurable states are perfectly known. Second, non-negative functions φ_1 and φ_2 are determined such that

$$\begin{aligned}\left| \frac{\partial V^*}{\partial \tilde{\boldsymbol{x}}_2} [\tilde{\boldsymbol{f}}_2 - \boldsymbol{L}_2 \boldsymbol{L}_1^{-1} \tilde{\boldsymbol{f}}_1](\tilde{\boldsymbol{x}}_1, \boldsymbol{L}_2 \boldsymbol{L}_1^{-1} \tilde{\boldsymbol{x}}_1; \boldsymbol{x}_1, \hat{\boldsymbol{x}}_2; \boldsymbol{u}) + \tilde{\boldsymbol{x}}_1 \boldsymbol{L}_1^{-1} \tilde{\boldsymbol{f}}_1(\tilde{\boldsymbol{x}}_1, \tilde{\boldsymbol{x}}_2 + \boldsymbol{L}_2 \boldsymbol{L}_1^{-1} \tilde{\boldsymbol{x}}_1; \boldsymbol{x}_1, \hat{\boldsymbol{x}}_2 - \tilde{\boldsymbol{x}}_2; \boldsymbol{u}) \right| \\ \leq \varphi_1(\tilde{\boldsymbol{x}}_1, \boldsymbol{x}_1, \hat{\boldsymbol{x}}_2, \boldsymbol{u}) \|\tilde{\boldsymbol{x}}_1\|^2 + \varphi_2(\tilde{\boldsymbol{x}}_1, \boldsymbol{x}_1, \hat{\boldsymbol{x}}_2, \boldsymbol{u}) \sqrt{\varphi^*(\|\tilde{\boldsymbol{x}}_2\|)} \|\tilde{\boldsymbol{x}}_1\|\end{aligned} \tag{37}$$

In this expression, parentheses contain arguments for all functions in square brackets. The requirement that there exist these *bounding functions* comes from the sufficient conditions for output feedback passivation developed in [25]. It essentially ensures the coupling between the output dynamics ($\dot{\tilde{\boldsymbol{x}}}_1$) and the unmeasurable dynamics ($\dot{\tilde{\boldsymbol{x}}}_2$) preserves strict passivity from $\boldsymbol{v}_\mathrm{p}$ to $\boldsymbol{y}_\mathrm{p}$, which is a result of the following.

Theorem 1 (Theorem 2 in [16])**.** *Suppose the Lyapunov function V^* proves the error dynamics augmented with the system dynamics are (globally) minimum phase with respect to $\mathcal{M}$. Also suppose there exist function φ_1 and φ_2 such that Eq. (37) holds. Then, the feedback*

$$\boldsymbol{v} = -k(\hat{\boldsymbol{x}}, \boldsymbol{y}) \boldsymbol{y}_\mathrm{p} + \boldsymbol{v}_\mathrm{p} \tag{38}$$

with

$$k(\hat{\boldsymbol{x}}, \boldsymbol{y}) = \varepsilon + \varphi_1(\hat{\boldsymbol{x}}_1 - \boldsymbol{y}, \boldsymbol{y}, \hat{\boldsymbol{x}}_2 - \boldsymbol{L}_2 \boldsymbol{L}_1^{-1}(\hat{\boldsymbol{x}}_1 - \boldsymbol{y})) + \varphi_2^2(\hat{\boldsymbol{x}}_1 - \boldsymbol{y}, \boldsymbol{y}, \hat{\boldsymbol{x}}_2 - \boldsymbol{L}_2 \boldsymbol{L}_1^{-1}(\hat{\boldsymbol{x}}_1 - \boldsymbol{y})), \quad \varepsilon > 0 \tag{39}$$

renders the augmented system strictly passive from $\boldsymbol{v}_\mathrm{p}$ to $\boldsymbol{y}_\mathrm{p}$ with respect to $\mathcal{M}$ with the storage function

$$W = V^*(\tilde{\boldsymbol{x}}_2 - \boldsymbol{L}_2 \boldsymbol{L}_1^{-1} \tilde{\boldsymbol{x}}_1, \boldsymbol{x}) + \frac{1}{2} \tilde{\boldsymbol{x}}_1^\intercal \boldsymbol{L}_1^{-1} \tilde{\boldsymbol{x}}_1 \tag{40}$$

Upon setting $\boldsymbol{v}_\mathrm{p} = \boldsymbol{0}$, $\mathcal{M}$ becomes positively invariant and (globally) asymptotically attractive.

While we do not use this theorem directly, the results in this paper follow its proof.

IV. Passivity-Based Observer Design for Aircraft in Wind

A. Minimum Phase and Relative Degree Sufficient Conditions

Consider the aircraft in wind described compactly by Eq. (28). The state observer takes the form

$$\dot{\hat{\boldsymbol{x}}}_1 = \boldsymbol{f}_1(\hat{\boldsymbol{x}}_1, \hat{\boldsymbol{x}}_2, \boldsymbol{u}) + \boldsymbol{L}_1 \boldsymbol{v} \tag{41a}$$

$$\dot{\hat{\boldsymbol{x}}}_2 = \boldsymbol{f}_2(\hat{\boldsymbol{x}}_1, \hat{\boldsymbol{x}}_2, \boldsymbol{u}) + \boldsymbol{L}_2(\boldsymbol{y}) \boldsymbol{v} \tag{41b}$$

The components of the vector field $\tilde{\boldsymbol{f}}$ appearing in the error dynamics, Eq. (34), are

$$\tilde{\boldsymbol{f}}_{1_q} = \boldsymbol{R}_{\mathrm{IB}}(\tilde{\boldsymbol{\lambda}} + \boldsymbol{\lambda}, \tilde{\boldsymbol{\zeta}} + \boldsymbol{\zeta})(\tilde{\boldsymbol{v}}_{\mathrm{r}} + \boldsymbol{v}_{\mathrm{r}}) - \boldsymbol{R}_{\mathrm{IB}}(\boldsymbol{\lambda}, \boldsymbol{\zeta}) \boldsymbol{v}_{\mathrm{r}} + \tilde{\boldsymbol{w}} \tag{42a}$$

$$\tilde{\boldsymbol{f}}_{1_\lambda} = \boldsymbol{S}(\tilde{\boldsymbol{\lambda}} + \boldsymbol{\lambda})(\tilde{\boldsymbol{\omega}} + \boldsymbol{\omega}) - \boldsymbol{S}(\boldsymbol{\lambda}) \boldsymbol{\omega} \tag{42b}$$

$$\tilde{\boldsymbol{f}}_{1_\zeta} = \boldsymbol{S}(\tilde{\boldsymbol{\zeta}} + \boldsymbol{\zeta})(\tilde{\boldsymbol{\omega}} + \boldsymbol{\omega}) - \boldsymbol{S}(\boldsymbol{\zeta}) \boldsymbol{\omega} \tag{42c}$$

$$\tilde{\boldsymbol{f}}_{1_\omega} = \boldsymbol{I}^{-1}\big(\boldsymbol{S}(\boldsymbol{I}\tilde{\boldsymbol{\omega}} + \boldsymbol{I}\boldsymbol{\omega})(\tilde{\boldsymbol{\omega}} + \boldsymbol{\omega}) - \boldsymbol{S}(\boldsymbol{I}\boldsymbol{\omega})\boldsymbol{\omega} + \boldsymbol{M}_v \tilde{\boldsymbol{v}}_{\mathrm{r}} + \boldsymbol{M}_\omega \tilde{\boldsymbol{\omega}}\big) \tag{42d}$$

$$\tilde{\boldsymbol{f}}_{2_{v_{\mathrm{r}}}} = \boldsymbol{S}(\tilde{\boldsymbol{v}}_{\mathrm{r}} + \boldsymbol{v}_{\mathrm{r}})(\tilde{\boldsymbol{\omega}} + \boldsymbol{\omega}) - \boldsymbol{S}(\boldsymbol{v}_{\mathrm{r}})\boldsymbol{\omega} + g\tilde{\boldsymbol{\zeta}} + \frac{1}{m}\left(\boldsymbol{F}_v \tilde{\boldsymbol{v}}_{\mathrm{r}} + \boldsymbol{F}_\omega \tilde{\boldsymbol{\omega}}\right) \tag{42e}$$

$$\tilde{\boldsymbol{f}}_{2_w} = \boldsymbol{0} \tag{42f}$$

With the error dynamics defined, we now aim to design the observer gain matrix $\boldsymbol{L}$ such that the first condition in Theorem 1 holds, where

$$\boldsymbol{L}_1 = \mathbf{diag}\left(\boldsymbol{L}_{1_q}, \boldsymbol{L}_{1_\lambda}, \boldsymbol{L}_{1_\zeta}, \boldsymbol{L}_{1_\omega}\right) \tag{43a}$$

$$\boldsymbol{L}_2 = \begin{bmatrix} \boldsymbol{L}_{2_{v_r}} \\ \boldsymbol{L}_{2_w} \end{bmatrix} = \begin{bmatrix} \boldsymbol{L}_{2_{v,q}} & \boldsymbol{L}_{2_{v,\lambda}} & \boldsymbol{L}_{2_{v,\zeta}} & \boldsymbol{L}_{2_{v,\omega}} \\ \boldsymbol{L}_{2_{w,q}} & \boldsymbol{L}_{2_{w,\lambda}} & \boldsymbol{L}_{2_{w,\zeta}} & \boldsymbol{L}_{2_{w,\omega}} \end{bmatrix} \tag{43b}$$

That is, we find conditions on $\boldsymbol{L}$ such that a given candidate Lyapunov function proves the error dynamics are minimum phase. Considering the output injection term in Eq. (38), the zero dynamics of the *augmented system* composed of Eqs. (26) and (42) is analyzed in view of the input-output pair $\{\boldsymbol{v}_{\mathrm{p}}, \boldsymbol{y}_{\mathrm{p}}\}$. In general, the *zero dynamics* of the augmented system with respect to $\boldsymbol{y}_{\mathrm{p}}$ exist in some neighborhood $\mathcal{Z} \subseteq \mathbb{R}^n \times \mathbb{R}^n$ about $\tilde{\boldsymbol{x}} = \boldsymbol{0}$ [24] and evolve on

$$\mathcal{Z}^* = \{(\tilde{\boldsymbol{x}}, \boldsymbol{x}) \in \mathcal{Z} \mid \tilde{\boldsymbol{x}}_1 \equiv \boldsymbol{0}\} \tag{44}$$

As discussed in [16], the zero dynamics can can be shown to satisfy

$$\dot{\tilde{\boldsymbol{x}}}_2 = \tilde{\boldsymbol{f}}_2(\boldsymbol{0}, \tilde{\boldsymbol{x}}_2; \boldsymbol{x}_1, \boldsymbol{x}_2; \boldsymbol{u}) - \boldsymbol{L}_2(\boldsymbol{x}_1)\boldsymbol{L}_1^{-1}\tilde{\boldsymbol{f}}_1(\boldsymbol{0}, \tilde{\boldsymbol{x}}_2; \boldsymbol{x}_1, \boldsymbol{x}_2; \boldsymbol{u}) \tag{45a}$$

$$\dot{\boldsymbol{x}} = \boldsymbol{f}(\boldsymbol{x}, \boldsymbol{u}) \tag{45b}$$

Therefore, we must choose $\boldsymbol{L}$ such that $\tilde{\boldsymbol{x}}_2 = \boldsymbol{0}$ is asymptotically stable on $\mathcal{Z}^*$. Here, we see that the global existence of the zero dynamics only requires $\boldsymbol{L}_1$ to be invertible, a condition that also implies the error dynamics have vector relative degree $\{1, \cdots, 1\}$ [25]. For convenience, denote

$$\tilde{\boldsymbol{\phi}}_2(\tilde{\boldsymbol{x}}_1, \tilde{\boldsymbol{x}}_2; \boldsymbol{x}_1, \boldsymbol{x}_2; \boldsymbol{u}) := \tilde{\boldsymbol{f}}_2(\tilde{\boldsymbol{x}}_1, \tilde{\boldsymbol{x}}_2; \boldsymbol{x}_1, \boldsymbol{x}_2; \boldsymbol{u}) - \boldsymbol{L}_2(\boldsymbol{x}_1)\boldsymbol{L}_1^{-1}\tilde{\boldsymbol{f}}_1(\tilde{\boldsymbol{x}}_1, \tilde{\boldsymbol{x}}_2; \boldsymbol{x}_1, \boldsymbol{x}_2; \boldsymbol{u}) \tag{46}$$

$$\implies \tilde{\boldsymbol{\phi}}_2^* := \tilde{\boldsymbol{\phi}}_2(\boldsymbol{0}, \tilde{\boldsymbol{x}}_2; \boldsymbol{x}_1, \boldsymbol{x}_2; \boldsymbol{u}) \tag{47}$$

where $\tilde{\boldsymbol{\phi}}_2^*$ is called the *zero dynamics vector field*. Referring to (43), we compute $\tilde{\boldsymbol{\phi}}_{2_{v_\mathrm{r}}}$ and $\tilde{\boldsymbol{\phi}}_{2_w}$ as

$$\begin{aligned}\tilde{\boldsymbol{\phi}}_{2_{v_\mathrm{r}}}(\tilde{\boldsymbol{x}}_1,\tilde{\boldsymbol{x}}_2;\boldsymbol{x}_1,\boldsymbol{x}_2;\boldsymbol{u}) &= \boldsymbol{S}(\tilde{\boldsymbol{v}}_\mathrm{r}+\boldsymbol{v}_\mathrm{r})(\tilde{\boldsymbol{\omega}}+\boldsymbol{\omega}) - \boldsymbol{S}(\boldsymbol{v}_\mathrm{r})\boldsymbol{\omega} + g\tilde{\boldsymbol{\zeta}} + \frac{1}{m}\left(\boldsymbol{F}_v\tilde{\boldsymbol{v}}_\mathrm{r} + \boldsymbol{F}_\omega\tilde{\boldsymbol{\omega}}\right)\\ &\quad - \boldsymbol{L}_{2_{v,q}}\boldsymbol{L}_{1_q}^{-1}\left(\boldsymbol{R}_\mathrm{IB}(\tilde{\boldsymbol{\lambda}}+\boldsymbol{\lambda},\tilde{\boldsymbol{\zeta}}+\boldsymbol{\zeta})(\tilde{\boldsymbol{v}}_\mathrm{r}+\boldsymbol{v}_\mathrm{r}) - \boldsymbol{R}_\mathrm{IB}(\boldsymbol{\lambda},\boldsymbol{\zeta})\boldsymbol{v}_\mathrm{r} + \tilde{\boldsymbol{w}}\right)\\ &\quad - \boldsymbol{L}_{2_{v,\lambda}}\boldsymbol{L}_{1_\lambda}^{-1}\left(\boldsymbol{S}(\tilde{\boldsymbol{\lambda}}+\boldsymbol{\lambda})(\tilde{\boldsymbol{\omega}}+\boldsymbol{\omega}) - \boldsymbol{S}(\boldsymbol{\lambda})\boldsymbol{\omega}\right)\\ &\quad - \boldsymbol{L}_{2_{v,\zeta}}\boldsymbol{L}_{1_\zeta}^{-1}\left(\boldsymbol{S}(\tilde{\boldsymbol{\zeta}}+\boldsymbol{\zeta})(\tilde{\boldsymbol{\omega}}+\boldsymbol{\omega}) - \boldsymbol{S}(\boldsymbol{\zeta})\boldsymbol{\omega}\right)\\ &\quad - \boldsymbol{L}_{2_{v,\omega}}\boldsymbol{L}_{1_\omega}^{-1}\Big(\boldsymbol{I}^{-1}\left(\boldsymbol{S}(\boldsymbol{I}\tilde{\boldsymbol{\omega}}+\boldsymbol{I}\boldsymbol{\omega})(\tilde{\boldsymbol{\omega}}+\boldsymbol{\omega}) - \boldsymbol{S}(\boldsymbol{I}\boldsymbol{\omega})\boldsymbol{\omega} + \boldsymbol{M}_v\tilde{\boldsymbol{v}}_\mathrm{r} + \boldsymbol{M}_\omega\tilde{\boldsymbol{\omega}}\right)\Big) \qquad (48a)\\ \tilde{\boldsymbol{\phi}}_{2_w}(\tilde{\boldsymbol{x}}_1,\tilde{\boldsymbol{x}}_2;\boldsymbol{x}_1,\boldsymbol{x}_2;\boldsymbol{u}) &= -\boldsymbol{L}_{2_{w,q}}\boldsymbol{L}_{1_q}^{-1}\left(\boldsymbol{R}_\mathrm{IB}(\tilde{\boldsymbol{\lambda}}+\boldsymbol{\lambda},\tilde{\boldsymbol{\zeta}}+\boldsymbol{\zeta})(\tilde{\boldsymbol{v}}_\mathrm{r}+\boldsymbol{v}_\mathrm{r}) - \boldsymbol{R}_\mathrm{IB}(\boldsymbol{\lambda},\boldsymbol{\zeta})\boldsymbol{v}_\mathrm{r} + \tilde{\boldsymbol{w}}\right)\\ &\quad - \boldsymbol{L}_{2_{w,\lambda}}\boldsymbol{L}_{1_\lambda}^{-1}\left(\boldsymbol{S}(\tilde{\boldsymbol{\lambda}}+\boldsymbol{\lambda})(\tilde{\boldsymbol{\omega}}+\boldsymbol{\omega}) - \boldsymbol{S}(\boldsymbol{\lambda})\boldsymbol{\omega}\right)\\ &\quad - \boldsymbol{L}_{2_{w,\zeta}}\boldsymbol{L}_{1_\zeta}^{-1}\left(\boldsymbol{S}(\tilde{\boldsymbol{\zeta}}+\boldsymbol{\zeta})(\tilde{\boldsymbol{\omega}}+\boldsymbol{\omega}) - \boldsymbol{S}(\boldsymbol{\zeta})\boldsymbol{\omega}\right)\\ &\quad - \boldsymbol{L}_{2_{w,\omega}}\boldsymbol{L}_{1_\omega}^{-1}\Big(\boldsymbol{I}^{-1}\left(\boldsymbol{S}(\boldsymbol{I}\tilde{\boldsymbol{\omega}}+\boldsymbol{I}\boldsymbol{\omega})(\tilde{\boldsymbol{\omega}}+\boldsymbol{\omega}) - \boldsymbol{S}(\boldsymbol{I}\boldsymbol{\omega})\boldsymbol{\omega} + \boldsymbol{M}_v\tilde{\boldsymbol{v}}_\mathrm{r} + \boldsymbol{M}_\omega\tilde{\boldsymbol{\omega}}\right)\Big) \qquad (48b)\end{aligned}$$

The zero dynamics are obtained by simply evaluating Eq. (48) at $\boldsymbol{y}_\mathrm{p} = \tilde{\boldsymbol{x}}_1 = \boldsymbol{0}$. As a result,

$$\tilde{\boldsymbol{\phi}}_{2_{v_\mathrm{r}}}^* = -\boldsymbol{S}(\boldsymbol{\omega})\tilde{\boldsymbol{v}}_\mathrm{r} + \frac{1}{m}\boldsymbol{F}_v\tilde{\boldsymbol{v}}_\mathrm{r} - \boldsymbol{L}_{2_{v,\omega}}\boldsymbol{L}_{1_\omega}^{-1}\boldsymbol{I}^{-1}\boldsymbol{M}_v\tilde{\boldsymbol{v}}_\mathrm{r} - \boldsymbol{L}_{2_{v,q}}\boldsymbol{L}_{1_q}^{-1}\left(\boldsymbol{R}_\mathrm{IB}(\boldsymbol{\lambda},\boldsymbol{\zeta})\tilde{\boldsymbol{v}}_\mathrm{r} + \tilde{\boldsymbol{w}}\right) \qquad (49a)$$

$$\tilde{\boldsymbol{\phi}}_{2_w}^* = -\boldsymbol{L}_{2_{w,q}}\boldsymbol{L}_{1_q}^{-1}\left(\boldsymbol{R}_\mathrm{IB}(\boldsymbol{\lambda},\boldsymbol{\zeta})\tilde{\boldsymbol{v}}_\mathrm{r} + \tilde{\boldsymbol{w}}\right) - \boldsymbol{L}_{2_{w,\omega}}\boldsymbol{L}_{1_\omega}^{-1}\boldsymbol{I}^{-1}\boldsymbol{M}_v\tilde{\boldsymbol{v}}_\mathrm{r} \qquad (49b)$$

Consider the zero-error manifold, $\mathcal{M}$, defined in Eq. (35). We aim to find a proper Lyapunov function $V^*(\tilde{\boldsymbol{x}}_2,\boldsymbol{x})$ that proves $\mathcal{M}^*$ is positively invariant and globally asymptotically attractive on $\mathcal{Z}^*$. That is, we seek V^* such that

$$\psi_1(\|\tilde{\boldsymbol{x}}_2\|) \leq V^*(\tilde{\boldsymbol{x}}_2,\boldsymbol{x}) \leq \psi_2(\|\tilde{\boldsymbol{x}}_2\|) \qquad (50)$$

$$\dot{V}^* = \frac{\partial V^*}{\partial\tilde{\boldsymbol{x}}_2}\tilde{\boldsymbol{\phi}}_2^* + \frac{\partial V^*}{\partial\boldsymbol{x}}\boldsymbol{f} \leq -\varphi^*(\|\tilde{\boldsymbol{x}}_2\|) \qquad (51)$$

where ψ_1,ψ_2 are class $\mathcal{K}_\infty$ functions and φ^* is a smooth, positive definite function. Note that V^* does not necessarily depend on $\boldsymbol{x}$, but allowing it to do so may admit observer designs for a wider class of systems [16]. By Assumption 2, we need only consider the candidate Lyapunov function

$$V^*(\tilde{\boldsymbol{x}}_2,\boldsymbol{x}) = \frac{1}{2}\tilde{\boldsymbol{x}}_2^\mathsf{T}\tilde{\boldsymbol{x}}_2 \qquad (52)$$

which satisfies Eq. (50). It follows that

$$\begin{aligned}\dot{V}^* = -\tilde{\boldsymbol{v}}_\mathrm{r}^\mathsf{T}\boldsymbol{S}(\boldsymbol{\omega})\tilde{\boldsymbol{v}}_\mathrm{r} + \tilde{\boldsymbol{v}}_\mathrm{r}^\mathsf{T}\frac{1}{m}\boldsymbol{F}_v\tilde{\boldsymbol{v}}_\mathrm{r} - \tilde{\boldsymbol{v}}_\mathrm{r}^\mathsf{T}\boldsymbol{L}_{2_{v,q}}\boldsymbol{L}_{1_q}^{-1}\tilde{\boldsymbol{w}} - \tilde{\boldsymbol{v}}_\mathrm{r}^\mathsf{T}\boldsymbol{L}_{2_{v,q}}\boldsymbol{L}_{1_q}^{-1}\boldsymbol{R}_\mathrm{IB}\tilde{\boldsymbol{v}}_\mathrm{r} - \tilde{\boldsymbol{v}}_\mathrm{r}^\mathsf{T}\boldsymbol{L}_{2_{v,\omega}}\boldsymbol{L}_{1_\omega}^{-1}\boldsymbol{I}^{-1}\boldsymbol{M}_v\tilde{\boldsymbol{v}}_\mathrm{r}\\ - \tilde{\boldsymbol{w}}^\mathsf{T}\boldsymbol{L}_{2_{w,q}}\boldsymbol{L}_{1_q}^{-1}\boldsymbol{R}_\mathrm{IB}\tilde{\boldsymbol{v}}_\mathrm{r} - \tilde{\boldsymbol{w}}^\mathsf{T}\boldsymbol{L}_{2_{w,q}}\boldsymbol{L}_{1_q}^{-1}\tilde{\boldsymbol{w}} - \tilde{\boldsymbol{w}}^\mathsf{T}\boldsymbol{L}_{2_{w,\omega}}\boldsymbol{L}_{1_\omega}^{-1}\boldsymbol{I}^{-1}\boldsymbol{M}_v\tilde{\boldsymbol{v}}_\mathrm{r} \qquad (53)\end{aligned}$$

Here we have dropped the argument to $\boldsymbol{R}_\mathrm{IB}$ for compactness. From here on, it is implied that $\boldsymbol{R}_\mathrm{IB} = \boldsymbol{R}_\mathrm{IB}(\boldsymbol{\lambda},\boldsymbol{\zeta})$ unless explicitly stated. Notice the term $\tilde{\boldsymbol{v}}_\mathrm{r}^\mathsf{T}\boldsymbol{S}(\boldsymbol{\omega})\tilde{\boldsymbol{v}}_\mathrm{r}$ is identically equal to zero since the quadratic form of a skew-symmetric matrix is zero. We may then write Eq. (53) as

$$\dot{V}^* = -\tilde{\boldsymbol{x}}_2^\mathsf{T}\boldsymbol{P}\tilde{\boldsymbol{x}}_2 \qquad (54)$$

where

$$\boldsymbol{P}_{11} = -\frac{1}{m}\boldsymbol{F}_v + \boldsymbol{L}_{2_{v,q}}\boldsymbol{L}_{1_q}^{-1}\boldsymbol{R}_\mathrm{IB} + \boldsymbol{L}_{2_{v,\omega}}\boldsymbol{L}_{1_\omega}^{-1}\boldsymbol{I}^{-1}\boldsymbol{M}_v \qquad (55a)$$

$$\boldsymbol{P}_{12} = \boldsymbol{L}_{2_{v,q}}\boldsymbol{L}_{1_q}^{-1} \qquad (55b)$$

$$\boldsymbol{P}_{21} = \boldsymbol{L}_{2_{w,q}}\boldsymbol{L}_{1_q}^{-1}\boldsymbol{R}_\mathrm{IB} + \boldsymbol{L}_{2_{w,\omega}}\boldsymbol{L}_{1_\omega}^{-1}\boldsymbol{I}^{-1}\boldsymbol{M}_v \qquad (55c)$$

$$\boldsymbol{P}_{22} = \boldsymbol{L}_{2_{w,q}}\boldsymbol{L}_{1_q}^{-1} \qquad (55d)$$

Therefore, we choose the gain matrix $\boldsymbol{L}$ such that

$$\begin{bmatrix} \boldsymbol{Q}_{11} & \boldsymbol{Q}_{12} \\ \boldsymbol{Q}_{12}^{\mathsf{T}} & \boldsymbol{Q}_{22} \end{bmatrix} := \boldsymbol{Q} := \frac{1}{2}\left(\boldsymbol{P} + \boldsymbol{P}^{\mathsf{T}}\right) \succ \boldsymbol{0}$$

where

$$\boldsymbol{Q}_{11} = \frac{1}{2}\left(-\frac{1}{m}(\boldsymbol{F}_v + \boldsymbol{F}_v^{\mathsf{T}}) + \boldsymbol{L}_{2_{v,q}}\boldsymbol{L}_{1_q}^{-1}\boldsymbol{R}_{\mathrm{IB}} + \boldsymbol{R}_{\mathrm{IB}}^{\mathsf{T}}\boldsymbol{L}_{1_q}^{-\mathsf{T}}\boldsymbol{L}_{2_{v,q}}^{\mathsf{T}} + \boldsymbol{L}_{2_{v,\omega}}\boldsymbol{L}_{1_\omega}^{-1}\boldsymbol{I}^{-1}\boldsymbol{M}_v + \boldsymbol{M}_v^{\mathsf{T}}\boldsymbol{I}^{-1}\boldsymbol{L}_{1_\omega}^{-\mathsf{T}}\boldsymbol{L}_{2_{v,\omega}}^{\mathsf{T}}\right) \tag{56a}$$

$$\boldsymbol{Q}_{12} = \frac{1}{2}\left(\boldsymbol{L}_{2_{v,q}}\boldsymbol{L}_{1_q}^{-1} + \boldsymbol{R}_{\mathrm{IB}}^{\mathsf{T}}\boldsymbol{L}_{1_q}^{-\mathsf{T}}\boldsymbol{L}_{2_{w,q}}^{\mathsf{T}} + \boldsymbol{M}_v^{\mathsf{T}}\boldsymbol{I}^{-1}\boldsymbol{L}_{1_\omega}^{-\mathsf{T}}\boldsymbol{L}_{2_{w,\omega}}^{\mathsf{T}}\right) \tag{56b}$$

$$\boldsymbol{Q}_{22} = \frac{1}{2}\left(\boldsymbol{L}_{2_{w,q}}\boldsymbol{L}_{1_q}^{-1} + \boldsymbol{L}_{1_q}^{-\mathsf{T}}\boldsymbol{L}_{2_{w,q}}^{\mathsf{T}}\right) \tag{56c}$$

Choosing $\boldsymbol{L}$ such that $\boldsymbol{Q} \succ \boldsymbol{0}$ is sufficient for proving $\dot{V}^*$ is negative definite. Let

$$\boldsymbol{L}_{2_{v,q}} = \boldsymbol{\Gamma}_{v,q}\boldsymbol{R}_{\mathrm{IB}}^{\mathsf{T}}\boldsymbol{L}_{1_q} \tag{57a}$$

$$\boldsymbol{L}_{2_{v,\omega}} = \boldsymbol{\Gamma}_{v,\omega}\boldsymbol{M}_v^{\mathsf{T}}\boldsymbol{I}\boldsymbol{L}_{1_\omega} \tag{57b}$$

$$\boldsymbol{L}_{2_{w,q}} = \boldsymbol{R}_{\mathrm{IB}}\boldsymbol{\Gamma}_{w,q}\boldsymbol{R}_{\mathrm{IB}}^{\mathsf{T}}\boldsymbol{L}_{1_q} \tag{57c}$$

$$\boldsymbol{L}_{2_{w,\omega}} = \boldsymbol{R}_{\mathrm{IB}}\boldsymbol{\Gamma}_{w,\omega}\boldsymbol{M}_v^{\mathsf{T}}\boldsymbol{I}\boldsymbol{L}_{1_\omega} \tag{57d}$$

where the matrix

$$\boldsymbol{\Gamma} = \begin{bmatrix} \boldsymbol{\Gamma}_{v,q} & \boldsymbol{\Gamma}_{v,\omega} \\ \boldsymbol{\Gamma}_{w,q} & \boldsymbol{\Gamma}_{w,\omega} \end{bmatrix} \tag{58}$$

is a constant parameter used for tuning. Notice we have chosen $\boldsymbol{L}_2$ to make the design of $\boldsymbol{L}_1$ independent of the tuning of the zero dynamics. The matrix $\boldsymbol{Q}$ reduces to

$$\boldsymbol{Q}_{11} = -\frac{1}{2m}\left(\boldsymbol{F}_v + \boldsymbol{F}_v^{\mathsf{T}}\right) + \frac{1}{2}\left(\boldsymbol{\Gamma}_{v,q} + \boldsymbol{\Gamma}_{v,q}^{\mathsf{T}}\right) + \frac{1}{2}\left(\boldsymbol{\Gamma}_{v,\omega}\boldsymbol{M}_v^{\mathsf{T}}\boldsymbol{M}_v + \boldsymbol{M}_v^{\mathsf{T}}\boldsymbol{M}_v\boldsymbol{\Gamma}_{v,\omega}^{\mathsf{T}}\right) \tag{59a}$$

$$\boldsymbol{Q}_{12} = \frac{1}{2}\left(\boldsymbol{\Gamma}_{v,q} + \boldsymbol{\Gamma}_{w,q}^{\mathsf{T}} + \boldsymbol{M}_v^{\mathsf{T}}\boldsymbol{M}_v\boldsymbol{\Gamma}_{w,\omega}^{\mathsf{T}}\right)\boldsymbol{R}_{\mathrm{IB}}^{\mathsf{T}} \tag{59b}$$

$$\boldsymbol{Q}_{22} = \frac{1}{2}\boldsymbol{R}_{\mathrm{IB}}\left(\boldsymbol{\Gamma}_{w,q} + \boldsymbol{\Gamma}_{w,q}^{\mathsf{T}}\right)\boldsymbol{R}_{\mathrm{IB}}^{\mathsf{T}} \tag{59c}$$

The rotation matrix, $\boldsymbol{R}_{\mathrm{IB}}$, does not influence the definiteness of $\boldsymbol{Q}$. This can be seen using the Schur complement where $\boldsymbol{Q} \succ \boldsymbol{0}$ if and only if

$$\boldsymbol{\Gamma}_{w,q} + \boldsymbol{\Gamma}_{w,q}^{\mathsf{T}} \succ \boldsymbol{0} \tag{60a}$$

$$\boldsymbol{Q}_{11} - \boldsymbol{Q}_{12}\boldsymbol{Q}_{22}^{-1}\boldsymbol{Q}_{12}^{\mathsf{T}} \succ \boldsymbol{0} \tag{60b}$$

Therefore, we may choose $\boldsymbol{\Gamma}$ such that

$$\begin{bmatrix} -\frac{1}{m}\boldsymbol{F}_v + \boldsymbol{\Gamma}_{v,q} + \boldsymbol{\Gamma}_{v,\omega}\boldsymbol{M}_v^{\mathsf{T}}\boldsymbol{M}_v & \boldsymbol{\Gamma}_{v,q} \\ \boldsymbol{\Gamma}_{w,q} + \boldsymbol{\Gamma}_{w,\omega}\boldsymbol{M}_v^{\mathsf{T}}\boldsymbol{M}_v & \boldsymbol{\Gamma}_{w,q} \end{bmatrix} + \begin{bmatrix} -\frac{1}{m}\boldsymbol{F}_v + \boldsymbol{\Gamma}_{v,q} + \boldsymbol{\Gamma}_{v,\omega}\boldsymbol{M}_v^{\mathsf{T}}\boldsymbol{M}_v & \boldsymbol{\Gamma}_{v,q} \\ \boldsymbol{\Gamma}_{w,q} + \boldsymbol{\Gamma}_{w,\omega}\boldsymbol{M}_v^{\mathsf{T}}\boldsymbol{M}_v & \boldsymbol{\Gamma}_{w,q} \end{bmatrix}^{\mathsf{T}} \succ \boldsymbol{0} \tag{61}$$

This condition may be stated as the linear matrix inequality (LMI)

$$\boldsymbol{\Gamma}\mathcal{A} + \mathcal{A}^{\mathsf{T}}\boldsymbol{\Gamma}^{\mathsf{T}} + \mathcal{Q} \succ \boldsymbol{0} \tag{62}$$

where

$$\mathcal{A} = \begin{bmatrix} \mathbb{I} & \mathbb{I} \\ \boldsymbol{M}_v^{\mathsf{T}}\boldsymbol{M}_v & \boldsymbol{0} \end{bmatrix} \qquad \text{and} \qquad \mathcal{Q} = \begin{bmatrix} -\frac{1}{m}(\boldsymbol{F}_v + \boldsymbol{F}_v^{\mathsf{T}}) & \boldsymbol{0} \\ \boldsymbol{0} & \boldsymbol{0} \end{bmatrix} \tag{63}$$

Since $\dot{V}^* = -\tilde{\boldsymbol{x}}_2^{\mathsf{T}}\boldsymbol{Q}\tilde{\boldsymbol{x}}_2$, we choose to lower bound the smallest eigenvalue of $\boldsymbol{Q}$, denoted $\lambda_{\min}(\boldsymbol{Q})$, by some positive constant $\underline{\gamma}$. This constant lower bounds the convergence rate of the zero dynamics. Similarly, we can ensure the observer

gain is not arbitrarily large by setting an upper bound, $\overline{\gamma}$, on the largest eigenvalue of $\boldsymbol{Q}$, denoted $\lambda_{\max}(\boldsymbol{Q})$. This is important for ensuring the numerical integration of the observer is well-conditioned. Since $\boldsymbol{R}_{\mathrm{IB}}(\boldsymbol{\lambda}, \boldsymbol{\zeta})$ does not influence the definiteness of $\boldsymbol{Q}$, we can incorporate the additional convex constraints

$$\lambda_{\min}(\bar{\boldsymbol{Q}}) \geq \underline{\gamma} \tag{64a}$$

$$\lambda_{\max}(\bar{\boldsymbol{Q}}) \leq \overline{\gamma} \tag{64b}$$

where $\bar{\boldsymbol{Q}} := \boldsymbol{Q}|_{\boldsymbol{R}_{\mathrm{IB}}=\mathbb{I}}$ is a constant symmetric matrix. Hence, for some given $\underline{\gamma}$ and $\overline{\gamma}$, we have the convex feasibility problem

$$\text{Find } \boldsymbol{\Gamma} \qquad \text{such that} \quad \begin{array}{l} \boldsymbol{\Gamma}\mathcal{A} + \mathcal{A}^{\mathsf{T}}\boldsymbol{\Gamma}^{\mathsf{T}} + \mathcal{Q} \succ \boldsymbol{0} \\ \boldsymbol{\Gamma}_{w,q} + \boldsymbol{\Gamma}_{w,q}^{\mathsf{T}} \succ \boldsymbol{0} \\ \lambda_{\min}(\bar{\boldsymbol{Q}}) \geq \underline{\gamma} \\ \lambda_{\max}(\bar{\boldsymbol{Q}}) \leq \overline{\gamma} \end{array} \tag{65}$$

It may be desirable to further constrain the set of solutions to (65). In some cases, the norm of $\boldsymbol{\Gamma}$ can still be quite large despite the addition of the bound $\overline{\gamma}$. Accordingly, an additional upper bound can be placed on the norm of $\boldsymbol{\Gamma}$.

If $\underline{\gamma}$ is upper bounded for the aerodynamic model of interest, (65) can be optimally solved by maximizing $\underline{\gamma}$ for some given $\overline{\gamma}$ greater then the maximal $\underline{\gamma}$. As seen in Eq. (59), the upper bound on the zero dynamics convergence rate then directly depends on the aircraft mass, $\boldsymbol{F}_v$, and $\boldsymbol{M}_v$. In other words, the dissipation rate of relative velocity and wind observation error is dependent on the aircraft's physical dissipation due to drag. Practically, this means there may be an upper limit on the time scale of wind fluctuations that can be accurately resolved. Conversely, if $\overline{\gamma}$ is lower bounded for some given $\underline{\gamma}$ less than the minimal $\overline{\gamma}$, then it may be minimized to ensure $\boldsymbol{Q}$ is well-conditioned.

While we have arrived at Eq. (62) assuming perfect knowledge of m, $\boldsymbol{F}_v$, and $\boldsymbol{M}_v$, we may want to prescribe a solution that is more robust to uncertainty or changes in these parameters. Suppose the matrices $\mathcal{A}$, $\mathcal{Q}$, and $\bar{\boldsymbol{Q}}$ are polytopic uncertain with

$$\left\{\mathcal{A},\ \mathcal{Q},\ \bar{\boldsymbol{Q}}\right\} \in \mathbb{P} := \sum_{i=1}^{N} \alpha_i \left\{\mathcal{A}_i,\ \mathcal{Q}_i,\ \bar{\boldsymbol{Q}}_i\right\}, \quad \sum_{i=1}^{N} \alpha_i = 1 \tag{66}$$

Then, we may choose $\boldsymbol{\Gamma}$ as a solution to the

$$\text{Find } \boldsymbol{\Gamma} \qquad \text{such that} \quad \begin{array}{l} \boldsymbol{\Gamma}\mathcal{A}_i + \mathcal{A}_i^{\mathsf{T}}\boldsymbol{\Gamma}^{\mathsf{T}} + \mathcal{Q}_i \succ \boldsymbol{0} \\ \boldsymbol{\Gamma}_{w,q} + \boldsymbol{\Gamma}_{w,q}^{\mathsf{T}} \succ \boldsymbol{0} \\ \lambda_{\min}(\bar{\boldsymbol{Q}}_i) \geq \underline{\gamma} \\ \lambda_{\max}(\bar{\boldsymbol{Q}}_i) \leq \overline{\gamma} \end{array} \qquad \text{for } i = 1, \cdots, N \tag{67}$$

This approach may be used for the case where one chooses to "gain-schedule" the linear aerodynamics matrices based on the current flight condition. This can be done in principle as long as $\boldsymbol{F}_v$, $\boldsymbol{F}_\omega$, $\boldsymbol{M}_v$, and $\boldsymbol{M}_\omega$ vary sufficiently slowly.

With $\boldsymbol{\Gamma}$ chosen such that (65) holds, we see that

$$\dot{V}^* = -\tilde{\boldsymbol{x}}_2^{\mathsf{T}}\boldsymbol{Q}\tilde{\boldsymbol{x}}_2 \leq -\underline{\gamma}\|\tilde{\boldsymbol{x}}_2\|^2 =: -\varphi^*(\|\tilde{\boldsymbol{x}}_2\|) \tag{68}$$

thus proving the error system is globally minimum phase with respect to $\boldsymbol{y}_{\mathrm{p}} = \hat{\boldsymbol{y}} - \boldsymbol{y}$.

B. Bounding Functions and Strict Passivity

Having proven that the augmented system is minimum phase, we follow the second step in [16] and consider the change of coordinates

$$\boldsymbol{\xi}_1 = \tilde{\boldsymbol{x}}_1 \tag{69a}$$

$$\boldsymbol{\xi}_2 = \tilde{\boldsymbol{x}}_2 - \boldsymbol{L}_2(\boldsymbol{y})\boldsymbol{L}_1^{-1}\tilde{\boldsymbol{x}}_1 \tag{69b}$$

Specifically, the components of $\boldsymbol{\xi}_2$ for the aircraft in wind are

$$\boldsymbol{\xi}_{2_{v_{\mathrm{r}}}} = \tilde{\boldsymbol{v}}_{\mathrm{r}} - \boldsymbol{\Gamma}_{v,q}\boldsymbol{R}_{\mathrm{IB}}^{\mathsf{T}}\tilde{\boldsymbol{q}} - \boldsymbol{\Gamma}_{v,\omega}\boldsymbol{M}_v^{\mathsf{T}}\boldsymbol{I}\tilde{\boldsymbol{\omega}} \tag{70a}$$

$$\boldsymbol{\xi}_{2_w} = \tilde{\boldsymbol{w}} - \boldsymbol{R}_{\mathrm{IB}}\boldsymbol{\Gamma}_{w,q}\boldsymbol{R}_{\mathrm{IB}}^{\mathsf{T}}\tilde{\boldsymbol{q}} - \boldsymbol{R}_{\mathrm{IB}}\boldsymbol{\Gamma}_{w,\omega}\boldsymbol{M}_v^{\mathsf{T}}\boldsymbol{I}\tilde{\boldsymbol{\omega}} \tag{70b}$$

It follows that

$$\dot{\boldsymbol{\xi}}_2 = \tilde{\boldsymbol{\phi}}_2(\boldsymbol{\xi}_1, \boldsymbol{\xi}_2 + \boldsymbol{L}_2\boldsymbol{L}_1^{-1}\boldsymbol{\xi}_1; \boldsymbol{x}_1, \boldsymbol{x}_2; \boldsymbol{u}) - \frac{\mathrm{d}}{\mathrm{d}t}\left(\boldsymbol{L}_2(\boldsymbol{x}_1)\boldsymbol{L}_1^{-1}\right)\tilde{\boldsymbol{x}}_1 \tag{71}$$

The only difference here from [16] is the second term. We will see shortly its effect can be incorporated into our choice of gain function, $\boldsymbol{K}$. Consider the storage function

$$W(\boldsymbol{\xi}, \boldsymbol{x}) = V^*(\boldsymbol{\xi}_2, \boldsymbol{x}) + \frac{1}{2}\boldsymbol{\xi}_1^{\mathsf{T}}\boldsymbol{L}_1^{-1}\boldsymbol{\xi}_1 \tag{72}$$

It can be shown the time derivative of W satisfies

$$\begin{aligned}\dot{W} = \frac{\partial V^*}{\partial \boldsymbol{x}}\boldsymbol{f}(\boldsymbol{x}, \boldsymbol{u}) + \frac{\partial V^*}{\partial \boldsymbol{\xi}_2}\tilde{\boldsymbol{\phi}}_2^*(\boldsymbol{\xi}_2, \boldsymbol{x}, \boldsymbol{u}) + \frac{\partial V^*}{\partial \boldsymbol{\xi}_2}\tilde{\boldsymbol{\phi}}_2(\boldsymbol{\xi}_1, \boldsymbol{L}_2\boldsymbol{L}_1^{-1}\boldsymbol{\xi}_1; \boldsymbol{x}_1, \boldsymbol{x}_2; \boldsymbol{u}) \\ + \boldsymbol{\xi}_1^{\mathsf{T}}\boldsymbol{L}_1^{-1}\tilde{\boldsymbol{f}}_1(\tilde{\boldsymbol{x}}_1, \tilde{\boldsymbol{x}}_2 + \boldsymbol{L}_2\boldsymbol{L}_1^{-1}\tilde{\boldsymbol{x}}_1; \boldsymbol{x}_1, \hat{\boldsymbol{x}}_2 - \tilde{\boldsymbol{x}}_2; \boldsymbol{u}) + \frac{\partial V^*}{\partial \boldsymbol{\xi}_2}\frac{\mathrm{d}}{\mathrm{d}t}\left(\boldsymbol{L}_2(\boldsymbol{x}_1)\boldsymbol{L}_1^{-1}\right)\boldsymbol{\xi}_1 + \boldsymbol{\xi}_1^{\mathsf{T}}\boldsymbol{v}\end{aligned} \tag{73}$$

where the term $\frac{\mathrm{d}}{\mathrm{d}t}\left(\boldsymbol{L}_2(\boldsymbol{x}_1)\boldsymbol{L}_1^{-1}\right)$ for the aircraft in wind is

$$\frac{\mathrm{d}}{\mathrm{d}t}\left(\boldsymbol{L}_2(\boldsymbol{x}_1)\boldsymbol{L}_1^{-1}\right) = \begin{bmatrix} -\boldsymbol{\Gamma}_{v,q}\boldsymbol{S}(\boldsymbol{\omega})\boldsymbol{R}_{\mathrm{IB}}^{\mathsf{T}} & \boldsymbol{0} & \boldsymbol{0} & \boldsymbol{0} \\ \boldsymbol{R}_{\mathrm{IB}}\left(\boldsymbol{S}(\boldsymbol{\omega})\boldsymbol{\Gamma}_{w,q} - \boldsymbol{\Gamma}_{w,q}\boldsymbol{S}(\boldsymbol{\omega})\right)\boldsymbol{R}_{\mathrm{IB}}^{\mathsf{T}} & \boldsymbol{0} & \boldsymbol{0} & \boldsymbol{R}_{\mathrm{IB}}\boldsymbol{S}(\boldsymbol{\omega})\boldsymbol{\Gamma}_{w,\omega}\boldsymbol{M}_v^{\mathsf{T}}\boldsymbol{I} \end{bmatrix} \tag{74}$$

Then by Eq. (68), we have

$$\begin{aligned}\dot{W} \leq -\varphi^*(\|\boldsymbol{\xi}_2\|) + \frac{\partial V^*}{\partial \boldsymbol{\xi}_2}\tilde{\boldsymbol{\phi}}_2(\boldsymbol{\xi}_1, \boldsymbol{L}_2(\boldsymbol{y})\boldsymbol{L}_1^{-1}\boldsymbol{\xi}_1; \boldsymbol{x}_1, \boldsymbol{\xi}_2 + \boldsymbol{x}_2; \boldsymbol{u}) \\ + \boldsymbol{\xi}_1^{\mathsf{T}}\boldsymbol{L}_1^{-1}\tilde{\boldsymbol{f}}_1(\boldsymbol{\xi}_1, \boldsymbol{\xi}_2 + \boldsymbol{L}_2(\boldsymbol{y})\boldsymbol{L}_1^{-1}\boldsymbol{\xi}_1; \boldsymbol{x}_1, \boldsymbol{x}_2; \boldsymbol{u}) - \frac{\partial V^*}{\partial \boldsymbol{\xi}_2}\frac{\mathrm{d}}{\mathrm{d}t}\left(\boldsymbol{L}_2(\boldsymbol{y})\boldsymbol{L}_1^{-1}\right)\boldsymbol{\xi}_1 + \boldsymbol{\xi}_1^{\mathsf{T}}\boldsymbol{v}\end{aligned} \tag{75}$$

Here we see the feedback $\boldsymbol{v}$ can be chosen to render the augmented dynamics strictly passive. Specifically, consider the following result.

Proposition 1. *There exist a symmetric matrix function $\boldsymbol{\Psi} : \mathbb{R}^p \times \mathbb{R}^{n-p} \times \mathbb{R}^p \times \mathcal{U} \to \mathbb{R}^{p\times p}$ and a matrix function $\boldsymbol{\Lambda} : \mathbb{R}^p \times \mathbb{R}^{n-p} \times \mathbb{R}^p \times \mathcal{U} \to \mathbb{R}^{(n-p)\times p}$ such that*

$$\begin{aligned}\frac{\partial V^*}{\partial \boldsymbol{\xi}_2}\tilde{\boldsymbol{\phi}}_2(\boldsymbol{\xi}_1, \boldsymbol{L}_2(\boldsymbol{y})\boldsymbol{L}_1^{-1}\boldsymbol{\xi}_1; \boldsymbol{x}_1, \boldsymbol{\xi}_2 + \boldsymbol{x}_2; \boldsymbol{u}) + \boldsymbol{\xi}_1^{\mathsf{T}}\boldsymbol{L}_1^{-1}\tilde{\boldsymbol{f}}_1(\boldsymbol{\xi}_1, \boldsymbol{\xi}_2 + \boldsymbol{L}_2(\boldsymbol{y})\boldsymbol{L}_1^{-1}\boldsymbol{\xi}_1; \boldsymbol{x}_1, \boldsymbol{x}_2; \boldsymbol{u}) \\ - \frac{\partial V^*}{\partial \boldsymbol{\xi}_2}\frac{\mathrm{d}}{\mathrm{d}t}\left(\boldsymbol{L}_2(\boldsymbol{y})\boldsymbol{L}_1^{-1}\right)\boldsymbol{\xi}_1 \leq \sqrt{\varphi^*(\|\boldsymbol{\xi}_2\|)}\|\boldsymbol{\Lambda}(\boldsymbol{\xi}_1, \boldsymbol{\xi}_2 + \boldsymbol{x}_2, \boldsymbol{x}_1, \boldsymbol{u})\boldsymbol{\xi}_1\| + \boldsymbol{\xi}_1^{\mathsf{T}}\boldsymbol{\Psi}(\boldsymbol{\xi}_1, \boldsymbol{\xi}_2 + \boldsymbol{x}_2, \boldsymbol{x}_1, \boldsymbol{u})\boldsymbol{\xi}_1\end{aligned} \tag{76}$$

Proof. The proof of Proposition 1 is given in Appendix A. □

Using Proposition 1, we write Eq. (75) as

$$\dot{W} \leq -\varphi^*(\|\boldsymbol{\xi}_2\|) + \sqrt{\varphi^*(\|\boldsymbol{\xi}_2\|)}\|\boldsymbol{\Lambda}(\boldsymbol{\xi}_1, \boldsymbol{\xi}_2 + \boldsymbol{x}_2, \boldsymbol{x}_1, \boldsymbol{u})\boldsymbol{\xi}_1\| + \boldsymbol{\xi}_1^{\mathsf{T}}\boldsymbol{\Psi}(\boldsymbol{\xi}_1, \boldsymbol{\xi}_2 + \boldsymbol{x}_2, \boldsymbol{x}_1, \boldsymbol{u})\boldsymbol{\xi}_1 + \boldsymbol{\xi}_1^{\mathsf{T}}\boldsymbol{v} \tag{77}$$

Consider the feedback law

$$\boldsymbol{v} = -\boldsymbol{K}(\hat{\boldsymbol{x}}, \boldsymbol{y})\boldsymbol{y}_{\mathrm{p}} + \boldsymbol{v}_{\mathrm{p}} \tag{78}$$

where

$$\boldsymbol{K}(\hat{\boldsymbol{x}}, \boldsymbol{y}, \boldsymbol{u}) = \varepsilon\mathbb{I} + \left[\boldsymbol{\Psi} + \boldsymbol{\Lambda}^{\mathsf{T}}\boldsymbol{\Lambda}\right]\left(\hat{\boldsymbol{x}}_1 - \boldsymbol{y}, \hat{\boldsymbol{x}}_2 - \boldsymbol{L}_2(\boldsymbol{y})\boldsymbol{L}_1^{-1}(\hat{\boldsymbol{x}}_1 - \boldsymbol{y}), \boldsymbol{y}, \boldsymbol{u}\right) \tag{79}$$

for any $\varepsilon > 0$. Here, parentheses contain arguments for all functions in square brackets. Substituting this feedback law under the coordinate transformation into Eq. (77), we obtain

$$\begin{aligned}\dot{W} \leq \boldsymbol{y}_{\mathrm{p}}^{\mathsf{T}}\boldsymbol{v}_{\mathrm{p}} - \varphi^*(\|\boldsymbol{\xi}_2\|) + \sqrt{\varphi^*(\|\boldsymbol{\xi}_2\|)}\|\boldsymbol{\Lambda}(\boldsymbol{\xi}_1, \boldsymbol{\xi}_2 + \boldsymbol{x}_2, \boldsymbol{x}_1, \boldsymbol{u})\boldsymbol{\xi}_1\| \\ + \boldsymbol{\xi}_1^{\mathsf{T}}\boldsymbol{\Psi}(\boldsymbol{\xi}_1, \boldsymbol{\xi}_2 + \boldsymbol{x}_2, \boldsymbol{x}_1, \boldsymbol{u})\boldsymbol{\xi}_1 - \boldsymbol{\xi}_1^{\mathsf{T}}\left(\varepsilon\mathbb{I} + \left[\boldsymbol{\Psi} + \boldsymbol{\Lambda}^{\mathsf{T}}\boldsymbol{\Lambda}\right](\boldsymbol{\xi}_1, \boldsymbol{\xi}_2 + \boldsymbol{x}_2, \boldsymbol{x}_1, \boldsymbol{u})\right)\boldsymbol{\xi}_1\end{aligned} \tag{80}$$

After writing Eq. (80) as

$$\dot{W} \leq \boldsymbol{y}_{\mathrm{p}}^{\mathsf{T}}\boldsymbol{v}_{\mathrm{p}} - \frac{3}{4}\varphi^*(\|\boldsymbol{\xi}_2\|) - \varepsilon\boldsymbol{\xi}_1^{\mathsf{T}}\boldsymbol{\xi}_1 \\ - \frac{1}{4}\varphi^*(\|\boldsymbol{\xi}_2\|) + \sqrt{\varphi^*(\|\boldsymbol{\xi}_2\|)}\|\boldsymbol{\Lambda}(\boldsymbol{\xi}_1, \boldsymbol{\xi}_2 + \boldsymbol{x}_2, \boldsymbol{x}_1, \boldsymbol{u})\boldsymbol{\xi}_1\| - \boldsymbol{\xi}_1^{\mathsf{T}}\left[\boldsymbol{\Lambda}^{\mathsf{T}}\boldsymbol{\Lambda}\right](\boldsymbol{\xi}_1, \boldsymbol{\xi}_2 + \boldsymbol{x}_2, \boldsymbol{x}_1, \boldsymbol{u})\boldsymbol{\xi}_1 \quad (81)$$

and noticing

$$-\frac{1}{4}\varphi^*(\|\boldsymbol{\xi}_2\|) + \sqrt{\varphi^*(\|\boldsymbol{\xi}_2\|)}\|\boldsymbol{\Lambda}\boldsymbol{\xi}_1\| - \boldsymbol{\xi}_1^{\mathsf{T}}\boldsymbol{\Lambda}^{\mathsf{T}}\boldsymbol{\Lambda}\boldsymbol{\xi}_1 = -\left(\frac{1}{2}\sqrt{\varphi^*(\|\boldsymbol{\xi}_2\|)} - \|\boldsymbol{\Lambda}\boldsymbol{\xi}_1\|\right)^2$$

we see that

$$\dot{W} \leq \boldsymbol{y}_{\mathrm{p}}^{\mathsf{T}}\boldsymbol{v}_{\mathrm{p}} - \frac{3}{4}\varphi^*(\|\boldsymbol{\xi}_2\|) - \varepsilon\boldsymbol{\xi}_1^{\mathsf{T}}\boldsymbol{\xi}_1 - \left(\frac{1}{2}\sqrt{\varphi^*(\|\boldsymbol{\xi}_2\|)} - \|\boldsymbol{\Lambda}\boldsymbol{\xi}_1\|\right)^2 \quad (82)$$

Hence, the storage function

$$W = V^*(\tilde{\boldsymbol{x}}_2 - \boldsymbol{L}_2\boldsymbol{L}_1^{-1}\tilde{\boldsymbol{x}}_1, \boldsymbol{x}) + \frac{1}{2}\tilde{\boldsymbol{x}}_1^{\mathsf{T}}\boldsymbol{L}_1^{-1}\tilde{\boldsymbol{x}}_1 \quad (83)$$

proves the feedback law in Eq. (78) renders the augmented system strictly passive from $\boldsymbol{v}_{\mathrm{p}}$ to $\boldsymbol{y}_{\mathrm{p}}$ with respect to $\mathcal{M}$. Upon setting $\boldsymbol{v}_{\mathrm{p}} = \boldsymbol{0}$, $\mathcal{M}$ becomes positively invariant and globally asymptotically attractive [30]. In other words, the origin of the error system (34) is asymptotically stable. In fact, since $\boldsymbol{L}_2(\boldsymbol{y})$ is bounded, there exist positive constants κ_1, κ_2, and κ_3 such that $\kappa_1\|\tilde{\boldsymbol{x}}\|^2 \leq W \leq \kappa_2\|\tilde{\boldsymbol{x}}\|^2$ and $\dot{W} \leq -\kappa_3\|\tilde{\boldsymbol{x}}\|^2$. Specifically, define the constant symmetric matrices

$$\boldsymbol{G}_{1,2} = \begin{bmatrix} \boldsymbol{L}_1^{-\mathsf{T}}\bar{\boldsymbol{L}}_2^{\mathsf{T}}\bar{\boldsymbol{L}}_2\boldsymbol{L}_1^{-1} + (\boldsymbol{L}_1^{-1} + \boldsymbol{L}_1^{-\mathsf{T}})/2 & \boldsymbol{L}_1^{-\mathsf{T}}\bar{\boldsymbol{L}}_2^{\mathsf{T}} \\ \bar{\boldsymbol{L}}_2\boldsymbol{L}_1^{-1} & \mathbb{I} \end{bmatrix}, \qquad \boldsymbol{G}_3 = \begin{bmatrix} \frac{3}{4}\underline{\gamma}\boldsymbol{L}_1^{-\mathsf{T}}\bar{\boldsymbol{L}}_2^{\mathsf{T}}\bar{\boldsymbol{L}}_2\boldsymbol{L}_1^{-1} + \varepsilon\mathbb{I} & \frac{3}{8}\underline{\gamma}\boldsymbol{L}_1^{-\mathsf{T}}\bar{\boldsymbol{L}}_2^{\mathsf{T}} \\ \frac{3}{4}\underline{\gamma}\bar{\boldsymbol{L}}_2\boldsymbol{L}_1^{-1} & \frac{3}{4}\underline{\gamma}\mathbb{I} \end{bmatrix}$$

where

$$\bar{\boldsymbol{L}}_2 := \boldsymbol{L}_2|_{\boldsymbol{R}_{\mathrm{IB}}=\mathbb{I}}$$

Then, the origin of the error system (34) is globally exponentially stable with trajectories satisfying

$$\|\tilde{\boldsymbol{x}}(t)\| \leq \sqrt{\frac{\kappa_2}{\kappa_1}}\|\tilde{\boldsymbol{x}}(0)\|e^{-\frac{1}{2}\frac{\kappa_3}{\kappa_2}t} \quad (84)$$

where $\kappa_1 = \frac{1}{2}\lambda_{\min}(\boldsymbol{G}_{1,2})$, $\kappa_2 = \frac{1}{2}\lambda_{\max}(\boldsymbol{G}_{1,2})$, and $\kappa_3 = \lambda_{\min}(\boldsymbol{G}_3)$. These results give an explicit upper bound for the convergence rate of the state estimate error. Note that this upper bound may be conservative since the contribution of the last term in Eq. (82) is neglected.

The matrix $\boldsymbol{L}_1$ is left as a tuning parameter that can be chosen using familiar methods of observer gain design by linearizing about a nominal flight condition and defining weighted objectives (similar to the process and measurement noise covariance matrices for a Kalman filter). Also note the choice of bounding matrix functions $\boldsymbol{\Psi}$ and $\boldsymbol{\Lambda}$ given in Appendix A hold for any finite $\boldsymbol{L}_{2_{v,\lambda}}$, $\boldsymbol{L}_{2_{v,\zeta}}$, $\boldsymbol{L}_{2_{w,\lambda}}$, $\boldsymbol{L}_{2_{w,\zeta}}$. However, the observer gain is then also arbitrarily large. Therefore, it is judicious to choose these gains to make $\boldsymbol{\Psi}$ and $\boldsymbol{\Lambda}$ as small as possible. Setting $\boldsymbol{L}_{2_{v,\lambda}}$, $\boldsymbol{L}_{2_{v,\zeta}}$, $\boldsymbol{L}_{2_{w,\lambda}}$, and $\boldsymbol{L}_{2_{w,\zeta}}$ to be zero matrices is sufficient this task. Intuitively, this is because the attitude kinematics do not explicitly encode any information about the relative velocity and wind states. They only depend on the measured angular velocity. Altogether, the matrix $\boldsymbol{L}$ is given as

$$\boldsymbol{L} = \begin{bmatrix} \boldsymbol{L}_{1_q} & \boldsymbol{0} & \boldsymbol{0} & \boldsymbol{0} \\ \boldsymbol{0} & \boldsymbol{L}_{1_\lambda} & \boldsymbol{0} & \boldsymbol{0} \\ \boldsymbol{0} & \boldsymbol{0} & \boldsymbol{L}_{1_\zeta} & \boldsymbol{0} \\ \boldsymbol{0} & \boldsymbol{0} & \boldsymbol{0} & \boldsymbol{L}_{1_\omega} \\ \boldsymbol{\Gamma}_{v,q}\boldsymbol{R}_{\mathrm{IB}}^{\mathsf{T}}(\boldsymbol{\lambda}, \boldsymbol{\zeta})\boldsymbol{L}_{1_q} & \boldsymbol{0} & \boldsymbol{0} & \boldsymbol{\Gamma}_{v,\omega}\boldsymbol{M}_v^{\mathsf{T}}\boldsymbol{I}\boldsymbol{L}_{1_\omega} \\ \boldsymbol{R}_{\mathrm{IB}}(\boldsymbol{\lambda}, \boldsymbol{\zeta})\boldsymbol{\Gamma}_{w,q}\boldsymbol{R}_{\mathrm{IB}}^{\mathsf{T}}(\boldsymbol{\lambda}, \boldsymbol{\zeta})\boldsymbol{L}_{1_q} & \boldsymbol{0} & \boldsymbol{0} & \boldsymbol{R}_{\mathrm{IB}}(\boldsymbol{\lambda}, \boldsymbol{\zeta})\boldsymbol{\Gamma}_{w,\omega}\boldsymbol{M}_v^{\mathsf{T}}\boldsymbol{I}\boldsymbol{L}_{1_\omega} \end{bmatrix} \quad (85)$$

V. Experimental Demonstration

A. Research Aircraft

The proposed observer was implemented both in simulation and flight test of a small fixed-wing UAS called the My Twin Dream (MTD), shown in Figure 2. It is a radio-controlled foam aircraft with counter-rotating electric motors and 10 in. diameter, 6 in. pitch (10x6) propellers. The aircraft was instrumented with a Cubepilot Cubeorange flight computer running PX4 firmware. The sensors onboard the aircraft include triple-redundant accelerometers and gyroscopes, two magnetometers, a Real-Time Kinematic (RTK) global navigation satellite system (GNSS) receiver, and a vaned air data unit for validation. The MTD was chosen for its simple construction, propeller location to accommodate the air data boom, and endurance of approximately 25 minutes. The MTD's physical properties are listed in Table 1.

Fig. 2 My Twin Dream research aircraft.

Table 1 My Twin Dream properties.

Property	Symbol	Value	Units
Mass	m	3.311	kg
Mean aerodynamic chord	$\bar{c}$	0.254	m
Projected wing span	b	1.800	m
Wing planform area	S	0.457	m^2
Roll moment of inertia	I_{xx}	0.319	kg-m^2
Pitch moment of inertia	I_{yy}	0.267	kg-m^2
Yaw moment of inertia	I_{zz}	0.471	kg-m^2
Product of inertia	I_{xz}	0.024	kg-m^2
Product of inertia	I_{xy}, I_{yz}	≈ 0	kg-m^2

A nonlinear aero-propulsive model for the MTD was identified from flight data using the methods detailed in [31–33]. For brevity, only a short overview of the system identification process is presented here. See [31–33] and references therein for representative details. Flight data was collected for the MTD in calm conditions using orthogonal phase-optimized multisine inputs [34] and was processed according to [31, 33]. Next, multivariate orthogonal function modeling [35] was used to determine the model structure with the minimum predicted squared error. The resulting non-dimensional force and moment coefficient models are

$$C_x = C_{x_\alpha}\alpha + C_{x_q}\frac{q\bar{c}}{2V} + C_{x_{\alpha^2}}\alpha^2 + C_{x_{\mathcal{J}_c}}\mathcal{J}_c + C_{x_0} \tag{86a}$$

$$C_y = C_{y_\beta}\beta + C_{y_r}\frac{rb}{2V} + C_{y_{\delta a}}\delta a + C_{y_{\delta r}}\delta r \tag{86b}$$

$$C_z = C_{z_\alpha}\alpha + C_{z_q}\frac{q\bar{c}}{2V} + C_{z_{\delta e}}\delta e + C_{z_0} \tag{86c}$$

$$C_l = C_{l_\beta}\beta + C_{l_p}\frac{pb}{2V} + C_{l_{\delta a}}\delta a \tag{86d}$$

$$C_m = C_{m_\alpha}\alpha + C_{m_q}\frac{q\bar{c}}{2V} + C_{m_{\delta e}}\delta e + C_{m_{\alpha^3}}\alpha^3 + C_{m_0} \tag{86e}$$

$$C_n = C_{n_\beta}\beta + C_{n_r}\frac{rb}{2V} + C_{n_{\delta a}}\delta a + C_{n_{\delta r}}\delta r \tag{86f}$$

Here, $\mathcal{J}_c = \mathcal{J} - \mathcal{J}_0$ where $\mathcal{J} = \Omega D/V$ is the inverse advance ratio [32], $\mathcal{J}_0$ is its nominal value, Ω is the propeller speed in rad/s, and D is the propeller diameter. Next, maximum likelihood parameter estimates were obtained using the output error method [34] in MATLAB using the System IDentification Programs for AirCraft (SIDPAC) software toolbox [36]. The final model structure is given in Appendix B. The model parameter estimates are shown in Table 3 and the valid model domain is given in Table 4. Figure 10 shows state prediction results obtained by integrating the final model with input data that were used in obtaining the model.

B. Wind Reconstruction

The wind estimates were compared to reconstructed wind data from a vaned air data unit (ADU) mounted out the nose of the aircraft as pictured in Figure 2. This sensor was developed, manufactured, and calibrated by the Nonlinear Systems Laboratory at Virginia Tech [37]. It consists of two 3D printed vanes attached to magnetic rotary encoders and a 3D printed Kiel probe connected to a MS5525DSO commercial off-the-shelf digital pressure sensor. The PWM rotary encoders are read at a sample rate of 200 Hz by a microcontroller that communicates with the autopilot over the CAN bus via a custom PX4 driver. The pressure sensor is natively supported by PX4 and configured to log calibrated airspeed data at 10 Hz.

Let V, α, and β_f be the airspeed, angle-of-attack, and flank angle reported by the ADU, respectively. By using GPS velocity measurements $\boldsymbol{v}_{\mathrm{i}}$ (accuracy of 0.05 m/s), autopilot attitude estimates (quaternion estimate standard deviations on the order of 10^{-3}), and angular velocity measurements from the calibrated gyroscope (noise and bias removed), the wind velocity may be reconstructed as

$$\boldsymbol{w} = \boldsymbol{v}_{\mathrm{i}} - \boldsymbol{R}_{\mathrm{IB}} \left(\boldsymbol{v}_{\mathrm{ADU}} - \boldsymbol{\omega} \times \boldsymbol{r}_{\mathrm{ADU}} \right) \tag{87}$$

where

$$\boldsymbol{v}_{\mathrm{ADU}} = \boldsymbol{R}_{\mathrm{BW}}(\alpha, \beta) \boldsymbol{e}_1 V$$

where $\boldsymbol{v}_{\mathrm{ADU}}$ is the air-relative velocity at the geometric center of the ADU vanes, whose position in the body frame is denoted $\boldsymbol{r}_{\mathrm{ADU}}$. The rotation matrix $\boldsymbol{R}_{\mathrm{BW}}(\alpha, \beta) = e^{-\boldsymbol{S}(\boldsymbol{e}_2)\alpha} e^{\boldsymbol{S}(\boldsymbol{e}_3)\beta}$, which maps free vectors from the wind frame to the body frame, is parameterized by the measured angle-of-attack, α, and the sideslip angle, $\beta = \tan^{-1}(\tan(\beta_f)\cos(\alpha))$. The accuracy of the reconstructed wind data can be characterized by propagating the measurement uncertainty through Eq. (87).

C. Simulation

First, the proposed observer was implemented in simulation with all assumptions satisfied in order to demonstrate the theoretical convergence guarantees. That is, the model is perfectly known, there is no measurement noise, and the wind is constant. The nonlinear system with linearized aerodynamics (Eq. (26)) was simulated in a uniform wind field with components $W_N = 10$ m/s, $W_E = -15$ m/s, and $W_D = -3$ m/s using MATLAB. The aircraft was given large-amplitude open loop controls resulting in the trajectory shown in Figure 3. The nonlinear passivity-based observer

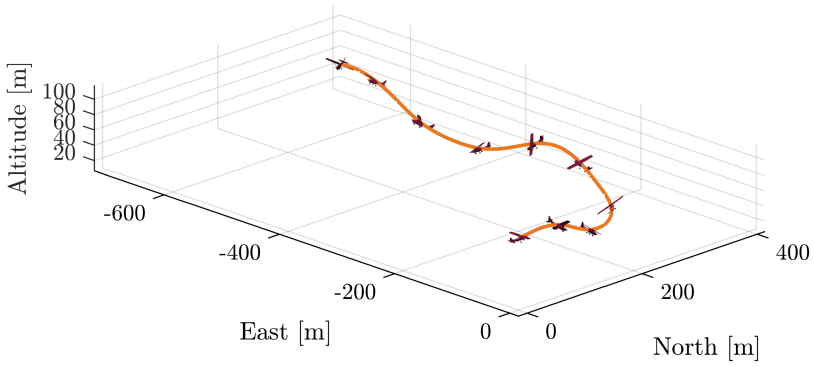

Fig. 3 Simulated aircraft trajectory in wind.

was implemented on this data. The set of LMIs in (65) were solved using CVX [38, 39] with the Mosek solver [40]. The lower bound $\underline{\gamma}$ was maximized for a fixed upper bound of $\overline{\gamma} = 5$, resulting in an optimal value of $\underline{\gamma} = 0.27$. The time history of wind estimate results are shown in Figure 4. The storage function, W, was also plotted for the simulation data and is shown in Figure 5. Here, we see W is strictly decreasing in time – consistent with Eq. (82).

D. Flight Test

Next, the proposed observer was implemented on flight test data for the MTD. These data were collected as part of a flight test campaign at Virginia Tech's Kentland Experimental Aerial Systems (KEAS) airfield on September 28th, 2022. The wind conditions were moderately turbulent for the aircraft's size (varying between 3 and 12 m/s) with a mean wind speed of 7.5 m/s coming from the northwest.

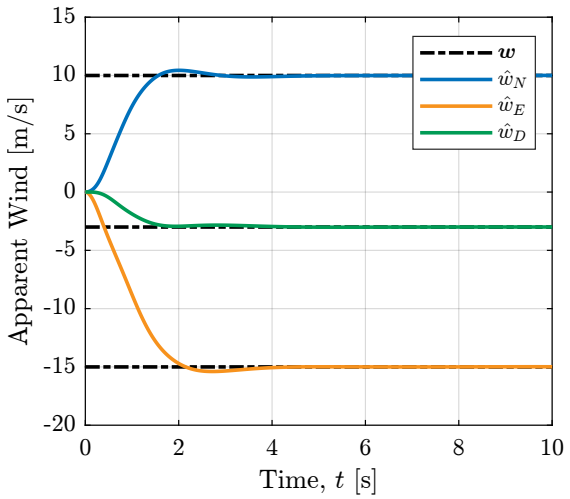

Fig. 4 Simulated wind estimates.

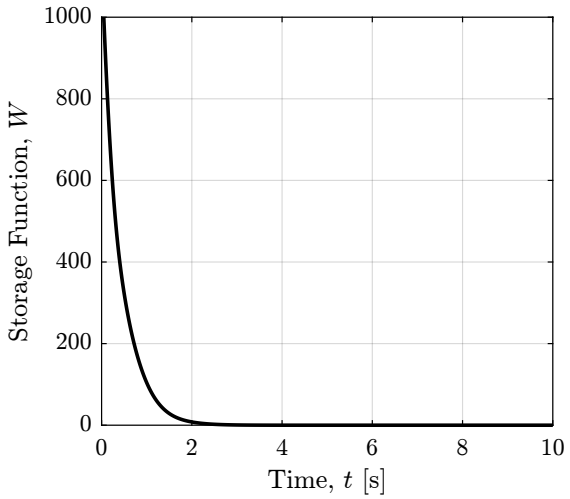

Fig. 5 Storage function.

Data were gathered in a grid pattern for two flights – one at 400 ft and the other at 700 ft above ground level (AGL). Since we are interested in maneuvering flight, nine maneuvers were selected in which the aircraft sharply executed a banked turn resulting in a heading change of 180 degrees.

The robust feasibility problem (67) was solved over the valid range of state and input values for the aerodynamic model (Table 4). The upper bound $\overline{\gamma}$ was fixed at 5, while the lower bound $\underline{\gamma}$ was maximized to yield an optimal value of 0.056. An additional constraint was placed such that the norm of $\boldsymbol{\Gamma}$ was less than 20 in order to maintain efficient and accurate numerical integration of the observer. The injection gain of the measured states, $\boldsymbol{L}_1$, was found by linearizing the aircraft dynamics about the nominal cruise flight condition, $\{\boldsymbol{x}_0, \boldsymbol{u}_0\}$, for the MTD and solving the algebraic Riccati equation, $\boldsymbol{AP} + \boldsymbol{PA}^\mathsf{T} - \boldsymbol{PC}^\mathsf{T}\boldsymbol{R}_c^{-1}\boldsymbol{CP} + \boldsymbol{Q}_c = \boldsymbol{0}$. Here, $\boldsymbol{A} = \partial \boldsymbol{f}/\partial \boldsymbol{x}|_{\boldsymbol{x}_0,\boldsymbol{u}_0}$ and $\boldsymbol{C} = [\mathbb{I}\ \ \boldsymbol{0}]^\mathsf{T}$. Using historical data collected for the MTD, the $\boldsymbol{Q}_c$ and $\boldsymbol{R}_c$ matrices were selected as typically done for a Kalman-Bucy filter. That is, $\boldsymbol{Q}_c$ was selected as the maximum power spectral density of the difference between the modeled and measured state derivatives over the frequency range of interest. The matrix $\boldsymbol{R}_c$ was chosen to be a time-averaged state estimate error covariance of $\boldsymbol{y} = \boldsymbol{x}_1$ from the autopilot's extended Kalman filter. The block-diagonal elements of the resulting gain matrix, $\boldsymbol{PC}^\mathsf{T}\boldsymbol{R}_c^{-1}$, were checked for invertibility and then selected to be the respective block-diagonal elements of $\boldsymbol{L}_1$. The initial conditions of the measured states, $\hat{\boldsymbol{x}}_1(0)$ were set to their initial measured values, $\boldsymbol{y}(0)$. The initial condition for the relative velocity, $\hat{\boldsymbol{v}}_\mathrm{r}(0)$ was set to be the aircraft's nominal trim value in calm air, while the initial wind estimate, $\hat{\boldsymbol{w}}$ was set to zero.

The passivity-based observer was implemented on all nine turn maneuvers with the same tuning parameters. The root-mean-squared error, $\mathrm{RMSE}(x) = (\frac{1}{N}\sum_{k=1}^{N}(\hat{x}(t_k) - x(t_k))^2)^{1/2}$, of the wind components were computed for each 40 second maneuver, as tabulated in Table 2. The typical RMSE value is less than 1 m/s. The RMSE for the vertical component is typically smaller than for the horizontal components, due to a fixed-wing aircraft's inherent sensitivity to vertical velocity fluctuations.

As an example, the passivity-based observer results for Maneuver 9 are considered. The trajectory that the aircraft follows during this maneuver is shown in Figure 6. The time histories of the apparent wind estimates are shown in Figure 7 along with the "truth values" reconstructed according to Section V.B. Examining Figure 7, the wind estimates appear to converge within an ultimate bound around the true values. Suppose we consider the modeling error as a disturbance to the error system, on which we can place some upper bound. Then since the state estimate error is globally asymptotically stable for the ideal system, there exists some neighborhood about the origin for which the error system is locally input-to-state stable with respect to these disturbances [41, Ch. 5]. The norms of the matrix-valued bounding functions, $\boldsymbol{\Psi}$ and $\boldsymbol{\Lambda}$, are also plotted in Figure 8. Recall, the function $\boldsymbol{\Psi}$ bounds the nonlinear growth of of $\tilde{\boldsymbol{x}}_1$, which is typically smaller than that of $\tilde{\boldsymbol{x}}_2$ (bounded by $\boldsymbol{\Lambda}$).

The variation in convergence among the set of maneuvers was also analyzed. Point-wise in time, the sample mean and standard deviations were computed across the set of wind estimate error trajectories. Time histories for the first one second of these data are shown in Figure 9, where we see consistent convergence towards some ultimate bound about zero error.

Table 2 Flight test maneuvers.

Maneuver	Flight Number	RMSE(w_N) [m/s]	RMSE(w_E) [m/s]	RMSE(w_D) [m/s]
1	1	0.97	0.58	0.59
2	1	0.83	0.70	0.68
3	1	0.86	0.76	0.69
4	1	0.74	0.55	0.56
5	1	0.75	0.75	0.56
6	2	1.06	0.68	0.41
7	2	1.11	0.81	0.46
8	2	0.84	0.93	0.70
9	2	1.32	1.04	0.63

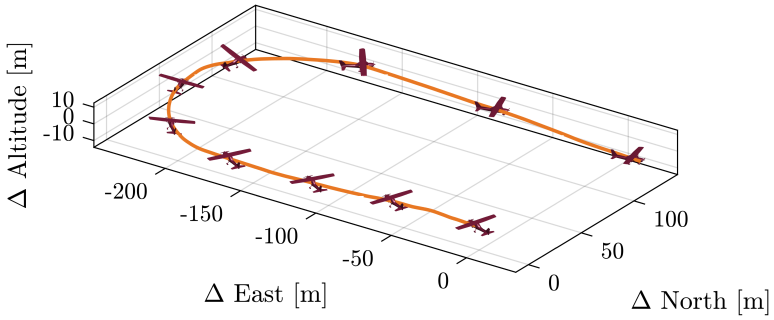

Fig. 6 Trajectory of maneuver 9 (aircraft not to scale)**.**

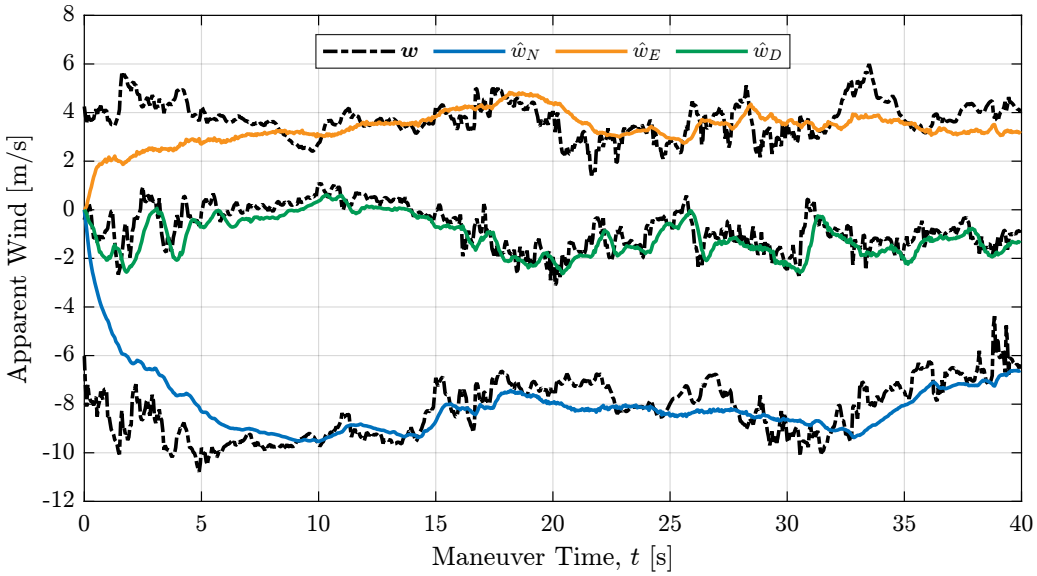

Fig. 7 Wind estimates for maneuver 9.

VI. Conclusions and Future Work

The design and experimental demonstration of a global nonlinear passivity-based wind observer for aircraft was presented. Under some mild assumptions about the wind field and aircraft's aerodynamics, we obtain rigorous guarantees on the convergence of wind estimates across the entire flight envelope. Such strong results help expand the range

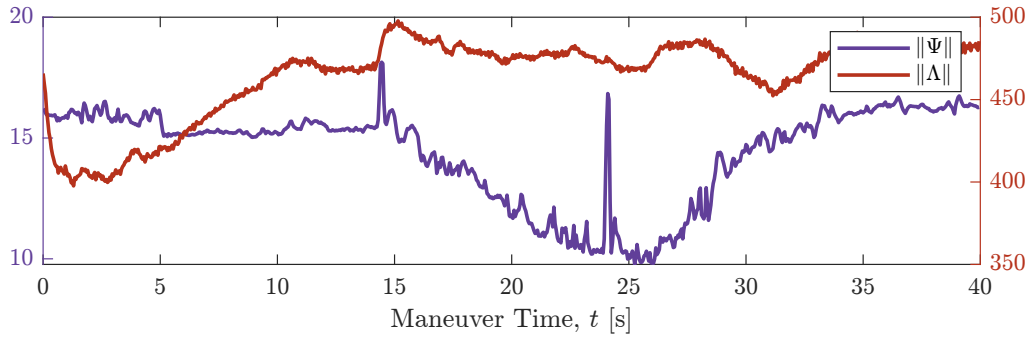

Fig. 8 Bounding functions for maneuver 9.

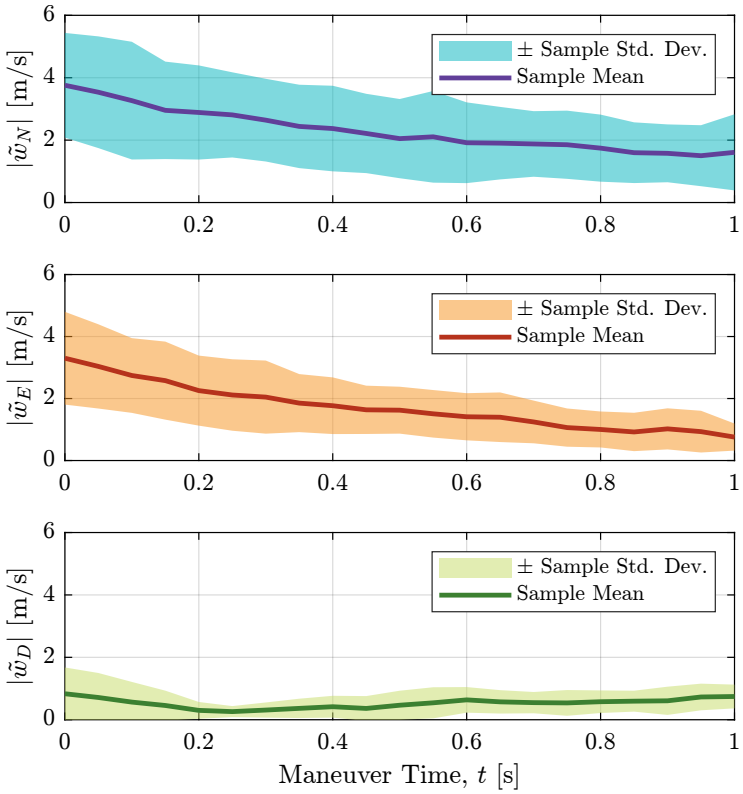

Fig. 9 Variation in wind estimate error transients.

of flight conditions for which accurate wind estimates can be made. Through a judicious choice of the output error injection gain matrix (specifically, the component denoted $\boldsymbol{L}_2$ in the narrative), linear matrix inequality conditions were obtained that not only prove the observer error dynamics are globally minimum phase, but also provide a constructive design procedure. Explicit formulas were derived for the bounding functions that define the matrix-valued output error scaling (denoted $\boldsymbol{K}$ in the narrative), allowing the observer to be implemented on flight data. The result of this paper is generally applicable to a wide variety of aircraft, providing a powerful capability to estimate wind with rigorous guarantees even in adverse conditions. Future work involves relaxing the assumption of linear aerodynamics, as well as analyzing the effect of aircraft and wind modeling error on stability of the observer.

Acknowledgments

The authors gratefully acknowledge the Virginia Space Grant Consortium under the graduate research fellowship and NASA under Grant No. 80NSSC20M0162. The first author thanks Jean-Michel Fahmi, Ying-Chun Chen, and

Zakia Ahmed of the Virginia Tech Nonlinear Systems Laboratory for their discussions on energy-based and nonlinear control theory.

A. Proof of Proposition 1

We start by expanding

$$\frac{\partial V^*}{\partial \tilde{\boldsymbol{x}}_2}\tilde{\boldsymbol{\phi}}_2(\tilde{\boldsymbol{x}}_1, \boldsymbol{L}_2(\boldsymbol{y})\boldsymbol{L}_1^{-1}\tilde{\boldsymbol{x}}_1; \boldsymbol{x}_1, \tilde{\boldsymbol{x}}_2 + \boldsymbol{x}_2; \boldsymbol{u}) - \frac{\partial V^*}{\partial \tilde{\boldsymbol{x}}_2}\frac{\mathrm{d}}{\mathrm{d}t}\left(\boldsymbol{L}_2(\boldsymbol{y})\boldsymbol{L}_1^{-1}\right)\tilde{\boldsymbol{x}}_1 + \tilde{\boldsymbol{x}}_1^{\mathsf{T}}\boldsymbol{L}_1^{-1}\tilde{\boldsymbol{f}}_1(\tilde{\boldsymbol{x}}_1, \tilde{\boldsymbol{x}}_2 + \boldsymbol{L}_2(\boldsymbol{y})\boldsymbol{L}_1^{-1}\tilde{\boldsymbol{x}}_1; \boldsymbol{x}_1, \boldsymbol{x}_2; \boldsymbol{u}) \quad \text{(A.1)}$$

and replacing $\boldsymbol{x}_2$ with $\hat{\boldsymbol{x}}_2 - \tilde{\boldsymbol{x}}_2$ to yield

$$\begin{aligned}
&- \tilde{\boldsymbol{x}}_2^{\mathsf{T}}\frac{\mathrm{d}}{\mathrm{d}t}\left(\boldsymbol{L}_2(\boldsymbol{y})\boldsymbol{L}_1^{-1}\right)\tilde{\boldsymbol{x}}_1 + \tilde{\boldsymbol{v}}_{\mathrm{r}}^{\mathsf{T}}\tilde{\boldsymbol{\phi}}_{2_{v_{\mathrm{r}}}}(\tilde{\boldsymbol{x}}_1, \boldsymbol{L}_2\boldsymbol{L}_1^{-1}\tilde{\boldsymbol{x}}_1; \boldsymbol{x}_1, \hat{\boldsymbol{x}}_2; \boldsymbol{u}) + \tilde{\boldsymbol{w}}^{\mathsf{T}}\tilde{\boldsymbol{\phi}}_{2_w}(\tilde{\boldsymbol{x}}_1, \boldsymbol{L}_2\boldsymbol{L}_1^{-1}\tilde{\boldsymbol{x}}_1; \boldsymbol{x}_1, \hat{\boldsymbol{x}}_2; \boldsymbol{u}) \\
&\quad + \tilde{\boldsymbol{q}}^{\mathsf{T}}\boldsymbol{L}_{1_q}^{-1}\tilde{\boldsymbol{f}}_{1_q}(\tilde{\boldsymbol{x}}_1, \tilde{\boldsymbol{x}}_2 + \boldsymbol{L}_2\boldsymbol{L}_1^{-1}\tilde{\boldsymbol{x}}_1; \boldsymbol{x}_1, \hat{\boldsymbol{x}}_2 - \tilde{\boldsymbol{x}}_2; \boldsymbol{u}) + \tilde{\boldsymbol{\lambda}}^{\mathsf{T}}\boldsymbol{L}_{1_\lambda}^{-1}\tilde{\boldsymbol{f}}_{1_\lambda}(\tilde{\boldsymbol{x}}_1, \tilde{\boldsymbol{x}}_2 + \boldsymbol{L}_2\boldsymbol{L}_1^{-1}\tilde{\boldsymbol{x}}_1; \boldsymbol{x}_1, \hat{\boldsymbol{x}}_2 - \tilde{\boldsymbol{x}}_2; \boldsymbol{u}) \\
&\quad + \tilde{\boldsymbol{\zeta}}^{\mathsf{T}}\boldsymbol{L}_{1_\zeta}^{-1}\tilde{\boldsymbol{f}}_{1_\zeta}(\tilde{\boldsymbol{x}}_1, \tilde{\boldsymbol{x}}_2 + \boldsymbol{L}_2\boldsymbol{L}_1^{-1}\tilde{\boldsymbol{x}}_1; \boldsymbol{x}_1, \hat{\boldsymbol{x}}_2 - \tilde{\boldsymbol{x}}_2; \boldsymbol{u}) + \tilde{\boldsymbol{\omega}}^{\mathsf{T}}\boldsymbol{L}_{1_\omega}^{-1}\tilde{\boldsymbol{f}}_{1_\omega}(\tilde{\boldsymbol{x}}_1, \tilde{\boldsymbol{x}}_2 + \boldsymbol{L}_2\boldsymbol{L}_1^{-1}\tilde{\boldsymbol{x}}_1; \boldsymbol{x}_1, \hat{\boldsymbol{x}}_2 - \tilde{\boldsymbol{x}}_2; \boldsymbol{u}) \quad \text{(A.2)}
\end{aligned}$$

With $\boldsymbol{L}_2$ given in Eq. (57), let us rewrite the components of $\tilde{\boldsymbol{\phi}}_2$ from Eq. (48) as

$$\begin{aligned}
\tilde{\boldsymbol{\phi}}_{2_{v_{\mathrm{r}}}}(\tilde{\boldsymbol{x}}_1, \tilde{\boldsymbol{x}}_2; \boldsymbol{x}_1, \boldsymbol{x}_2; \boldsymbol{u}) &= \boldsymbol{S}(\boldsymbol{v}_{\mathrm{r}})\tilde{\boldsymbol{\omega}} - \boldsymbol{S}(\tilde{\boldsymbol{\omega}} + \boldsymbol{\omega})\tilde{\boldsymbol{v}}_{\mathrm{r}} + g\tilde{\boldsymbol{\zeta}} + \frac{1}{m}\boldsymbol{F}_v\tilde{\boldsymbol{v}}_{\mathrm{r}} + \frac{1}{m}\boldsymbol{F}_\omega\tilde{\boldsymbol{\omega}} \\
&\quad - \boldsymbol{\Gamma}_{v,q}\boldsymbol{R}_{\mathrm{IB}}^{\mathsf{T}}(\boldsymbol{\lambda}, \boldsymbol{\zeta})\left(\boldsymbol{R}_{\mathrm{IB}}(\tilde{\boldsymbol{\lambda}} + \boldsymbol{\lambda}, \tilde{\boldsymbol{\zeta}} + \boldsymbol{\zeta})\tilde{\boldsymbol{v}}_{\mathrm{r}} + \left(\boldsymbol{R}_{\mathrm{IB}}(\tilde{\boldsymbol{\lambda}} + \boldsymbol{\lambda}, \tilde{\boldsymbol{\zeta}} + \boldsymbol{\zeta}) - \boldsymbol{R}_{\mathrm{IB}}(\boldsymbol{\lambda}, \boldsymbol{\zeta})\right)\boldsymbol{v}_{\mathrm{r}} + \tilde{\boldsymbol{w}}\right) \\
&\quad - \boldsymbol{\Gamma}_{v,\omega}\boldsymbol{M}_v^{\mathsf{T}}\Big(\boldsymbol{S}(\boldsymbol{I}(\tilde{\boldsymbol{\omega}} + \boldsymbol{\omega}))\tilde{\boldsymbol{\omega}} - \boldsymbol{S}(\boldsymbol{\omega})\boldsymbol{I}\tilde{\boldsymbol{\omega}} + \boldsymbol{M}_v\tilde{\boldsymbol{v}}_{\mathrm{r}} + \boldsymbol{M}_\omega\tilde{\boldsymbol{\omega}}\Big) \quad \text{(A.3a)} \\
\tilde{\boldsymbol{\phi}}_{2_w}(\tilde{\boldsymbol{x}}_1, \tilde{\boldsymbol{x}}_2; \boldsymbol{x}_1, \boldsymbol{x}_2; \boldsymbol{u}) &= -\boldsymbol{R}_{\mathrm{IB}}(\boldsymbol{\lambda}, \boldsymbol{\zeta})\boldsymbol{\Gamma}_{w,q}\boldsymbol{R}_{\mathrm{IB}}^{\mathsf{T}}(\boldsymbol{\lambda}, \boldsymbol{\zeta})\Big(\boldsymbol{R}_{\mathrm{IB}}(\tilde{\boldsymbol{\lambda}} + \boldsymbol{\lambda}, \tilde{\boldsymbol{\zeta}} + \boldsymbol{\zeta})\tilde{\boldsymbol{v}}_{\mathrm{r}} \\
&\quad + \left(\boldsymbol{R}_{\mathrm{IB}}(\tilde{\boldsymbol{\lambda}} + \boldsymbol{\lambda}, \tilde{\boldsymbol{\zeta}} + \boldsymbol{\zeta}) - \boldsymbol{R}_{\mathrm{IB}}(\boldsymbol{\lambda}, \boldsymbol{\zeta})\right)\boldsymbol{v}_{\mathrm{r}} + \tilde{\boldsymbol{w}}\Big) - \boldsymbol{R}_{\mathrm{IB}}(\boldsymbol{\lambda}, \boldsymbol{\zeta})\boldsymbol{\Gamma}_{w,\omega}\boldsymbol{M}_v^{\mathsf{T}}\Big(\boldsymbol{S}(\boldsymbol{I}(\tilde{\boldsymbol{\omega}} + \boldsymbol{\omega}))\tilde{\boldsymbol{\omega}} \\
&\quad - \boldsymbol{S}(\boldsymbol{\omega})\boldsymbol{I}\tilde{\boldsymbol{\omega}} + \boldsymbol{M}_v\tilde{\boldsymbol{v}}_{\mathrm{r}} + \boldsymbol{M}_\omega\tilde{\boldsymbol{\omega}}\Big) \quad \text{(A.3b)}
\end{aligned}$$

Using

$$\boldsymbol{L}_2\boldsymbol{L}_1^{-1}\tilde{\boldsymbol{x}}_1 = \begin{bmatrix}\boldsymbol{L}_{2_{v,q}}\boldsymbol{L}_{1_q}^{-1}\tilde{\boldsymbol{q}} + \boldsymbol{L}_{2_{v,\omega}}\boldsymbol{L}_{1_\omega}^{-1}\tilde{\boldsymbol{\omega}} \\ \boldsymbol{L}_{2_{w,q}}\boldsymbol{L}_{1_q}^{-1}\tilde{\boldsymbol{q}} + \boldsymbol{L}_{2_{w,\omega}}\boldsymbol{L}_{1_\omega}^{-1}\tilde{\boldsymbol{\omega}}\end{bmatrix} = \begin{bmatrix}\boldsymbol{\Gamma}_{v,q}\boldsymbol{R}_{\mathrm{IB}}^{\mathsf{T}}(\boldsymbol{\lambda}, \boldsymbol{\zeta})\tilde{\boldsymbol{q}} + \boldsymbol{\Gamma}_{v,\omega}\boldsymbol{M}_v^{\mathsf{T}}\boldsymbol{I}\tilde{\boldsymbol{\omega}} \\ \boldsymbol{R}_{\mathrm{IB}}(\boldsymbol{\lambda}, \boldsymbol{\zeta})\boldsymbol{\Gamma}_{w,q}\boldsymbol{R}_{\mathrm{IB}}^{\mathsf{T}}(\boldsymbol{\lambda}, \boldsymbol{\zeta})\tilde{\boldsymbol{q}} + \boldsymbol{R}_{\mathrm{IB}}(\boldsymbol{\lambda}, \boldsymbol{\zeta})\boldsymbol{\Gamma}_{w,\omega}\boldsymbol{M}_v^{\mathsf{T}}\boldsymbol{I}\tilde{\boldsymbol{\omega}}\end{bmatrix} \quad \text{(A.4)}$$

and the expressions for $\tilde{\boldsymbol{\phi}}_2$ in Eq. (A.3), we compute the necessary terms in Eq. (A.2) as

$$\begin{aligned}
\tilde{\boldsymbol{\phi}}_{2_{v_{\mathrm{r}}}}(\tilde{\boldsymbol{x}}_1, \boldsymbol{L}_2\boldsymbol{L}_1^{-1}\tilde{\boldsymbol{x}}_1; \boldsymbol{x}_1, \hat{\boldsymbol{x}}_2; \boldsymbol{u}) &= \Big(\Big(\frac{1}{m}\boldsymbol{F}_v - \boldsymbol{S}(\tilde{\boldsymbol{\omega}} + \boldsymbol{\omega})\Big)\boldsymbol{\Gamma}_{v,q} - \boldsymbol{\Gamma}_{v,q}\boldsymbol{R}_{\mathrm{IB}}^{\mathsf{T}}(\boldsymbol{\lambda}, \boldsymbol{\zeta})\boldsymbol{R}_{\mathrm{IB}}(\tilde{\boldsymbol{\lambda}} + \boldsymbol{\lambda}, \tilde{\boldsymbol{\zeta}} + \boldsymbol{\zeta})\boldsymbol{\Gamma}_{v,q} - \boldsymbol{\Gamma}_{v,q}\boldsymbol{\Gamma}_{w,q} \\
&\quad - \boldsymbol{\Gamma}_{v,\omega}\boldsymbol{M}_v^{\mathsf{T}}\boldsymbol{M}_v\boldsymbol{\Gamma}_{v,q}\Big)\boldsymbol{R}_{\mathrm{IB}}^{\mathsf{T}}(\boldsymbol{\lambda}, \boldsymbol{\zeta})\tilde{\boldsymbol{q}} + g\tilde{\boldsymbol{\zeta}} + \Big(\Big(\frac{1}{m}\boldsymbol{F}_v - \boldsymbol{S}(\tilde{\boldsymbol{\omega}} + \boldsymbol{\omega})\Big)\boldsymbol{\Gamma}_{v,\omega}\boldsymbol{M}_v^{\mathsf{T}}\boldsymbol{I} \\
&\quad + \frac{1}{m}\boldsymbol{F}_\omega + \boldsymbol{S}(\hat{\boldsymbol{v}}_{\mathrm{r}}) - \boldsymbol{\Gamma}_{v,q}\left(\boldsymbol{R}_{\mathrm{IB}}^{\mathsf{T}}(\boldsymbol{\lambda}, \boldsymbol{\zeta})\boldsymbol{R}_{\mathrm{IB}}(\tilde{\boldsymbol{\lambda}} + \boldsymbol{\lambda}, \tilde{\boldsymbol{\zeta}} + \boldsymbol{\zeta})\boldsymbol{\Gamma}_{v,\omega} + \boldsymbol{\Gamma}_{w,\omega}\right)\boldsymbol{M}_v^{\mathsf{T}}\boldsymbol{I} \\
&\quad - \boldsymbol{\Gamma}_{v,\omega}\boldsymbol{M}_v^{\mathsf{T}}\Big(\boldsymbol{S}(\boldsymbol{I}(\tilde{\boldsymbol{\omega}} + \boldsymbol{\omega})) - \boldsymbol{S}(\boldsymbol{\omega})\boldsymbol{I} + \boldsymbol{M}_\omega + \boldsymbol{M}_v\boldsymbol{\Gamma}_{v,\omega}\boldsymbol{M}_v^{\mathsf{T}}\boldsymbol{I}\Big)\Big)\tilde{\boldsymbol{\omega}} \\
&\quad - \boldsymbol{\Gamma}_{v,q}\boldsymbol{R}_{\mathrm{IB}}^{\mathsf{T}}(\boldsymbol{\lambda}, \boldsymbol{\zeta})\left(\boldsymbol{R}_{\mathrm{IB}}(\tilde{\boldsymbol{\lambda}} + \boldsymbol{\lambda}, \tilde{\boldsymbol{\zeta}} + \boldsymbol{\zeta}) - \boldsymbol{R}_{\mathrm{IB}}(\boldsymbol{\lambda}, \boldsymbol{\zeta})\right)\hat{\boldsymbol{v}}_{\mathrm{r}} \quad \text{(A.5a)}
\end{aligned}$$

$$\begin{aligned}\tilde{\boldsymbol{\phi}}_{2_w}(\tilde{\boldsymbol{x}}_1, \boldsymbol{L}_2\boldsymbol{L}_1^{-1}\tilde{\boldsymbol{x}}_1; \boldsymbol{x}_1, \hat{\boldsymbol{x}}_2; \boldsymbol{u}) = \boldsymbol{R}_{\mathrm{IB}}(\boldsymbol{\lambda}, \boldsymbol{\zeta})\Big(&- \boldsymbol{\Gamma}_{w,q}\left(\boldsymbol{R}_{\mathrm{IB}}^{\mathsf{T}}(\boldsymbol{\lambda}, \boldsymbol{\zeta})\boldsymbol{R}_{\mathrm{IB}}(\tilde{\boldsymbol{\lambda}} + \boldsymbol{\lambda}, \tilde{\boldsymbol{\zeta}} + \boldsymbol{\zeta})\boldsymbol{\Gamma}_{v,q} + \boldsymbol{\Gamma}_{w,q}\right) \\ &- \boldsymbol{\Gamma}_{w,\omega}\boldsymbol{M}_v^{\mathsf{T}}\boldsymbol{M}_v\boldsymbol{\Gamma}_{v,q}\Big)\boldsymbol{R}_{\mathrm{IB}}^{\mathsf{T}}(\boldsymbol{\lambda}, \boldsymbol{\zeta})\tilde{\boldsymbol{q}} \\ &+ \boldsymbol{R}_{\mathrm{IB}}(\boldsymbol{\lambda}, \boldsymbol{\zeta})\Big(- \boldsymbol{\Gamma}_{w,q}\left(\boldsymbol{R}_{\mathrm{IB}}^{\mathsf{T}}(\boldsymbol{\lambda}, \boldsymbol{\zeta})\boldsymbol{R}_{\mathrm{IB}}(\tilde{\boldsymbol{\lambda}} + \boldsymbol{\lambda}, \tilde{\boldsymbol{\zeta}} + \boldsymbol{\zeta})\boldsymbol{\Gamma}_{v,\omega} + \boldsymbol{\Gamma}_{w,\omega}\right)\boldsymbol{M}_v^{\mathsf{T}}\boldsymbol{I} \\ &- \boldsymbol{\Gamma}_{w,\omega}\boldsymbol{M}_v^{\mathsf{T}}\Big(\boldsymbol{S}(\boldsymbol{I}(\tilde{\boldsymbol{\omega}} + \boldsymbol{\omega})) - \boldsymbol{S}(\boldsymbol{\omega})\boldsymbol{I} + \boldsymbol{M}_\omega + \boldsymbol{M}_v\boldsymbol{\Gamma}_{v,\omega}\boldsymbol{M}_v^{\mathsf{T}}\boldsymbol{I}\Big)\Big)\tilde{\boldsymbol{\omega}} \\ &- \boldsymbol{R}_{\mathrm{IB}}(\boldsymbol{\lambda}, \boldsymbol{\zeta})\boldsymbol{\Gamma}_{w,q}\boldsymbol{R}_{\mathrm{IB}}^{\mathsf{T}}(\boldsymbol{\lambda}, \boldsymbol{\zeta})\left(\boldsymbol{R}_{\mathrm{IB}}(\tilde{\boldsymbol{\lambda}} + \boldsymbol{\lambda}, \tilde{\boldsymbol{\zeta}} + \boldsymbol{\zeta}) - \boldsymbol{R}_{\mathrm{IB}}(\boldsymbol{\lambda}, \boldsymbol{\zeta})\right)\hat{\boldsymbol{v}}_{\mathrm{r}} \end{aligned} \tag{A.5b}$$

$$\begin{aligned}\tilde{\boldsymbol{f}}_{1_q}(\tilde{\boldsymbol{x}}_1, \tilde{\boldsymbol{x}}_2 + \boldsymbol{L}_2\boldsymbol{L}_1^{-1}\tilde{\boldsymbol{x}}_1; \boldsymbol{x}_1, \hat{\boldsymbol{x}}_2 - \tilde{\boldsymbol{x}}_2; \boldsymbol{u}) = &\Big(\boldsymbol{R}_{\mathrm{IB}}(\boldsymbol{\lambda}, \boldsymbol{\zeta})\boldsymbol{\Gamma}_{w,q}\boldsymbol{R}_{\mathrm{IB}}^{\mathsf{T}}(\boldsymbol{\lambda}, \boldsymbol{\zeta}) + \boldsymbol{R}_{\mathrm{IB}}(\tilde{\boldsymbol{\lambda}} + \boldsymbol{\lambda}, \tilde{\boldsymbol{\zeta}} + \boldsymbol{\zeta})\boldsymbol{\Gamma}_{v,q}\boldsymbol{R}_{\mathrm{IB}}^{\mathsf{T}}(\boldsymbol{\lambda}, \boldsymbol{\zeta})\Big)\tilde{\boldsymbol{q}} \\ &+ \Big(\boldsymbol{R}_{\mathrm{IB}}(\boldsymbol{\lambda}, \boldsymbol{\zeta})\boldsymbol{\Gamma}_{w,\omega} + \boldsymbol{R}_{\mathrm{IB}}(\tilde{\boldsymbol{\lambda}} + \boldsymbol{\lambda}, \tilde{\boldsymbol{\zeta}} + \boldsymbol{\zeta})\boldsymbol{\Gamma}_{v,\omega}\Big)\boldsymbol{M}_v^{\mathsf{T}}\boldsymbol{I}\tilde{\boldsymbol{\omega}} + \tilde{\boldsymbol{w}} \\ &+ \boldsymbol{R}_{\mathrm{IB}}(\boldsymbol{\lambda}, \boldsymbol{\zeta})\tilde{\boldsymbol{v}}_{\mathrm{r}} + \Big(\boldsymbol{R}_{\mathrm{IB}}(\tilde{\boldsymbol{\lambda}} + \boldsymbol{\lambda}, \tilde{\boldsymbol{\zeta}} + \boldsymbol{\zeta}) - \boldsymbol{R}_{\mathrm{IB}}(\boldsymbol{\lambda}, \boldsymbol{\zeta})\Big)\hat{\boldsymbol{v}}_{\mathrm{r}} \end{aligned} \tag{A.5c}$$

$$\tilde{\boldsymbol{f}}_{1_\lambda}(\tilde{\boldsymbol{x}}_1, \tilde{\boldsymbol{x}}_2 + \boldsymbol{L}_2\boldsymbol{L}_1^{-1}\tilde{\boldsymbol{x}}_1; \boldsymbol{x}_1, \hat{\boldsymbol{x}}_2 - \tilde{\boldsymbol{x}}_2; \boldsymbol{u}) = \boldsymbol{S}(\tilde{\boldsymbol{\lambda}} + \boldsymbol{\lambda})\tilde{\boldsymbol{\omega}} - \boldsymbol{S}(\boldsymbol{\omega})\tilde{\boldsymbol{\lambda}} \tag{A.5d}$$

$$\tilde{\boldsymbol{f}}_{1_\zeta}(\tilde{\boldsymbol{x}}_1, \tilde{\boldsymbol{x}}_2 + \boldsymbol{L}_2\boldsymbol{L}_1^{-1}\tilde{\boldsymbol{x}}_1; \boldsymbol{x}_1, \hat{\boldsymbol{x}}_2 - \tilde{\boldsymbol{x}}_2; \boldsymbol{u}) = \boldsymbol{S}(\tilde{\boldsymbol{\zeta}} + \boldsymbol{\zeta})\tilde{\boldsymbol{\omega}} - \boldsymbol{S}(\boldsymbol{\omega})\tilde{\boldsymbol{\zeta}} \tag{A.5e}$$

$$\begin{aligned}\tilde{\boldsymbol{f}}_{1_\omega}(\tilde{\boldsymbol{x}}_1, \tilde{\boldsymbol{x}}_2 + \boldsymbol{L}_2\boldsymbol{L}_1^{-1}\tilde{\boldsymbol{x}}_1; \boldsymbol{x}_1, \hat{\boldsymbol{x}}_2 - \tilde{\boldsymbol{x}}_2; \boldsymbol{u}) = &\boldsymbol{I}^{-1}\boldsymbol{M}_v\boldsymbol{\Gamma}_{v,q}\boldsymbol{R}_{\mathrm{IB}}^{\mathsf{T}}(\boldsymbol{\lambda}, \boldsymbol{\zeta})\tilde{\boldsymbol{q}} + \boldsymbol{I}^{-1}\boldsymbol{M}_v\tilde{\boldsymbol{v}}_{\mathrm{r}} \\ &+ \boldsymbol{I}^{-1}\left(\boldsymbol{S}(\boldsymbol{I}(\tilde{\boldsymbol{\omega}} + \boldsymbol{\omega})) - \boldsymbol{S}(\boldsymbol{\omega})\boldsymbol{I} + \boldsymbol{M}_\omega + \boldsymbol{M}_v\boldsymbol{\Gamma}_{v,\omega}\boldsymbol{M}_v^{\mathsf{T}}\boldsymbol{I}\right)\tilde{\boldsymbol{\omega}} \end{aligned} \tag{A.5f}$$

These expressions in Eq. (A.5) are then substituted into Eq. (A.2) along with the expression for $\frac{\mathrm{d}}{\mathrm{d}t}(\boldsymbol{L}_2(\boldsymbol{y})\boldsymbol{L}_1^{-1})$ from Eq. (74) to yield

$$
\begin{aligned}
&\tilde{\boldsymbol{v}}_{\mathrm{r}}^{\mathsf{T}}\boldsymbol{\Gamma}_{v,q}\boldsymbol{S}(\boldsymbol{\omega})\boldsymbol{R}_{\mathrm{IB}}^{\mathsf{T}}\tilde{\boldsymbol{q}} - \tilde{\boldsymbol{w}}^{\mathsf{T}}\boldsymbol{R}_{\mathrm{IB}}\left(\boldsymbol{S}(\boldsymbol{\omega})\boldsymbol{\Gamma}_{w,q} - \boldsymbol{\Gamma}_{w,q}\boldsymbol{S}(\boldsymbol{\omega})\right)\boldsymbol{R}_{\mathrm{IB}}^{\mathsf{T}}\tilde{\boldsymbol{q}} - \tilde{\boldsymbol{w}}^{\mathsf{T}}\boldsymbol{R}_{\mathrm{IB}}\boldsymbol{S}(\boldsymbol{\omega})\boldsymbol{\Gamma}_{w,\omega}\boldsymbol{M}_v^{\mathsf{T}}\boldsymbol{I}\tilde{\boldsymbol{\omega}} \\
&+\tilde{\boldsymbol{v}}_{\mathrm{r}}^{\mathsf{T}}\Bigg(\Big(\frac{1}{m}\boldsymbol{F}_v - \boldsymbol{S}(\tilde{\boldsymbol{\omega}}+\boldsymbol{\omega})\Big)\boldsymbol{\Gamma}_{v,q} - \boldsymbol{\Gamma}_{v,q}\boldsymbol{R}_{\mathrm{IB}}^{\mathsf{T}}(\boldsymbol{\lambda},\boldsymbol{\zeta})\boldsymbol{R}_{\mathrm{IB}}(\tilde{\boldsymbol{\lambda}}+\boldsymbol{\lambda},\tilde{\boldsymbol{\zeta}}+\boldsymbol{\zeta})\boldsymbol{\Gamma}_{v,q} - \boldsymbol{\Gamma}_{v,q}\boldsymbol{\Gamma}_{w,q} - \boldsymbol{\Gamma}_{v,\omega}\boldsymbol{M}_v^{\mathsf{T}}\boldsymbol{M}_v\boldsymbol{\Gamma}_{v,q}\Bigg)\boldsymbol{R}_{\mathrm{IB}}^{\mathsf{T}}(\boldsymbol{\lambda},\boldsymbol{\zeta})\tilde{\boldsymbol{q}} \\
&+\tilde{\boldsymbol{v}}_{\mathrm{r}}^{\mathsf{T}}g\tilde{\boldsymbol{\zeta}} + \tilde{\boldsymbol{v}}_{\mathrm{r}}^{\mathsf{T}}\Bigg(\Big(\frac{1}{m}\boldsymbol{F}_v - \boldsymbol{S}(\tilde{\boldsymbol{\omega}}+\boldsymbol{\omega})\Big)\boldsymbol{\Gamma}_{v,\omega}\boldsymbol{M}_v^{\mathsf{T}}\boldsymbol{I} - \boldsymbol{\Gamma}_{v,q}\Big(\boldsymbol{R}_{\mathrm{IB}}^{\mathsf{T}}(\boldsymbol{\lambda},\boldsymbol{\zeta})\boldsymbol{R}_{\mathrm{IB}}(\tilde{\boldsymbol{\lambda}}+\boldsymbol{\lambda},\tilde{\boldsymbol{\zeta}}+\boldsymbol{\zeta})\boldsymbol{\Gamma}_{v,\omega} + \boldsymbol{\Gamma}_{w,\omega}\Big)\boldsymbol{M}_v^{\mathsf{T}}\boldsymbol{I} \\
&\qquad +\frac{1}{m}\boldsymbol{F}_\omega + \boldsymbol{S}(\hat{\boldsymbol{v}}_{\mathrm{r}}) - \boldsymbol{\Gamma}_{v,\omega}\boldsymbol{M}_v^{\mathsf{T}}\Big(\boldsymbol{S}(\boldsymbol{I}(\tilde{\boldsymbol{\omega}}+\boldsymbol{\omega})) - \boldsymbol{S}(\boldsymbol{\omega})\boldsymbol{I} + \boldsymbol{M}_\omega + \boldsymbol{M}_v\boldsymbol{\Gamma}_{v,\omega}\boldsymbol{M}_v^{\mathsf{T}}\boldsymbol{I}\Big)\Bigg)\tilde{\boldsymbol{\omega}} \\
&\qquad -\tilde{\boldsymbol{v}}_{\mathrm{r}}^{\mathsf{T}}\boldsymbol{\Gamma}_{v,q}\boldsymbol{R}_{\mathrm{IB}}^{\mathsf{T}}(\boldsymbol{\lambda},\boldsymbol{\zeta})\Big(\boldsymbol{R}_{\mathrm{IB}}(\tilde{\boldsymbol{\lambda}}+\boldsymbol{\lambda},\tilde{\boldsymbol{\zeta}}+\boldsymbol{\zeta}) - \boldsymbol{R}_{\mathrm{IB}}(\boldsymbol{\lambda},\boldsymbol{\zeta})\Big)\hat{\boldsymbol{v}}_{\mathrm{r}} + \tilde{\boldsymbol{w}}^{\mathsf{T}}\boldsymbol{R}_{\mathrm{IB}}(\boldsymbol{\lambda},\boldsymbol{\zeta})\Bigg(-\boldsymbol{\Gamma}_{w,\omega}\boldsymbol{M}_v^{\mathsf{T}}\boldsymbol{M}_v\boldsymbol{\Gamma}_{v,q} \\
&\qquad -\boldsymbol{\Gamma}_{w,q}\Big(\boldsymbol{R}_{\mathrm{IB}}^{\mathsf{T}}(\boldsymbol{\lambda},\boldsymbol{\zeta})\boldsymbol{R}_{\mathrm{IB}}(\tilde{\boldsymbol{\lambda}}+\boldsymbol{\lambda},\tilde{\boldsymbol{\zeta}}+\boldsymbol{\zeta})\boldsymbol{\Gamma}_{v,q} + \boldsymbol{\Gamma}_{w,q}\Big)\Bigg)\boldsymbol{R}_{\mathrm{IB}}^{\mathsf{T}}(\boldsymbol{\lambda},\boldsymbol{\zeta})\tilde{\boldsymbol{q}} \\
&\qquad +\tilde{\boldsymbol{w}}^{\mathsf{T}}\boldsymbol{R}_{\mathrm{IB}}(\boldsymbol{\lambda},\boldsymbol{\zeta})\Bigg(-\boldsymbol{\Gamma}_{w,q}\Big(\boldsymbol{R}_{\mathrm{IB}}^{\mathsf{T}}(\boldsymbol{\lambda},\boldsymbol{\zeta})\boldsymbol{R}_{\mathrm{IB}}(\tilde{\boldsymbol{\lambda}}+\boldsymbol{\lambda},\tilde{\boldsymbol{\zeta}}+\boldsymbol{\zeta})\boldsymbol{\Gamma}_{v,\omega} + \boldsymbol{\Gamma}_{w,\omega}\Big)\boldsymbol{M}_v^{\mathsf{T}}\boldsymbol{I} \\
&\qquad -\boldsymbol{\Gamma}_{w,\omega}\boldsymbol{M}_v^{\mathsf{T}}\Big(\boldsymbol{S}(\boldsymbol{I}(\tilde{\boldsymbol{\omega}}+\boldsymbol{\omega})) - \boldsymbol{S}(\boldsymbol{\omega})\boldsymbol{I} + \boldsymbol{M}_\omega + \boldsymbol{M}_v\boldsymbol{\Gamma}_{v,\omega}\boldsymbol{M}_v^{\mathsf{T}}\boldsymbol{I}\Big)\Bigg)\tilde{\boldsymbol{\omega}} \\
&-\tilde{\boldsymbol{w}}^{\mathsf{T}}\boldsymbol{R}_{\mathrm{IB}}(\boldsymbol{\lambda},\boldsymbol{\zeta})\boldsymbol{\Gamma}_{w,q}\boldsymbol{R}_{\mathrm{IB}}^{\mathsf{T}}(\boldsymbol{\lambda},\boldsymbol{\zeta})\Big(\boldsymbol{R}_{\mathrm{IB}}(\tilde{\boldsymbol{\lambda}}+\boldsymbol{\lambda},\tilde{\boldsymbol{\zeta}}+\boldsymbol{\zeta}) - \boldsymbol{R}_{\mathrm{IB}}(\boldsymbol{\lambda},\boldsymbol{\zeta})\Big)\hat{\boldsymbol{v}}_{\mathrm{r}} + \tilde{\boldsymbol{q}}^{\mathsf{T}}\boldsymbol{L}_{1_q}^{-1}\Bigg(\boldsymbol{R}_{\mathrm{IB}}(\boldsymbol{\lambda},\boldsymbol{\zeta})\boldsymbol{\Gamma}_{w,q}\boldsymbol{R}_{\mathrm{IB}}^{\mathsf{T}}(\boldsymbol{\lambda},\boldsymbol{\zeta}) \\
&+\boldsymbol{R}_{\mathrm{IB}}(\tilde{\boldsymbol{\lambda}}+\boldsymbol{\lambda},\tilde{\boldsymbol{\zeta}}+\boldsymbol{\zeta})\boldsymbol{\Gamma}_{v,q}\boldsymbol{R}_{\mathrm{IB}}^{\mathsf{T}}(\boldsymbol{\lambda},\boldsymbol{\zeta})\Bigg)\tilde{\boldsymbol{q}} + \tilde{\boldsymbol{q}}^{\mathsf{T}}\boldsymbol{L}_{1_q}^{-1}\Bigg(\boldsymbol{R}_{\mathrm{IB}}(\boldsymbol{\lambda},\boldsymbol{\zeta})\boldsymbol{\Gamma}_{w,\omega} + \boldsymbol{R}_{\mathrm{IB}}(\tilde{\boldsymbol{\lambda}}+\boldsymbol{\lambda},\tilde{\boldsymbol{\zeta}}+\boldsymbol{\zeta})\boldsymbol{\Gamma}_{v,\omega}\Bigg)\boldsymbol{M}_v^{\mathsf{T}}\boldsymbol{I}\tilde{\boldsymbol{\omega}} \\
&\qquad + \tilde{\boldsymbol{q}}^{\mathsf{T}}\boldsymbol{L}_{1_q}^{-1}\boldsymbol{R}_{\mathrm{IB}}(\boldsymbol{\lambda},\boldsymbol{\zeta})\tilde{\boldsymbol{v}}_{\mathrm{r}} + \tilde{\boldsymbol{q}}^{\mathsf{T}}\boldsymbol{L}_{1_q}^{-1}\tilde{\boldsymbol{w}} + \tilde{\boldsymbol{q}}^{\mathsf{T}}\boldsymbol{L}_{1_q}^{-1}\Big(\boldsymbol{R}_{\mathrm{IB}}(\tilde{\boldsymbol{\lambda}}+\boldsymbol{\lambda},\tilde{\boldsymbol{\zeta}}+\boldsymbol{\zeta}) - \boldsymbol{R}_{\mathrm{IB}}(\boldsymbol{\lambda},\boldsymbol{\zeta})\Big)\hat{\boldsymbol{v}}_{\mathrm{r}} \\
&\qquad + \tilde{\boldsymbol{\lambda}}^{\mathsf{T}}\boldsymbol{L}_{1_\lambda}^{-1}\boldsymbol{S}(\tilde{\boldsymbol{\lambda}}+\boldsymbol{\lambda})\tilde{\boldsymbol{\omega}} - \tilde{\boldsymbol{\lambda}}^{\mathsf{T}}\boldsymbol{L}_{1_\lambda}^{-1}\boldsymbol{S}(\boldsymbol{\omega})\tilde{\boldsymbol{\lambda}} + \tilde{\boldsymbol{\zeta}}^{\mathsf{T}}\boldsymbol{L}_{1_\zeta}^{-1}\boldsymbol{S}(\tilde{\boldsymbol{\zeta}}+\boldsymbol{\zeta})\tilde{\boldsymbol{\omega}} - \tilde{\boldsymbol{\zeta}}^{\mathsf{T}}\boldsymbol{L}_{1_\zeta}^{-1}\boldsymbol{S}(\boldsymbol{\omega})\tilde{\boldsymbol{\zeta}} + \tilde{\boldsymbol{\omega}}^{\mathsf{T}}\boldsymbol{L}_{1_\omega}^{-1}\boldsymbol{I}^{-1}\boldsymbol{M}_v\tilde{\boldsymbol{v}}_{\mathrm{r}} \\
&\qquad \tilde{\boldsymbol{\omega}}^{\mathsf{T}}\boldsymbol{L}_{1_\omega}^{-1}\boldsymbol{I}^{-1}\boldsymbol{M}_v\boldsymbol{\Gamma}_{v,q}\boldsymbol{R}_{\mathrm{IB}}^{\mathsf{T}}(\boldsymbol{\lambda},\boldsymbol{\zeta})\tilde{\boldsymbol{q}} + \tilde{\boldsymbol{\omega}}^{\mathsf{T}}\boldsymbol{L}_{1_\omega}^{-1}\boldsymbol{I}^{-1}\left(\boldsymbol{S}(\boldsymbol{I}(\tilde{\boldsymbol{\omega}}+\boldsymbol{\omega})) - \boldsymbol{S}(\boldsymbol{\omega})\boldsymbol{I} + \boldsymbol{M}_\omega + \boldsymbol{M}_v\boldsymbol{\Gamma}_{v,\omega}\boldsymbol{M}_v^{\mathsf{T}}\boldsymbol{I}\right)\tilde{\boldsymbol{\omega}} \qquad \text{(A.6)}
\end{aligned}
$$

Here we have color-coded terms by those that can be written as $\tilde{\boldsymbol{x}}_1^{\mathsf{T}}(\bullet)\tilde{\boldsymbol{x}}_1$ and those that can be written as $\tilde{\boldsymbol{x}}_2^{\mathsf{T}}(\bullet)\tilde{\boldsymbol{x}}_1$. The terms in violet are not immediately seen to follow either of these two forms. However, consider the common term

$$
\Big(\boldsymbol{R}_{\mathrm{IB}}(\tilde{\boldsymbol{\lambda}}+\boldsymbol{\lambda},\tilde{\boldsymbol{\zeta}}+\boldsymbol{\zeta}) - \boldsymbol{R}_{\mathrm{IB}}(\boldsymbol{\lambda},\boldsymbol{\zeta})\Big)\hat{\boldsymbol{v}}_{\mathrm{r}} \qquad \text{(A.7)}
$$

with each element of the vector result given by

$$
\begin{aligned}
\Big[\Big(\boldsymbol{R}_{\mathrm{IB}}(\tilde{\boldsymbol{\lambda}}+\boldsymbol{\lambda},\tilde{\boldsymbol{\zeta}}+\boldsymbol{\zeta}) - \boldsymbol{R}_{\mathrm{IB}}(\boldsymbol{\lambda},\boldsymbol{\zeta})\Big)\hat{\boldsymbol{v}}_{\mathrm{r}}\Big]_1 &= \tilde{\lambda}_1\hat{u}_{\mathrm{r}} + \tilde{\lambda}_2\hat{v}_{\mathrm{r}} + \tilde{\lambda}_3\hat{w}_{\mathrm{r}} && \text{(A.8a)} \\
\Big[\Big(\boldsymbol{R}_{\mathrm{IB}}(\tilde{\boldsymbol{\lambda}}+\boldsymbol{\lambda},\tilde{\boldsymbol{\zeta}}+\boldsymbol{\zeta}) - \boldsymbol{R}_{\mathrm{IB}}(\boldsymbol{\lambda},\boldsymbol{\zeta})\Big)\hat{\boldsymbol{v}}_{\mathrm{r}}\Big]_2 &= (\tilde{\zeta}_2\tilde{\lambda}_3 + \tilde{\zeta}_2\lambda_3 + \zeta_2\tilde{\lambda}_3 - \tilde{\zeta}_3\tilde{\lambda}_2 - \tilde{\zeta}_3\lambda_2 - \zeta_3\tilde{\lambda}_2)\hat{u}_{\mathrm{r}} \\
&\quad + (\tilde{\zeta}_3\tilde{\lambda}_1 + \tilde{\zeta}_3\lambda_1 + \zeta_3\tilde{\lambda}_1 - \tilde{\zeta}_1\tilde{\lambda}_3 - \tilde{\zeta}_1\lambda_3 - \zeta_1\tilde{\lambda}_3)\hat{v}_{\mathrm{r}} \\
&\quad + (\tilde{\zeta}_1\tilde{\lambda}_2 + \tilde{\zeta}_1\lambda_2 + \zeta_1\tilde{\lambda}_2 - \tilde{\zeta}_2\tilde{\lambda}_1 - \tilde{\zeta}_2\lambda_1 - \zeta_2\tilde{\lambda}_1)\hat{w}_{\mathrm{r}} && \text{(A.8b)} \\
\Big[\Big(\boldsymbol{R}_{\mathrm{IB}}(\tilde{\boldsymbol{\lambda}}+\boldsymbol{\lambda},\tilde{\boldsymbol{\zeta}}+\boldsymbol{\zeta}) - \boldsymbol{R}_{\mathrm{IB}}(\boldsymbol{\lambda},\boldsymbol{\zeta})\Big)\hat{\boldsymbol{v}}_{\mathrm{r}}\Big]_3 &= \tilde{\zeta}_1\hat{u}_{\mathrm{r}} + \tilde{\zeta}_2\hat{v}_{\mathrm{r}} + \tilde{\zeta}_3\hat{w}_{\mathrm{r}} && \text{(A.8c)}
\end{aligned}
$$

It is apparent the first and third elements can be written in the form $(\bullet)\tilde{\boldsymbol{\lambda}} + (\bullet)\tilde{\boldsymbol{\zeta}}$. The second element may be written as

$$\begin{aligned}\left[\Big(\boldsymbol{R}_{\mathrm{IB}}(\tilde{\boldsymbol{\lambda}}+\boldsymbol{\lambda},\tilde{\boldsymbol{\zeta}}+\boldsymbol{\zeta}) - \boldsymbol{R}_{\mathrm{IB}}(\boldsymbol{\lambda},\boldsymbol{\zeta})\Big)\hat{\boldsymbol{v}}_{\mathrm{r}}\right]_2 &= \Big(\hat{v}_{\mathrm{r}}(\tilde{\zeta}_3+\zeta_3) - \hat{w}_{\mathrm{r}}(\tilde{\zeta}_2+\zeta_2)\Big)\tilde{\lambda}_1 \\ &+ \Big(-\hat{u}_{\mathrm{r}}(\tilde{\zeta}_3+\zeta_3) + \hat{w}_{\mathrm{r}}(\tilde{\zeta}_1+\zeta_1)\Big)\tilde{\lambda}_2 \\ &+ \Big(\hat{u}_{\mathrm{r}}(\tilde{\zeta}_2+\zeta_2) - \hat{v}_{\mathrm{r}}(\tilde{\zeta}_1+\zeta_1)\Big)\tilde{\lambda}_3 \\ &+ (-\hat{v}_{\mathrm{r}}\lambda_3 + \hat{w}_{\mathrm{r}}\lambda_2)\tilde{\zeta}_1 \\ &+ (\hat{u}_{\mathrm{r}}\lambda_3 - \hat{w}_{\mathrm{r}}\lambda_1)\tilde{\zeta}_2 \\ &+ (-\hat{u}_{\mathrm{r}}\lambda_2 + \hat{v}_{\mathrm{r}}\lambda_1)\tilde{\zeta}_3 \end{aligned} \tag{A.9}$$

Therefore,

$$\Big(\boldsymbol{R}_{\mathrm{IB}}(\tilde{\boldsymbol{\lambda}}+\boldsymbol{\lambda},\tilde{\boldsymbol{\zeta}}+\boldsymbol{\zeta}) - \boldsymbol{R}_{\mathrm{IB}}(\boldsymbol{\lambda},\boldsymbol{\zeta})\Big)\hat{\boldsymbol{v}}_{\mathrm{r}} = \begin{bmatrix}\boldsymbol{M}_{\lambda}(\tilde{\boldsymbol{\lambda}},\tilde{\boldsymbol{\zeta}},\hat{\boldsymbol{v}}_{\mathrm{r}}) & \boldsymbol{M}_{\zeta}(\tilde{\boldsymbol{\lambda}},\tilde{\boldsymbol{\zeta}},\hat{\boldsymbol{v}}_{\mathrm{r}})\end{bmatrix}\begin{bmatrix}\tilde{\boldsymbol{\lambda}}\\ \tilde{\boldsymbol{\zeta}}\end{bmatrix} \tag{A.10}$$

where

$$\boldsymbol{M}_{\lambda}^{\mathsf{T}}(\tilde{\boldsymbol{\zeta}},\boldsymbol{\zeta},\hat{\boldsymbol{v}}_{\mathrm{r}}) = \begin{bmatrix}\hat{u}_{\mathrm{r}} & \hat{v}_{\mathrm{r}}(\tilde{\zeta}_3+\zeta_3) - \hat{w}_{\mathrm{r}}(\tilde{\zeta}_2+\zeta_2) & 0\\ \hat{v}_{\mathrm{r}} & -\hat{u}_{\mathrm{r}}(\tilde{\zeta}_3+\zeta_3) + \hat{w}_{\mathrm{r}}(\tilde{\zeta}_1+\zeta_1) & 0\\ \hat{w}_{\mathrm{r}} & \hat{u}_{\mathrm{r}}(\tilde{\zeta}_2+\zeta_2) - \hat{v}_{\mathrm{r}}(\tilde{\zeta}_1+\zeta_1) & 0\end{bmatrix} \tag{A.11a}$$

$$\boldsymbol{M}_{\zeta}^{\mathsf{T}}(\boldsymbol{\lambda},\hat{\boldsymbol{v}}_{\mathrm{r}}) = \begin{bmatrix}0 & -\hat{v}_{\mathrm{r}}\lambda_3 + \hat{w}_{\mathrm{r}}\lambda_2 & \hat{u}_{\mathrm{r}}\\ 0 & \hat{u}_{\mathrm{r}}\lambda_3 - \hat{w}_{\mathrm{r}}\lambda_1 & \hat{v}_{\mathrm{r}}\\ 0 & -\hat{u}_{\mathrm{r}}\lambda_2 + \hat{v}_{\mathrm{r}}\lambda_1 & \hat{w}_{\mathrm{r}}\end{bmatrix} \tag{A.11b}$$

Note that these choices of $\boldsymbol{M}_{\lambda}$ and $\boldsymbol{M}_{\zeta}$ are non-unique. Turning back to Eq. (A.6), we have

$$\begin{aligned}&\tilde{\boldsymbol{v}}_{\mathrm{r}}^{\mathsf{T}}\boldsymbol{\Gamma}_{v,q}\boldsymbol{S}(\boldsymbol{\omega})\boldsymbol{R}_{\mathrm{IB}}^{\mathsf{T}}\tilde{\boldsymbol{q}} - \tilde{\boldsymbol{w}}^{\mathsf{T}}\boldsymbol{R}_{\mathrm{IB}}\left(\boldsymbol{S}(\boldsymbol{\omega})\boldsymbol{\Gamma}_{w,q} - \boldsymbol{\Gamma}_{w,q}\boldsymbol{S}(\boldsymbol{\omega})\right)\boldsymbol{R}_{\mathrm{IB}}^{\mathsf{T}}\tilde{\boldsymbol{q}} - \tilde{\boldsymbol{w}}^{\mathsf{T}}\boldsymbol{R}_{\mathrm{IB}}\boldsymbol{S}(\boldsymbol{\omega})\boldsymbol{\Gamma}_{w,\omega}\boldsymbol{M}_v^{\mathsf{T}}\boldsymbol{I}\tilde{\boldsymbol{\omega}}\\
&\tilde{\boldsymbol{v}}_{\mathrm{r}}^{\mathsf{T}}\Bigg(\Big(\frac{1}{m}\boldsymbol{F}_v - \boldsymbol{S}(\tilde{\boldsymbol{\omega}}+\boldsymbol{\omega})\Big)\boldsymbol{\Gamma}_{v,q} - \boldsymbol{\Gamma}_{v,q}\boldsymbol{R}_{\mathrm{IB}}^{\mathsf{T}}(\boldsymbol{\lambda},\boldsymbol{\zeta})\boldsymbol{R}_{\mathrm{IB}}(\tilde{\boldsymbol{\lambda}}+\boldsymbol{\lambda},\tilde{\boldsymbol{\zeta}}+\boldsymbol{\zeta})\boldsymbol{\Gamma}_{v,q} - \boldsymbol{\Gamma}_{v,q}\boldsymbol{\Gamma}_{w,q} - \boldsymbol{\Gamma}_{v,\omega}\boldsymbol{M}_v^{\mathsf{T}}\boldsymbol{M}_v\boldsymbol{\Gamma}_{v,q}\Bigg)\boldsymbol{R}_{\mathrm{IB}}^{\mathsf{T}}(\boldsymbol{\lambda},\boldsymbol{\zeta})\tilde{\boldsymbol{q}}\\
&+\tilde{\boldsymbol{v}}_{\mathrm{r}}^{\mathsf{T}}g\tilde{\boldsymbol{\zeta}} + \tilde{\boldsymbol{v}}_{\mathrm{r}}^{\mathsf{T}}\Bigg(\Big(\frac{1}{m}\boldsymbol{F}_v - \boldsymbol{S}(\tilde{\boldsymbol{\omega}}+\boldsymbol{\omega})\Big)\boldsymbol{\Gamma}_{v,\omega}\boldsymbol{M}_v^{\mathsf{T}}\boldsymbol{I} - \boldsymbol{\Gamma}_{v,q}\Big(\boldsymbol{R}_{\mathrm{IB}}^{\mathsf{T}}(\boldsymbol{\lambda},\boldsymbol{\zeta})\boldsymbol{R}_{\mathrm{IB}}(\tilde{\boldsymbol{\lambda}}+\boldsymbol{\lambda},\tilde{\boldsymbol{\zeta}}+\boldsymbol{\zeta})\boldsymbol{\Gamma}_{v,\omega} + \boldsymbol{\Gamma}_{w,\omega}\Big)\boldsymbol{M}_v^{\mathsf{T}}\boldsymbol{I}\\
&\qquad+\frac{1}{m}\boldsymbol{F}_{\omega} + \boldsymbol{S}(\hat{\boldsymbol{v}}_{\mathrm{r}}) - \boldsymbol{\Gamma}_{v,\omega}\boldsymbol{M}_v^{\mathsf{T}}\Big(\boldsymbol{S}(\boldsymbol{I}(\tilde{\boldsymbol{\omega}}+\boldsymbol{\omega})) - \boldsymbol{S}(\boldsymbol{\omega})\boldsymbol{I} + \boldsymbol{M}_{\omega} + \boldsymbol{M}_v\boldsymbol{\Gamma}_{v,\omega}\boldsymbol{M}_v^{\mathsf{T}}\boldsymbol{I}\Big)\Bigg)\tilde{\boldsymbol{\omega}}\\
&-\tilde{\boldsymbol{v}}_{\mathrm{r}}^{\mathsf{T}}\boldsymbol{\Gamma}_{v,q}\boldsymbol{R}_{\mathrm{IB}}^{\mathsf{T}}(\boldsymbol{\lambda},\boldsymbol{\zeta})\boldsymbol{M}_{\lambda}(\tilde{\boldsymbol{\lambda}},\tilde{\boldsymbol{\zeta}},\hat{\boldsymbol{v}}_{\mathrm{r}})\tilde{\boldsymbol{\lambda}} - \tilde{\boldsymbol{v}}_{\mathrm{r}}^{\mathsf{T}}\boldsymbol{\Gamma}_{v,q}\boldsymbol{R}_{\mathrm{IB}}^{\mathsf{T}}(\boldsymbol{\lambda},\boldsymbol{\zeta})\boldsymbol{M}_{\zeta}(\tilde{\boldsymbol{\lambda}},\tilde{\boldsymbol{\zeta}},\hat{\boldsymbol{v}}_{\mathrm{r}})\tilde{\boldsymbol{\zeta}} + \tilde{\boldsymbol{w}}^{\mathsf{T}}\boldsymbol{R}_{\mathrm{IB}}(\boldsymbol{\lambda},\boldsymbol{\zeta})\Bigg(-\boldsymbol{\Gamma}_{w,\omega}\boldsymbol{M}_v^{\mathsf{T}}\boldsymbol{M}_v\boldsymbol{\Gamma}_{v,q}\\
&\qquad-\boldsymbol{\Gamma}_{w,q}\Big(\boldsymbol{R}_{\mathrm{IB}}^{\mathsf{T}}(\boldsymbol{\lambda},\boldsymbol{\zeta})\boldsymbol{R}_{\mathrm{IB}}(\tilde{\boldsymbol{\lambda}}+\boldsymbol{\lambda},\tilde{\boldsymbol{\zeta}}+\boldsymbol{\zeta})\boldsymbol{\Gamma}_{v,q} + \boldsymbol{\Gamma}_{w,q}\Big)\Bigg)\boldsymbol{R}_{\mathrm{IB}}^{\mathsf{T}}(\boldsymbol{\lambda},\boldsymbol{\zeta})\tilde{\boldsymbol{q}}\\
&\qquad+\tilde{\boldsymbol{w}}^{\mathsf{T}}\boldsymbol{R}_{\mathrm{IB}}(\boldsymbol{\lambda},\boldsymbol{\zeta})\Bigg(-\boldsymbol{\Gamma}_{w,q}\Big(\boldsymbol{R}_{\mathrm{IB}}^{\mathsf{T}}(\boldsymbol{\lambda},\boldsymbol{\zeta})\boldsymbol{R}_{\mathrm{IB}}(\tilde{\boldsymbol{\lambda}}+\boldsymbol{\lambda},\tilde{\boldsymbol{\zeta}}+\boldsymbol{\zeta})\boldsymbol{\Gamma}_{v,\omega} + \boldsymbol{\Gamma}_{w,\omega}\Big)\boldsymbol{M}_v^{\mathsf{T}}\boldsymbol{I}\\
&-\boldsymbol{\Gamma}_{w,\omega}\boldsymbol{M}_v^{\mathsf{T}}\Big(\boldsymbol{S}(\boldsymbol{I}(\tilde{\boldsymbol{\omega}}+\boldsymbol{\omega})) - \boldsymbol{S}(\boldsymbol{\omega})\boldsymbol{I} + \boldsymbol{M}_{\omega} + \boldsymbol{M}_v\boldsymbol{\Gamma}_{v,\omega}\boldsymbol{M}_v^{\mathsf{T}}\boldsymbol{I}\Big)\Bigg)\tilde{\boldsymbol{\omega}} - \tilde{\boldsymbol{w}}^{\mathsf{T}}\boldsymbol{R}_{\mathrm{IB}}(\boldsymbol{\lambda},\boldsymbol{\zeta})\boldsymbol{\Gamma}_{w,q}\boldsymbol{R}_{\mathrm{IB}}^{\mathsf{T}}(\boldsymbol{\lambda},\boldsymbol{\zeta})\boldsymbol{M}_{\lambda}(\tilde{\boldsymbol{\lambda}},\tilde{\boldsymbol{\zeta}},\hat{\boldsymbol{v}}_{\mathrm{r}})\tilde{\boldsymbol{\lambda}}\\
&\qquad-\tilde{\boldsymbol{w}}^{\mathsf{T}}\boldsymbol{R}_{\mathrm{IB}}(\boldsymbol{\lambda},\boldsymbol{\zeta})\boldsymbol{\Gamma}_{w,q}\boldsymbol{R}_{\mathrm{IB}}^{\mathsf{T}}(\boldsymbol{\lambda},\boldsymbol{\zeta})\boldsymbol{M}_{\zeta}(\tilde{\boldsymbol{\lambda}},\tilde{\boldsymbol{\zeta}},\hat{\boldsymbol{v}}_{\mathrm{r}})\tilde{\boldsymbol{\zeta}} + \tilde{\boldsymbol{q}}^{\mathsf{T}}\boldsymbol{L}_{1_q}^{-1}\Bigg(\boldsymbol{R}_{\mathrm{IB}}(\boldsymbol{\lambda},\boldsymbol{\zeta})\boldsymbol{\Gamma}_{w,q}\boldsymbol{R}_{\mathrm{IB}}^{\mathsf{T}}(\boldsymbol{\lambda},\boldsymbol{\zeta})\\
&+\boldsymbol{R}_{\mathrm{IB}}(\tilde{\boldsymbol{\lambda}}+\boldsymbol{\lambda},\tilde{\boldsymbol{\zeta}}+\boldsymbol{\zeta})\boldsymbol{\Gamma}_{v,q}\boldsymbol{R}_{\mathrm{IB}}^{\mathsf{T}}(\boldsymbol{\lambda},\boldsymbol{\zeta})\Bigg)\tilde{\boldsymbol{q}} + \tilde{\boldsymbol{q}}^{\mathsf{T}}\boldsymbol{L}_{1_q}^{-1}\Bigg(\boldsymbol{R}_{\mathrm{IB}}(\boldsymbol{\lambda},\boldsymbol{\zeta})\boldsymbol{\Gamma}_{w,\omega} + \boldsymbol{R}_{\mathrm{IB}}(\tilde{\boldsymbol{\lambda}}+\boldsymbol{\lambda},\tilde{\boldsymbol{\zeta}}+\boldsymbol{\zeta})\boldsymbol{\Gamma}_{v,\omega}\Bigg)\boldsymbol{M}_v^{\mathsf{T}}\boldsymbol{I}\tilde{\boldsymbol{\omega}}\\
&+\tilde{\boldsymbol{q}}^{\mathsf{T}}\boldsymbol{L}_{1_q}^{-1}\boldsymbol{R}_{\mathrm{IB}}(\boldsymbol{\lambda},\boldsymbol{\zeta})\tilde{\boldsymbol{v}}_{\mathrm{r}} + \tilde{\boldsymbol{q}}^{\mathsf{T}}\boldsymbol{L}_{1_q}^{-1}\tilde{\boldsymbol{w}} + \tilde{\boldsymbol{q}}^{\mathsf{T}}\boldsymbol{L}_{1_q}^{-1}\boldsymbol{M}_{\lambda}(\tilde{\boldsymbol{\lambda}},\tilde{\boldsymbol{\zeta}},\hat{\boldsymbol{v}}_{\mathrm{r}})\tilde{\boldsymbol{\lambda}} + \tilde{\boldsymbol{q}}^{\mathsf{T}}\boldsymbol{L}_{1_q}^{-1}\boldsymbol{M}_{\zeta}(\tilde{\boldsymbol{\lambda}},\tilde{\boldsymbol{\zeta}},\hat{\boldsymbol{v}}_{\mathrm{r}})\tilde{\boldsymbol{\zeta}}\\
&+\tilde{\boldsymbol{\lambda}}^{\mathsf{T}}\boldsymbol{L}_{1_{\lambda}}^{-1}\boldsymbol{S}(\tilde{\boldsymbol{\lambda}}+\boldsymbol{\lambda})\tilde{\boldsymbol{\omega}} - \tilde{\boldsymbol{\lambda}}^{\mathsf{T}}\boldsymbol{L}_{1_{\lambda}}^{-1}\boldsymbol{S}(\boldsymbol{\omega})\tilde{\boldsymbol{\lambda}} + \tilde{\boldsymbol{\zeta}}^{\mathsf{T}}\boldsymbol{L}_{1_{\zeta}}^{-1}\boldsymbol{S}(\tilde{\boldsymbol{\zeta}}+\boldsymbol{\zeta})\tilde{\boldsymbol{\omega}} - \tilde{\boldsymbol{\zeta}}^{\mathsf{T}}\boldsymbol{L}_{1_{\zeta}}^{-1}\boldsymbol{S}(\boldsymbol{\omega})\tilde{\boldsymbol{\zeta}} + \tilde{\boldsymbol{\omega}}^{\mathsf{T}}\boldsymbol{L}_{1_{\omega}}^{-1}\boldsymbol{I}^{-1}\boldsymbol{M}_v\tilde{\boldsymbol{v}}_{\mathrm{r}}\\
&+\tilde{\boldsymbol{\omega}}^{\mathsf{T}}\boldsymbol{L}_{1_{\omega}}^{-1}\boldsymbol{I}^{-1}\boldsymbol{M}_v\boldsymbol{\Gamma}_{v,q}\boldsymbol{R}_{\mathrm{IB}}^{\mathsf{T}}(\boldsymbol{\lambda},\boldsymbol{\zeta})\tilde{\boldsymbol{q}} + \tilde{\boldsymbol{\omega}}^{\mathsf{T}}\boldsymbol{L}_{1_{\omega}}^{-1}\boldsymbol{I}^{-1}\left(\boldsymbol{S}(\boldsymbol{I}(\tilde{\boldsymbol{\omega}}+\boldsymbol{\omega})) - \boldsymbol{S}(\boldsymbol{\omega})\boldsymbol{I} + \boldsymbol{M}_{\omega} + \boldsymbol{M}_v\boldsymbol{\Gamma}_{v,\omega}\boldsymbol{M}_v^{\mathsf{T}}\boldsymbol{I}\right)\tilde{\boldsymbol{\omega}}\end{aligned} \tag{A.12}$$

Let the $p \times p$ matrix-valued function $\boldsymbol{A}$ be defined as

$$\boldsymbol{A}(\tilde{\boldsymbol{x}}_1, \boldsymbol{x}_1, \hat{\boldsymbol{x}}_2) = \begin{bmatrix} \boldsymbol{A}_{q,q} & \boldsymbol{A}_{q,\lambda} & \boldsymbol{A}_{q,\zeta} & \boldsymbol{A}_{q,\omega} \\ \boldsymbol{0} & \boldsymbol{A}_{\lambda,\lambda} & \boldsymbol{A}_{\lambda,\zeta} & \boldsymbol{A}_{\lambda,\omega} \\ \boldsymbol{0} & \boldsymbol{0} & \boldsymbol{A}_{\zeta,\zeta} & \boldsymbol{A}_{\zeta,\omega} \\ \boldsymbol{0} & \boldsymbol{0} & \boldsymbol{0} & \boldsymbol{A}_{\omega,\omega} \end{bmatrix} \tag{A.13}$$

where

$$\begin{aligned}
\boldsymbol{A}_{q,q} &= \boldsymbol{L}_{1_q}^{-1}\Big(\boldsymbol{R}_{\mathrm{IB}}(\boldsymbol{\lambda},\boldsymbol{\zeta})\boldsymbol{\Gamma}_{w,q}\boldsymbol{R}_{\mathrm{IB}}^{\mathsf{T}}(\boldsymbol{\lambda},\boldsymbol{\zeta}) + \boldsymbol{R}_{\mathrm{IB}}(\tilde{\boldsymbol{\lambda}}+\boldsymbol{\lambda},\tilde{\boldsymbol{\zeta}}+\boldsymbol{\zeta})\boldsymbol{\Gamma}_{v,q}\boldsymbol{R}_{\mathrm{IB}}^{\mathsf{T}}(\boldsymbol{\lambda},\boldsymbol{\zeta})\Big) \\
\boldsymbol{A}_{q,\lambda} &= \boldsymbol{L}_{1_q}^{-1}\boldsymbol{M}_{\lambda}(\tilde{\boldsymbol{\lambda}},\tilde{\boldsymbol{\zeta}},\hat{\boldsymbol{v}}_{\mathrm{r}}) \\
\boldsymbol{A}_{q,\zeta} &= \boldsymbol{L}_{1_q}^{-1}\boldsymbol{M}_{\zeta}(\tilde{\boldsymbol{\lambda}},\tilde{\boldsymbol{\zeta}},\hat{\boldsymbol{v}}_{\mathrm{r}}) \\
\boldsymbol{A}_{q,\omega} &= \boldsymbol{L}_{1_q}^{-1}\Big(\boldsymbol{R}_{\mathrm{IB}}(\boldsymbol{\lambda},\boldsymbol{\zeta})\boldsymbol{\Gamma}_{w,\omega} + \boldsymbol{R}_{\mathrm{IB}}(\tilde{\boldsymbol{\lambda}}+\boldsymbol{\lambda},\tilde{\boldsymbol{\zeta}}+\boldsymbol{\zeta})\boldsymbol{\Gamma}_{v,\omega}\Big)\boldsymbol{M}_v^{\mathsf{T}}\boldsymbol{I} + \boldsymbol{R}_{\mathrm{IB}}(\boldsymbol{\lambda},\boldsymbol{\zeta})\boldsymbol{\Gamma}_{v,q}^{\mathsf{T}}\boldsymbol{M}_v^{\mathsf{T}}\boldsymbol{I}^{-1}\boldsymbol{L}_{1_\omega}^{-\mathsf{T}} \\
\boldsymbol{A}_{\lambda,\lambda} &= -\boldsymbol{L}_{1_\lambda}^{-1}\boldsymbol{S}(\boldsymbol{\omega}) \\
\boldsymbol{A}_{\lambda,\zeta} &= \boldsymbol{0} \\
\boldsymbol{A}_{\lambda,\omega} &= \boldsymbol{L}_{1_\lambda}^{-1}\boldsymbol{S}(\tilde{\boldsymbol{\lambda}}+\boldsymbol{\lambda}) \\
\boldsymbol{A}_{\zeta,\zeta} &= -\boldsymbol{L}_{1_\zeta}^{-1}\boldsymbol{S}(\boldsymbol{\omega}) \\
\boldsymbol{A}_{\zeta,\omega} &= \boldsymbol{L}_{1_\zeta}^{-1}\boldsymbol{S}(\tilde{\boldsymbol{\zeta}}+\boldsymbol{\zeta}) \\
\boldsymbol{A}_{\omega,\omega} &= \boldsymbol{L}_{1_\omega}^{-1}\boldsymbol{I}^{-1}\left(\boldsymbol{S}(\boldsymbol{I}(\tilde{\boldsymbol{\omega}}+\boldsymbol{\omega})) - \boldsymbol{S}(\boldsymbol{\omega})\boldsymbol{I} + \boldsymbol{M}_{\omega} + \boldsymbol{M}_v\boldsymbol{\Gamma}_{v,\omega}\boldsymbol{M}_v^{\mathsf{T}}\boldsymbol{I}\right)
\end{aligned}$$

Also, define the $(n-p) \times p$ matrix-valued function $\boldsymbol{B}$ as

$$\boldsymbol{B}(\tilde{\boldsymbol{x}}_1, \boldsymbol{x}_1, \hat{\boldsymbol{x}}_2) = \begin{bmatrix} \boldsymbol{B}_{v_{\mathrm{r}},q} & \boldsymbol{B}_{v_{\mathrm{r}},\lambda} & \boldsymbol{B}_{v_{\mathrm{r}},\zeta} & \boldsymbol{B}_{v_{\mathrm{r}},\omega} \\ \boldsymbol{B}_{w,q} & \boldsymbol{B}_{w,\lambda} & \boldsymbol{B}_{w,\zeta} & \boldsymbol{B}_{w,\omega} \end{bmatrix} \tag{A.14}$$

where

$$\begin{aligned}
\boldsymbol{B}_{v_{\mathrm{r}},q} &= \Big(\boldsymbol{\Gamma}_{v,q}\boldsymbol{S}(\boldsymbol{\omega}) + \Big(\frac{1}{m}\boldsymbol{F}_v - \boldsymbol{S}(\tilde{\boldsymbol{\omega}}+\boldsymbol{\omega}) - \boldsymbol{\Gamma}_{v,q}\boldsymbol{R}_{\mathrm{IB}}^{\mathsf{T}}(\boldsymbol{\lambda},\boldsymbol{\zeta})\boldsymbol{R}_{\mathrm{IB}}(\tilde{\boldsymbol{\lambda}}+\boldsymbol{\lambda},\tilde{\boldsymbol{\zeta}}+\boldsymbol{\zeta}) - \boldsymbol{\Gamma}_{v,\omega}\boldsymbol{M}_v^{\mathsf{T}}\boldsymbol{M}_v\Big)\boldsymbol{\Gamma}_{v,q} \\
&\quad - \boldsymbol{\Gamma}_{v,q}\boldsymbol{\Gamma}_{w,q}\Big)\boldsymbol{R}_{\mathrm{IB}}^{\mathsf{T}}(\boldsymbol{\lambda},\boldsymbol{\zeta}) + \boldsymbol{R}_{\mathrm{IB}}^{\mathsf{T}}(\boldsymbol{\lambda},\boldsymbol{\zeta})\boldsymbol{L}_{1_q}^{-\mathsf{T}} \\
\boldsymbol{B}_{v_{\mathrm{r}},\lambda} &= -\boldsymbol{\Gamma}_{v,q}\boldsymbol{R}_{\mathrm{IB}}^{\mathsf{T}}(\boldsymbol{\lambda},\boldsymbol{\zeta})\boldsymbol{M}_{\lambda}(\tilde{\boldsymbol{\lambda}},\tilde{\boldsymbol{\zeta}},\hat{\boldsymbol{v}}_{\mathrm{r}}) \\
\boldsymbol{B}_{v_{\mathrm{r}},\zeta} &= g\mathbb{I} - \boldsymbol{\Gamma}_{v,q}\boldsymbol{R}_{\mathrm{IB}}^{\mathsf{T}}(\boldsymbol{\lambda},\boldsymbol{\zeta})\boldsymbol{M}_{\zeta}(\tilde{\boldsymbol{\lambda}},\tilde{\boldsymbol{\zeta}},\hat{\boldsymbol{v}}_{\mathrm{r}}) \\
\boldsymbol{B}_{v_{\mathrm{r}},\omega} &= \Big(\frac{1}{m}\boldsymbol{F}_v - \boldsymbol{S}(\tilde{\boldsymbol{\omega}}+\boldsymbol{\omega})\Big)\boldsymbol{\Gamma}_{v,\omega}\boldsymbol{M}_v^{\mathsf{T}}\boldsymbol{I} - \boldsymbol{\Gamma}_{v,q}\left(\boldsymbol{R}_{\mathrm{IB}}^{\mathsf{T}}(\boldsymbol{\lambda},\boldsymbol{\zeta})\boldsymbol{R}_{\mathrm{IB}}(\tilde{\boldsymbol{\lambda}}+\boldsymbol{\lambda},\tilde{\boldsymbol{\zeta}}+\boldsymbol{\zeta})\boldsymbol{\Gamma}_{v,\omega} + \boldsymbol{\Gamma}_{w,\omega}\right)\boldsymbol{M}_v^{\mathsf{T}}\boldsymbol{I} + \frac{1}{m}\boldsymbol{F}_{\omega} + \boldsymbol{S}(\hat{\boldsymbol{v}}_{\mathrm{r}}) \\
&\quad - \boldsymbol{\Gamma}_{v,\omega}\boldsymbol{M}_v^{\mathsf{T}}\Big(\boldsymbol{S}(\boldsymbol{I}(\tilde{\boldsymbol{\omega}}+\boldsymbol{\omega})) - \boldsymbol{S}(\boldsymbol{\omega})\boldsymbol{I} + \boldsymbol{M}_{\omega} + \boldsymbol{M}_v\boldsymbol{\Gamma}_{v,\omega}\boldsymbol{M}_v^{\mathsf{T}}\boldsymbol{I}\Big) + \boldsymbol{M}_v^{\mathsf{T}}\boldsymbol{I}^{-1}\boldsymbol{L}_{1_\omega}^{-\mathsf{T}} \\
\boldsymbol{B}_{w,q} &= \boldsymbol{R}_{\mathrm{IB}}(\boldsymbol{\lambda},\boldsymbol{\zeta})\Big(\boldsymbol{\Gamma}_{w,q}\boldsymbol{S}(\boldsymbol{\omega}) - \boldsymbol{S}(\boldsymbol{\omega})\boldsymbol{\Gamma}_{w,q} - \boldsymbol{\Gamma}_{w,\omega}\boldsymbol{M}_v^{\mathsf{T}}\boldsymbol{M}_v\boldsymbol{\Gamma}_{v,q} \\
&\quad - \boldsymbol{\Gamma}_{w,q}\left(\boldsymbol{R}_{\mathrm{IB}}^{\mathsf{T}}(\boldsymbol{\lambda},\boldsymbol{\zeta})\boldsymbol{R}_{\mathrm{IB}}(\tilde{\boldsymbol{\lambda}}+\boldsymbol{\lambda},\tilde{\boldsymbol{\zeta}}+\boldsymbol{\zeta})\boldsymbol{\Gamma}_{v,q} + \boldsymbol{\Gamma}_{w,q}\right)\Big)\boldsymbol{R}_{\mathrm{IB}}^{\mathsf{T}}(\boldsymbol{\lambda},\boldsymbol{\zeta}) + \boldsymbol{L}_{1_q}^{-\mathsf{T}} \\
\boldsymbol{B}_{w,\lambda} &= -\boldsymbol{R}_{\mathrm{IB}}(\boldsymbol{\lambda},\boldsymbol{\zeta})\boldsymbol{\Gamma}_{w,q}\boldsymbol{R}_{\mathrm{IB}}^{\mathsf{T}}(\boldsymbol{\lambda},\boldsymbol{\zeta})\boldsymbol{M}_{\lambda}(\tilde{\boldsymbol{\lambda}},\tilde{\boldsymbol{\zeta}},\hat{\boldsymbol{v}}_{\mathrm{r}}) \\
\boldsymbol{B}_{w,\zeta} &= -\boldsymbol{R}_{\mathrm{IB}}(\boldsymbol{\lambda},\boldsymbol{\zeta})\boldsymbol{\Gamma}_{w,q}\boldsymbol{R}_{\mathrm{IB}}^{\mathsf{T}}(\boldsymbol{\lambda},\boldsymbol{\zeta})\boldsymbol{M}_{\zeta}(\tilde{\boldsymbol{\lambda}},\tilde{\boldsymbol{\zeta}},\hat{\boldsymbol{v}}_{\mathrm{r}}) \\
\boldsymbol{B}_{w,\omega} &= \boldsymbol{R}_{\mathrm{IB}}(\boldsymbol{\lambda},\boldsymbol{\zeta})\Big(-\boldsymbol{S}(\boldsymbol{\omega})\boldsymbol{\Gamma}_{w,\omega}\boldsymbol{M}_v^{\mathsf{T}}\boldsymbol{I} - \boldsymbol{\Gamma}_{w,q}\left(\boldsymbol{R}_{\mathrm{IB}}^{\mathsf{T}}(\boldsymbol{\lambda},\boldsymbol{\zeta})\boldsymbol{R}_{\mathrm{IB}}(\tilde{\boldsymbol{\lambda}}+\boldsymbol{\lambda},\tilde{\boldsymbol{\zeta}}+\boldsymbol{\zeta})\boldsymbol{\Gamma}_{v,\omega} + \boldsymbol{\Gamma}_{w,\omega}\right)\boldsymbol{M}_v^{\mathsf{T}}\boldsymbol{I} \\
&\quad - \boldsymbol{\Gamma}_{w,\omega}\boldsymbol{M}_v^{\mathsf{T}}\Big(\boldsymbol{S}(\boldsymbol{I}(\tilde{\boldsymbol{\omega}}+\boldsymbol{\omega})) - \boldsymbol{S}(\boldsymbol{\omega})\boldsymbol{I} + \boldsymbol{M}_{\omega} + \boldsymbol{M}_v\boldsymbol{\Gamma}_{v,\omega}\boldsymbol{M}_v^{\mathsf{T}}\boldsymbol{I}\Big)\Big)
\end{aligned}$$

Therefore, the expression in Eq. (A.12) can be written as

$$\tilde{\boldsymbol{x}}_2^\mathsf{T}\boldsymbol{B}(\tilde{\boldsymbol{x}}_1,\boldsymbol{x}_1,\hat{\boldsymbol{x}}_2)\tilde{\boldsymbol{x}}_1+\tilde{\boldsymbol{x}}_1^\mathsf{T}\boldsymbol{A}(\tilde{\boldsymbol{x}}_1,\boldsymbol{x}_1,\hat{\boldsymbol{x}}_2)\tilde{\boldsymbol{x}}_1$$

Let

$$\boldsymbol{\Lambda}=\sqrt{\frac{1}{\gamma}}\boldsymbol{B}\qquad\text{and}\qquad\boldsymbol{\Psi}=\frac{1}{2}\left(\boldsymbol{A}+\boldsymbol{A}^\mathsf{T}\right)\tag{A.15}$$

Using a series of sub-multiplicative properties, and the definition of φ^* in Eq. (68), we have

$$\begin{aligned}\tilde{\boldsymbol{x}}_2^\mathsf{T}\boldsymbol{B}(\tilde{\boldsymbol{x}}_1,\boldsymbol{x}_1,\hat{\boldsymbol{x}}_2)\tilde{\boldsymbol{x}}_1+\tilde{\boldsymbol{x}}_1^\mathsf{T}\boldsymbol{A}(\tilde{\boldsymbol{x}}_1,\boldsymbol{x}_1,\hat{\boldsymbol{x}}_2)\tilde{\boldsymbol{x}}_1&\leq\left|\tilde{\boldsymbol{x}}_2^\mathsf{T}\boldsymbol{B}(\tilde{\boldsymbol{x}}_1,\boldsymbol{x}_1,\hat{\boldsymbol{x}}_2)\tilde{\boldsymbol{x}}_1\right|+\tilde{\boldsymbol{x}}_1^\mathsf{T}\boldsymbol{A}(\tilde{\boldsymbol{x}}_1,\boldsymbol{x}_1,\hat{\boldsymbol{x}}_2)\tilde{\boldsymbol{x}}_1 &\text{(A.16a)}\\&=\left|\tilde{\boldsymbol{x}}_2^\mathsf{T}\sqrt{\gamma}\boldsymbol{\Lambda}(\tilde{\boldsymbol{x}}_1,\boldsymbol{x}_1,\hat{\boldsymbol{x}}_2)\tilde{\boldsymbol{x}}_1\right|+\tilde{\boldsymbol{x}}_1^\mathsf{T}\boldsymbol{\Psi}(\tilde{\boldsymbol{x}}_1,\boldsymbol{x}_1,\hat{\boldsymbol{x}}_2)\tilde{\boldsymbol{x}}_1 &\text{(A.16b)}\\&\leq\sqrt{\gamma}\|\tilde{\boldsymbol{x}}_2\|\|\boldsymbol{\Lambda}(\tilde{\boldsymbol{x}}_1,\boldsymbol{x}_1,\hat{\boldsymbol{x}}_2)\tilde{\boldsymbol{x}}_1\|+\tilde{\boldsymbol{x}}_1^\mathsf{T}\boldsymbol{\Psi}(\tilde{\boldsymbol{x}}_1,\boldsymbol{x}_1,\hat{\boldsymbol{x}}_2)\tilde{\boldsymbol{x}}_1 &\text{(A.16c)}\\&=\sqrt{\varphi^*(\tilde{\boldsymbol{x}}_2)}\,\|\boldsymbol{\Lambda}(\tilde{\boldsymbol{x}}_1,\boldsymbol{x}_1,\hat{\boldsymbol{x}}_2)\tilde{\boldsymbol{x}}_1\|+\tilde{\boldsymbol{x}}_1^\mathsf{T}\boldsymbol{\Psi}(\tilde{\boldsymbol{x}}_1,\boldsymbol{x}_1,\hat{\boldsymbol{x}}_2)\tilde{\boldsymbol{x}}_1 &\text{(A.16d)}\end{aligned}$$

thereby proving Proposition 1. □

B. System Identification Results

Table 3 Maximum likelihood parameter estimates

Parameter	Estimate	Standard Deviation
C_{x_α}	-3.07×10^{-1}	4.45×10^{-3}
C_{x_q}	2.54	4.06×10^{-2}
$C_{x_{\alpha^2}}$	3.55	3.73×10^{-2}
$C_{x_{\mathcal{J}_c}}$	9.45×10^{-2}	5.33×10^{-4}
C_{x_0}	1.03×10^{-2}	1.87×10^{-4}
C_{y_β}	-4.62×10^{-1}	3.04×10^{-3}
C_{y_r}	5.37×10^{-1}	6.86×10^{-3}
$C_{y_{\delta a}}$	5.95×10^{-2}	1.02×10^{-3}
$C_{y_{\delta r}}$	-1.54×10^{-1}	2.15×10^{-3}
C_{z_α}	-4.95	2.29×10^{-2}
C_{z_q}	-8.80	1.45×10^{-1}
$C_{z_{\delta e}}$	7.90×10^{-2}	1.47×10^{-3}
C_{z_0}	1.32×10^{-1}	1.90×10^{-3}
C_{l_β}	-9.21×10^{-3}	1.49×10^{-4}
C_{l_p}	-3.97×10^{-1}	3.12×10^{-3}
$C_{l_{\delta a}}$	-1.16×10^{-1}	8.04×10^{-4}
C_{m_α}	-4.27×10^{-1}	4.08×10^{-3}
C_{m_q}	-4.88	6.11×10^{-2}
$C_{m_{\delta e}}$	2.66×10^{-1}	1.69×10^{-3}
$C_{m_{\alpha^3}}$	-2.16	4.53×10^{-2}
C_{m_0}	4.17×10^{-2}	3.92×10^{-4}
C_{n_β}	7.78×10^{-2}	4.32×10^{-4}
C_{n_r}	-1.61×10^{-1}	1.63×10^{-3}
$C_{n_{\delta a}}$	1.61×10^{-2}	2.57×10^{-4}
$C_{n_{\delta r}}$	5.51×10^{-2}	4.72×10^{-4}

Table 4 Aerodynamic model valid domain (taken to capture 95% of data)

Variable	Minimum	Mean	Maximum	Units
V	13.9	18.7	23.4	m/s
α	1.43	6.08	10.72	deg
β	-8.89	2.83	14.54	deg
p	-90.0	7.9	105.8	deg/s
q	-44.5	9.2	62.9	deg/s
r	-67.6	-0.03	67.5	deg/s
δa	-16.7	-1.2	14.3	deg
δe	-12.2	1.9	16.1	deg
δr	-13.0	-0.1	12.9	deg
Ω	196.7	212.6	228.5	rad/s

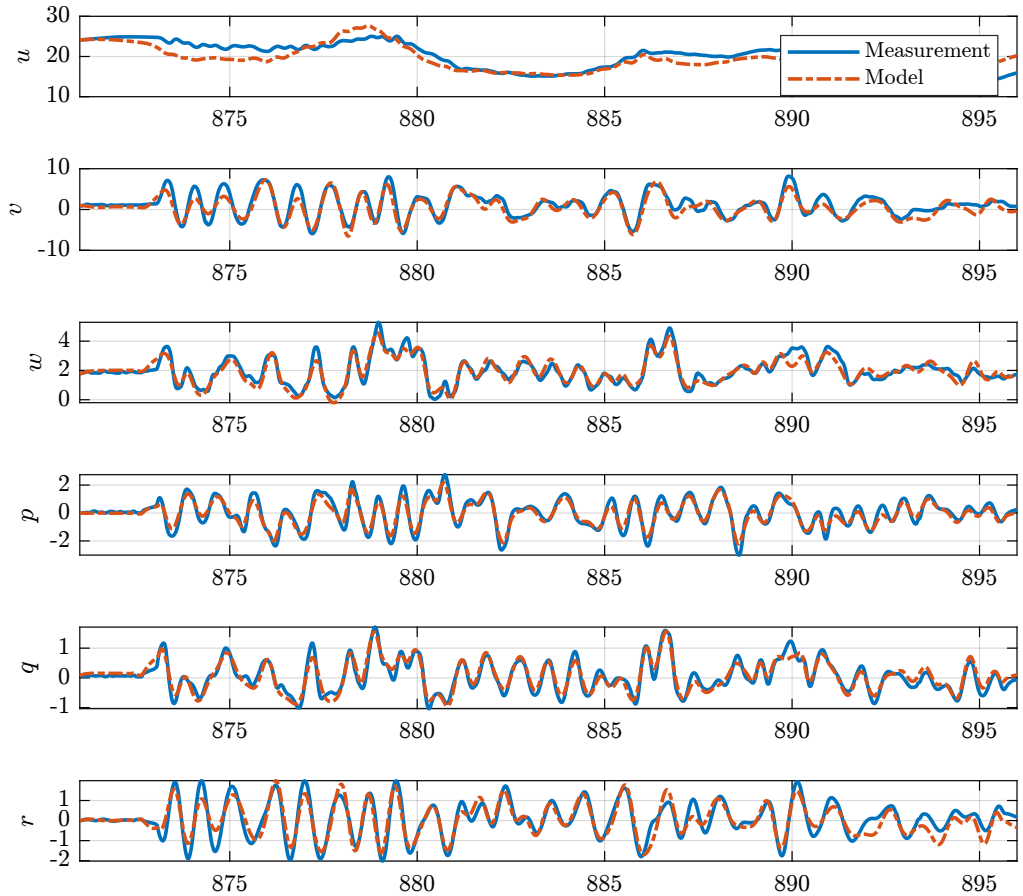

Fig. 10 Output error method model prediction.

References

[1] Reiche, C., Cohen, A. P., and Fernando, C., "An Initial Assessment of the Potential Weather Barriers of Urban Air Mobility," *IEEE Transactions on Intelligent Transportation Systems*, Vol. 22, No. 9, 2021, pp. 6018–6027. https://doi.org/10.1109/TITS.2020.3048364.

[2] "NASA Aeronautics Strategic Implementation Plan 2019 Update," Tech. rep., National Aeronautics and Space Administration, 2019.

[3] Hill, B., DeCarme, D., Metcalfe, M., Griffin, C., Wiggins, S., Metts, C., Bastedo, B., Patterson, M., and Mendonca, N., "UAM Vision Concept of Operations," Tech. rep., National Aeronautics and Space Administration, 2020.

[4] Patterson, M., Isaacson, D., and Mendonca, N., "Intermediate State UAM Vision Concept of Operations (ConOps) Overview," , Feb. 2021.

[5] Karr, D. A., Wing, D. J., Barney, T. L., Sharma, V., Etherington, T. J., and Sturdy, J. L., "Initial Design Guidelines for Onboard Automation of Flight Path Management," *AIAA AVIATION Forum*, VIRTUAL EVENT, 2021. https://doi.org/10.2514/6.2021-2326.

[6] Thipphavong, D. P., Apaza, R., Barmore, B., Battiste, V., Burian, B., Dao, Q., Feary, M., Go, S., Goodrich, K. H., Homola, J., Idris, H. R., Kopardekar, P. H., Lachter, J. B., Neogi, N. A., Ng, H. K., Oseguera-Lohr, R. M., Patterson, M. D., and Verma, S. A., "Urban Air Mobility Airspace Integration Concepts and Considerations," *2018 Aviation Technology, Integration, and Operations Conference*, American Institute of Aeronautics and Astronautics, Atlanta, Georgia, 2018. https://doi.org/10.2514/6.2018-3676.

[7] González-Rocha, J., Woolsey, C. A., Sultan, C., and De Wekker, S. F. J., "Sensing Wind from Quadrotor Motion," *Journal of Guidance, Control, and Dynamics*, Vol. 42, No. 4, 2019, pp. 836–852. https://doi.org/10.2514/1.G003542.

[8] Barbieri, L., Kral, S., Bailey, S., Frazier, A., Jacob, J., Reuder, J., Brus, D., Chilson, P., Crick, C., Detweiler, C., Doddi, A., Elston, J., Foroutan, H., González-Rocha, J., Greene, B., Guzman, M., Houston, A., Islam, A., Kemppinen, O., Lawrence, D., Pillar-Little, E., Ross, S., Sama, M., Schmale, D., Schuyler, T., Shankar, A., Smith, S., Waugh, S., Dixon, C., Borenstein, S., and de Boer, G., "Intercomparison of Small Unmanned Aircraft System (sUAS) Measurements for Atmospheric Science during the LAPSE-RATE Campaign," *Sensors*, Vol. 19, No. 9, 2019, p. 2179. https://doi.org/10.3390/s19092179.

[9] Jacob, J., Chilson, P., Houston, A., and Smith, S., "Considerations for Atmospheric Measurements with Small Unmanned Aircraft Systems," *Atmosphere*, Vol. 9, No. 7, 2018, p. 252. https://doi.org/10.3390/atmos9070252.

[10] Witte, B., Singler, R., and Bailey, S., "Development of an Unmanned Aerial Vehicle for the Measurement of Turbulence in the Atmospheric Boundary Layer," *Atmosphere*, Vol. 8, No. 10, 2017, p. 195. https://doi.org/10.3390/atmos8100195.

[11] Palomaki, R. T., Rose, N. T., van den Bossche, M., Sherman, T. J., and De Wekker, S. F. J., "Wind Estimation in the Lower Atmosphere Using Multirotor Aircraft," *Journal of Atmospheric and Oceanic Technology*, Vol. 34, No. 5, 2017, pp. 1183–1191. https://doi.org/10.1175/JTECH-D-16-0177.1.

[12] Langelaan, J. W., Alley, N., and Neidhoefer, J., "Wind Field Estimation for Small Unmanned Aerial Vehicles," *Journal of Guidance, Control, and Dynamics*, Vol. 34, No. 4, 2011, pp. 1016–1030. https://doi.org/10.2514/1.52532.

[13] Adkins, K. A., Akbas, M., and Compere, M., "Real-Time Urban Weather Observations for Urban Air Mobility," *International Journal of Aviation, Aeronautics, and Aerospace*, Vol. 7, No. 4, 2020. https://doi.org/10.15394/ijaaa.2020.1540.

[14] Trub, R., Moser, D., Schafer, M., Pinheiro, R., and Lenders, V., "Monitoring Meteorological Parameters with Crowdsourced Air Traffic Control Data," *2018 17th ACM/IEEE International Conference on Information Processing in Sensor Networks (IPSN)*, IEEE, Porto, 2018, pp. 25–36. https://doi.org/10.1109/IPSN.2018.00010.

[15] Shim, H., "A Passivity-based Nonlinear Observer and a Semi-global Separation Principle," Ph.D. thesis, School of Electrical Engineering, Seoul National University, Feb. 2000.

[16] Shim, H., Seo, J. H., and Teel, A. R., "Nonlinear Observer Design via Passivation of Error Dynamics," *Automatica*, Vol. 39, No. 5, 2003, pp. 885–892. https://doi.org/10.1016/S0005-1098(03)00023-2.

[17] Woolsey, C., and Techy, L., "Cross-Track Control of a Slender, Underactuated AUV Using Potential Shaping," *Ocean Engineering*, Vol. 36, No. 1, 2009, pp. 82–91. https://doi.org/10.1016/j.oceaneng.2008.07.010.

[18] Battista, T., Jung, S., Woolsey, C., and Paterson, E., "An Energy-Casimir Approach to Underwater Vehicle Depth and Heading Regulation in Short Crested Waves," *2017 IEEE Conference on Control Technology and Applications (CCTA)*, IEEE, Mauna Lani Resort, HI, USA, 2017, pp. 217–222. https://doi.org/10.1109/CCTA.2017.8062466.

[19] Fahmi, J.-M., and Woolsey, C. A., "Passivity Based Cross-Track Control of a Fixed-Wing Aircraft," *Conference on Guidance, Navigation and Control*, 2022.

[20] Fahmi, J.-M., and Woolsey, C. A., "Port-Hamiltonian Flight Control of a Fixed-Wing Aircraft," *IEEE Transactions on Control Systems Technology*, Vol. 30, No. 1, 2022, pp. 408–415. https://doi.org/10.1109/TCST.2021.3059928.

[21] Etkin, B., *Dynamics of Atmospheric Flight*, Wiley, New York, 1972.

[22] Thomasson, P. G., and Woolsey, C. A., "Vehicle Motion in Currents," *IEEE Journal of Oceanic Engineering*, Vol. 38, No. 2, 2013, pp. 226–242. https://doi.org/10.1109/JOE.2013.2238054.

[23] Etkin, B., "Turbulent Wind and Its Effect on Flight," *Journal of Aircraft*, Vol. 18, No. 5, 1981, pp. 327–345. https://doi.org/10.2514/3.57498.

[24] Byrnes, C. I., Isidori, A., and Willems, J. C., "Passivity, Feedback Equivalence, and the Global Stabilization of Minimum Phase Nonlinear Systems," *IEEE Transactions on Automatic Control*, Vol. 36, No. 11, 1991, pp. 1228–1240. https://doi.org/10.1109/9.100932.

[25] Jiang, Zhong-Ping, and Hill, D. J., "Passivity and Disturbance Attenuation via Output Feedback for Uncertain Nonlinear Systems," *IEEE Transactions on Automatic Control*, Vol. 43, No. 7, 1998, pp. 992–997. https://doi.org/10.1109/9.701109.

[26] Venkatraman, A., and van der Schaft, A., "Full-Order Observer Design for a Class of Port-Hamiltonian Systems," *Automatica*, Vol. 46, No. 3, 2010, pp. 555–561. https://doi.org/10.1016/j.automatica.2010.01.019.

[27] Chen, Y.-C., and Woolsey, C., "Passivity-Based Disturbance Observer Design," *ASME 2020 Dynamic Systems and Control Conference*, American Society of Mechanical Engineers, Virtual, Online, 2020, p. V001T21A007. https://doi.org/10.1115/DSCC2020-3287.

[28] Chen, Y.-C., and Woolsey, C. A., "Nonlinear, Model-Based Disturbance Estimation for Fixed-Wing Aircraft," *AIAA Scitech 2021 Forum*, American Institute of Aeronautics and Astronautics, VIRTUAL EVENT, 2021. https://doi.org/10.2514/6.2021-0018.

[29] Khalil, H. K., "Chapter 14: Nonlinear Design Tools," *Nonlinear Systems*, Prentice Hall, Upper Saddle Ridge, New Jersey, 2002, 3rd ed., pp. 551–646.

[30] Lin, Y., Sontag, E. D., and Wang, Y., "A Smooth Converse Lyapunov Theorem for Robust Stability," *SIAM Journal on Control and Optimization*, Vol. 34, No. 1, 1996, pp. 124–160. https://doi.org/10.1137/S0363012993259981.

[31] Gresham, J. L., Fahmi, J.-M. W., Simmons, B. M., Hopwood, J. W., Foster, W., and Woolsey, C. A., "Flight Test Approach for Modeling and Control Law Validation for Unmanned Aircraft," *AIAA SCITECH 2022 Forum*, American Institute of Aeronautics and Astronautics, San Diego, CA & Virtual, 2022. https://doi.org/10.2514/6.2022-2406.

[32] Simmons, B. M., Gresham, J. L., and Woolsey, C. A., "Aero-Propulsive Modeling for Propeller Aircraft Using Flight Data," *Journal of Aircraft*, Vol. 60, No. 1, 2023, pp. 81–96. https://doi.org/10.2514/1.C036773.

[33] Simmons, B. M., Gresham, J. L., and Woolsey, C. A., "Flight-Test System Identification Techniques and Applications for Small, Low-Cost, Fixed-Wing Aircraft," *Journal of Aircraft*, Vol. 60, No. 5, 2023, pp. 1503–1521. https://doi.org/10.2514/1.C037260.

[34] Morelli, E. A., and Klein, V., *Aircraft System Identification: Theory and Practice*, 2nd ed., Sunflyte Enterprises, Williamsburg, Virginia, 2016.

[35] Morelli, E. A., "Global Nonlinear Aerodynamic Modeling Using Multivariate Orthogonal Functions," *Journal of Aircraft*, Vol. 32, No. 2, 1995, pp. 270–277. https://doi.org/10.2514/3.46712.

[36] Morelli, E. A., "System IDentification Programs for AirCraft (SIDPAC), Version 4.0," NASA Langley Research Center, 2018.

[37] Gahan, K., Hopwood, J. W., and Woolsey, C. A., "Wind Estimation Using an H∞ Filter with Fixed-Wing Aircraft Flight Test Results," *AIAA SCITECH 2023 Forum*, American Institute of Aeronautics and Astronautics, National Harbor, MD & Online, 2023. https://doi.org/10.2514/6.2023-2252.

[38] Grant, M., and Boyd, S., "CVX: Matlab Software for Disciplined Convex Programming, Version 2.1," , Mar. 2014.

[39] Grauer, J. A., and Morelli, E. A., "Generic Global Aerodynamic Model for Aircraft," *Journal of Aircraft*, Vol. 52, No. 1, 2015, pp. 13–20. https://doi.org/10.2514/1.C032888.

[40] "The MOSEK Optimization Toolbox for MATLAB Manual," MOSEK ApS, 2022. URL https://www.mosek.com/.

[41] Khalil, H. K., *Nonlinear Systems*, 2nd ed., Prentice Hall, Upper Saddle Ridge, New Jersey, 1996.